NTNU – Trondheim
Norwegian University of
Science and Technology

Competitive Binding of Persistent Organic Pollutants to the Thyroid Hormone Transport Protein Transthyretin in Glaucous Gull (*Larus hyperboreus*).

Åse-Karen Mortensen

MSc in Biology
Submission date: May 2015
Supervisor: Bjørn Munro Jenssen, IBI
Co-supervisor: Geir Wing Gabrielsen, Norsk Polarinstitutt

Norwegian University of Science and Technology
Department of Biology

ACKNOWLEDGEMENTS

The work resulting in this master thesis was performed at the Department of Biology at the Norwegian University of Science and Technology (NTNU) in collaboration with the Norwegian Polar Institute (NPI), the Research Group of Medical Pharmacology and Toxicology at the Department of Medical Biology, University of Tromsø (UiT) and the Norwegian Institute of Air Research (NILU) from January 2014 to May 2015.

I want to thank everyone who helped me with this project and for everything they taught me. I am very grateful and it has been fun to work with you. I had the privilege to work under the great guidance of main supervisor Professor Bjørn Munro Jenssen (NTNU), and co-supervisors Senior Research Scientist Geir Wing Gabrielsen (NPI), Science Director Eldbjørg S. Heimstad (NILU) and Professor Ingebrigt Sylte (UiT). I also want to thank Associate Professor Kurt Kristiansen (UiT) for teaching me about molecular modelling and Senior Advisor Kjetil Sagerup (Akvaplan niva) for teaching me how to work in the field.

Trondheim, May 2015
Åse-Karen Mortensen

ABSTRACT

The glaucous gull (*Larus hyperboreus*) is one of the largest avian top predators in the Arctic. High levels of persistent organic pollutants (POPs) and their metabolites have been detected in the glaucous gull, and several studies indicate that high levels of different POPs can contribute to detrimental effects. The mechanism behind these disruptions could be that chemicals interfere with the endocrine system. Thyroid hormones (THs) are important for thermogenesis, reproduction, growth and differentiation. They are transported in the circulation system of glaucous gull mainly bound to the transport proteins globulin, albumin and transthyretin (TTR). The aim of this study was to use molecular modeling to construct a homology model of the TTR in glaucous gull and to dock several well-known and new emerging POPs in the models to predict the binding affinity of POPs to the TH binding site in glaucous gull TTR.

The models predicted that a large group of structurally diverse compounds would bind to glaucous gull TTR such as polychlorinated biphenyls (PCB), hydroxyl-PCB (OH-PCB), methyl sulfone-PCB ($MeSO_2$-PCB), polybrominated diphenyl ether (PBDE), OH-PBDE, methoxyl-PBDE (MeO-PBDE), bromophenols, 2-bromoallyl-2,4,6-tribromophenyl ether (BATE), bis-(2,4,5-tribromophenoxy)-ethane (BTBPE), allyl-2,4,6-tribromphenylether (ATE), 2,3-dibromopropyl-2,4,6-tribromophenyl ether (DPTE), triclocarban, triphenylphosphate (TPhP), 68399-95-1, 63734-62-3, 5059-77-9 and several perfluorinated compounds (PFCs).

The present of functional groups in the compounds like OH-groups were predicted to increase the binding affinity for the binding site, and if the functional groups were ionized then the binding affinity was predicted to further increased. However, the high scores of PBDEs indicate that functional groups are not necessary to bind to TTR. The models also predicted that brominated analogues had higher affinity to TTR than the corresponding chlorinated analogues. T_3 were predicted to bind stronger to TTR than T_4. The THs and the docked POPs were predicted to bind both in forward and reverse binding modes and had hydrogen-bonding interactions with the amino acids Lys15 and Ser117. The predicted binding affinityto TTR for some compounds like TBBPA were different from the results in studies of other species. This indicate that there is species-specific difference in binding to TTR. The docking of THs and the ROC-curves from the test set indicate that the constructed models of glaucous gull TTR are accurate in the predictions of whether a compound will bind to glaucous gull TTR or not.

Competitive binding of the POPs with THs for TTR in glaucous gull can potentially disrupt circulation of THs and possibly affect the TH homeostasis and TH-dependent functions. Many of the compounds predicted to bind to TTR have been detected in samples from glaucous gull or other seabirds from the Arctic. The POPs not yet detected should be measured in samples from glaucous gull. Further studies should investigate the binding affinity of the compound to TTR and their potential of competitive displacement of TH in the binding site of TTR *in vitro*. Studies looking at the potential biological effects on individual and population level of POPs binding to TTR are also necessary.

SAMMENDRAG

Polarmåke (*Larus hyperboreus*) er en av de største topp predatorene blant fugler i Arktis. Høye nivåer av persistente organiske miljøgifter (POPs) og deres metabolitter er blitt detektert i polarmåke, og flere studier indikerer at høye nivåer av forskjellige POPs kan bidra til utvikling, atferd og reproduktivt stress og abnormiteter. Årsaken til disse forstyrrelsene kan være at kjemikaliene forstyrrer hormonsystemet. Thyroidhormoner (THs) er viktig for termogenese, reproduksjon, vekst og differensiering. De er transportert i sirkulasjonssystemet til polarmåke bundet til transportproteinene globulin, albumin og transthyretin (TTR). Målet for denne studien var å bruke molekylær modellering for å konstruere en homologi modell av TTR i polarmåke og dokke flere velkjente og nye framtredende POPs i modellene for å predikere bindingsaffiniteten av POPs til TH bindingssete i polarmåke TTR.

Modellene predikterer at en stor gruppe strukturelt forskjellige forbindelser kan bindes til polarmåke TTR slik som polyklorerte bifenyler (PCB), hydroksyl-PCB (OH-PCB), metyl sulfon-PCB ($MeSO_2$-PCB), polybrominerte difenyl eter (PBDE), OH-PBDE, metoxyl-PBDE (MeO-PBDE), bromofenoler, 2-bromoallyl-2,4,6-tribromofenyl eter (BATE), bis-(2,4,5-tribromofenoksy)-etan (BTBPE), allyl-2,4,6-tribromfenyleter (ATE), 2,3-dibromopropyl-2,4,6-tribromophenyl eter (DPTE), triclocarban, trifenylfosfat (TPhP), 68399-95-1, 63734-62-3, 5059-77-9 og flere perfluorinerte forbindelser (PFCs).

Funksjonelle grupper i forbindelsen som hydroksylgrupper ble prediktert å øke bindingsaffiniteten for TH bindingssete og hvis de funksjonelle gruppene var ionisert ble bindingsaffiniteten ytterligere økt. Likevel, den høye skåren til PBDE indikerer at funksjonelle grupper ikke er nødvendig for at en forbindelse skal binde til TTR. Modellene predikerer også at brominerte forbindelser hadde høyere affinitet til TTR enn korresponderende klorinerte forbindelser. T_3 ble prediktert til å binde sterkere til TTR enn T_4. TH og dokkede forbindelsene var også predikert til å binde både i framover og revers bindings modus, og hadde hydrogenbindinger med aminosyrene Lys15 og Ser117. Den predikerte affiniteten til TTR for noen forbindelser som TBBPA var annerledes fra resultat i studier på andre arter. Dette indikerer at det er arts-spesifikke forskjeller i binding til. Dokking av THs og ROC-kurvene fra dokkingen av test-settet indikerer at de konstruerte homologi-modellene av polarmåke TTR er presise i prediksjonen av om en forbindelse vil binde til polarmåke TTR eller ikke.

Konkurrerende binding av POPs med THs for TTR i polarmåke kan potensielt forstyrre sirkulasjonen av THs og muligens påvirke TH homeostase og TH avhengige funksjoner. Mange av forbindelsene som ble predikterte å binde til TTR har blitt detektert i prøver fra polarmåke eller andre sjøfugler fra Arktis. POPs ennå ikke detektert bør måles i prøver fra polarmåke. Videre studier bør undersøke bindingsaffiniteten av forbindelsene til TTR og deres potensielle konkurrerende fortrengning av TH i bindingssete av TTR *in vitro*. Studier som ser på potensielle biologiske effekter på individ og populasjonsnivå av POPs som binder til TTR er også nødvendig.

TABLE OF CONTENTS

INDEX OF FIGURES, TABLES AND APPENDIX

FIGURES

TABLES

APPENDIX

ABBREVIATIONS

10:2 FTOH	3,3,4,4,5,5,6,6,7,7,8,8,9,9,10,10,11,11,12,12,12-henicosafluorododecan-1-ol
12:2 FTAC	pentacosafluorotetradecyl acrylate
12:2 FTMAC	pentacosafluorotetradecyl methacrylate
12:2 FTOH	3,3,4,4,5,5,6,6,7,7,8,8,9,9,10,10,11,11,12,12,13,13,14,14,14-pentacosafluorotetradecan-1-ol
14:2 FTAC	nonacosafluorohexadecyl acrylate
2,4,6-TBP	2,4,6-tribromophenol
2,4-DBP	2,4-Dibromophenol
6:2 FTMAC	perfluorooctyl methacrylate
6:2 FTOH	3,3,4,4,5,5,6,6,7,7,8,8,8-tridecafluorooctan-1-ol
8:2 FTOH	3,3,4,4,5,5,6,6,7,7,8,8,9,9,10,10,10-heptadecafluorodecan-1-ol
3D	three dimensional
aa	amino acid
ALB	albumin
ATE	allyl-2,4,6-tribromphenylether
AUC	area under curve
BAF	bioaccumulation factor
BATE	2-bromoallyl-2,4,6-tribromophenyl ether
BBP	butylbenzyl phthalates
BCPS	Bis-(4-chlorophenyl)sulfone
BFR	brominated flame retardants
BTBPE	bis-(2,4,5-tribromophenoxy)-ethane
C8-PFPA	C8-perfluorinated phosphonic acids
ChEMBL	chemical database of European Molecular Biology Laboratory
DDT	dichlorodiphenyltrichloroethane
DES	diethylstilbestrol
DPTE	2,3-dibromopropyl-2,4,6-tribromophenyl ether
DUD.E	A database of Useful Decoys: Enhanced
$\mathbf{E_{angle}}$	angle energy
$\mathbf{E_{bond}}$	bonding energy
$\mathbf{E_{dihedral}}$	torsional energy
$\mathbf{E_{elec}}$	electrostatic energy
$\mathbf{E_{non\text{-}bond}}$	non-bonding energy
$\mathbf{E_{tot}}$	total potential energy
$\mathbf{E_{vdw}}$	van der Waals energy
FA	fatty acid
FTAC	fluorotelomer acrylate
FTMAC	fluorotelomer methacrylate
FTOH	fluorotelomer alcohol
HBBz	hexabromobenzene
HBCD	hexabromocyclododecane

HCBD	hexachlorobutadiene
HBP	halogen binding pocket
IC50	half maximal inhibitory concentration
ICM	internal coordinate mechanics
MeO	methoxyl
$MeSO_2$	methyl sulfone
MM	molecular mechanically
N-Et-FOSA	N-ethyl perfluorooctane sulfonamide
N-Et-FOSE	N-ethyl perfluorooctane sulfonamidoethanol
N-Me-FOSA	N-methyl perfluorooctane sulfonamide
N-Me-FOSE	N-methyl perfluorooctane sulfonamidoethanol
NILU	Norwegian Institute of Air Research
NPI	Norwegian Polar Institute
NTNU	Norwegian University of Science and Technology
OCS	octachlorostyrene
OH	hydroxyl
OHC	organohalogenated compound
OC	organochlorine
PBDE	polybrominated diphenyl ether
PBEB	pentabromoethylbenzene
PBF	heptafluorobutyryl fluoride
PCA	pentachloroanisole
PCB	polychlorinated biphenyl
PCN	polychlorinated naphthalenes
PCNB	pentachloronitrobenzene
PCP	pentachlorophenol
PDB	protein data bank
PeCBz	pentachlorobenzene
PFC	perfluorinated compounds
PFCA	perfluoroalkyl carboxylates
PFDcA	perfluoroheptane sulfonate
PFHxA	perfluorohexanoic acid
PFHxS	perfluorohexane sulfonate
PFNA	perfluorononanoic acid
PFOA	perfluorooctanoic acid
PFOS	perfluorooctane sulfonate
PFPA	perfluoropentanoic acid
PFR	phosphours flame-retardants
PFSA	perfluoroalkyl sulfonates
PFTeA	perfluorotetradecanoic acid
PFTriA	perfluorotridecanoic acid
PHpF	Perfluoroheptanoic fluoride
POF	Perfluorooctanoic fluoride
POP	persistent organic pollutant

QM	quantum mechanically
RBP	retinol-binding protein
ROC	receiver operating curve
sbrTTR	sea bream recombinant TTR
SMILES	simplified molecular-input line-entry system
T_3	3,5,3´-triiodothyronine / triiodo-L-thyronine
T_4	3,5,3´,5´-tetraiodothyronine / thyroxine
TBB	2-ethylhexyl-2,3,4,5-tetrabromobenzoate
TBBPA	tetrabromobisphenol A
TBG	thyroxine-binding-globulin
TBPH	bis(2-ethyl-hexyl)tetrabromophthalate
TH	thyroid hormone
TPhP	Triphenylphosphate
TR	thyroid hormone receptor
TSH	thyroid stimulating hormone
TTR	transthyretin
UiT	University of Tromsø
UniProtKB	UniProt Knowledgebase
UPGMA	Unweighted Pair Group Method with Arithmetic Mean
VLS	virtual ligand screnning
Å	angstrom

1. INTRODUCTION

1.1 Persistent organic pollutants in the Arctic

Despite of almost no local sources persistent organic pollutants (POPs) are found in the arctic food webs. Man-made substances are transported over long distances from industrialized regions to the Arctic. The long-range transport of POPs occurs through atmospheric and ocean currents, as well as river discharge. The most important route is atmospheric circulation bringing the contaminants from lower latitudes within days (Burkow and Kallenborn, 2000).

POPs are a diverse group of anthropogenic pollutants of industrial and agricultural origin. Substances such as polychlorinated biphenyls (PCBs) and chlorinated pesticides (e.g. dichlorodiphenyltrichloroethane (DDT) have been documented in artic wildlife since the 1970s (Bourne and Bogan, 1972). The levels of some POPs (e.g. PCB and DDT) have decreased in the last 10-20 years after the introduction of bans and restrictions by the global treaty the Stockholm convention (www.pops.int), but new persistent pollutants are produced in large quantities and are therefore increasing in the environment. Some of these new compounds are brominated flame retardants (BFRs) and perfluorooctane sulfonate (PFOS) (de Wit, 2004).

POPs are characterized by their chemical properties, they are lipophilic, semi-volatile and persistent to degradation, and therefore POPs tend to accumulate in lipid rich food chains of the arctic marine ecosystem (Borga et al., 2001). Due to bioaccumulation and biomagnification POPs may reach very high concentrations in the apex predators (de Wit, 2004). POPs elicit a range of detrimental effects on biota, and the concerns about POPs have increased with the knowledge about them. The detrimental effects of POPs are related to enzyme-, immune-, hormone- and vitamin systems. Contaminants that have reproductive effects and mimics and disrupt the hormone system are of special concern (Giesy et al., 2003, Colborn et al., 1993).

Fluctuating external conditions expose the arctic wildlife to natural stress (e.g. food availability, temperature, precipitation, sea ice conditions) and combined with the effect of contaminations and anthropogenic stressors, organisms may be vulnerable to detrimental effects (Bustnes et al., 2008). Climate change might adverse this by increasing the amount of stress in wildlife when adapting to the environmental conditions, and possibly elicit the bioavailability and toxicity of POPs (Jenssen, 2006). During the last years several studies in the Arctic have investigated the relationship between contaminants and effects in organisms like polar bear (*Ursus maritimus*) and glaucous gull (*Larus hyperboreus*), and the documented levels are so high that they raise concern about the health of these species (Gabrielsen, 2007).

The increasing levels of some emerging POPs in arctic biota compared to the classic organochlorinated anthropogenic pollutants are a cause for concern. The new emerging chemicals tend to have different physiochemical properties compared to the classic pollutants such as the hydrophobic and oleophobic effects of perfluorinated compounds (PFCs) (Houde et al., 2006).

Most POPs are organohalogenated compounds (OHCs) and many are aromatic as well. OHCs includes both brominated, chlorinated and fluorinated chemicals. PCBs consists of paired phenyls rings with different degrees of chlorination. They have been used as flame-retardants and as coolants and lubricants in electrical equipment. The manufacturing peaked in the 1960s, but decreased drastically after being banned by the Stockholm convention. PCBs can be biotransformed into methyl sulfone ($MeSO_2$-) and hydroxylated (OH-) metabolites (Letcher et al., 2000). Following the ban new BFRs were produced to replace PCBs, and some of they are increasing in the environment (de Wit et al., 2010). Polybrominated biphenyl ethers (PBDEs) are widely used BFRs structurally similar to PCBs, consisting of paired phenyl rings connected by an ether bridge and having different degree of bromination. PBDEs can be biotransformed into hydroxylated and methoxylated (MeO-) metabolites (Kelly et al., 2008). Two out of three commercial PBDE mixtures, PentaBDE and OctaBDE have been included in the Stockholm Convention, and the last, DecaBDE, is under consideration for phase-out.

Therefore are the PBDEs being replaced by the rapid development of other BFRs. Examples of potential replacements include 2,3-dibromopropyl-2,4,6-tribromophenyl ether (DPTE), bis(2-ethyl-hexyl)tetrabromophthalate (TBPH), 2-ethylhexyl-2,3,4,5-tetrabromobenzoate (TBB), pentabromoethylbenzene (PBEB), hexabromobenzene (HBBz), tetrabromobisphenol A (TBBPA), hexabromocyclododecane (HBCD), bis-(2,4,5-tribromophenoxy)-ethane (BTBPE) and decabromodiphenylethane (DBDPE). These alternative flame-retardants have properties similar to those of PBDE mixtures: high bromination, aromatic moieties and low aqueous solubility, and mostly used as additive flame-retardants instead of reactive. The emerging BFRs are known to leak out into environment, are subject to long-range transport and are found in biotic and abiotic samples in the Arctic, but little is known about their toxicity and potential for bioaccumulation (Sagerup et al., 2010, Schlabach et al., 2011, Vorkamp and Riget, 2014).

PFCs have been in use for more than 50 years in a wide variety of industrial and commercial products. They are atypical to other POPs by possessing both lipophilic and hydrophilic properties and have strong carbon-fluorine bonds, making them thermally and chemically stable. This means that they are environmentally persistent (Houde et al., 2006). PFCs consist of a carbon chain of 4-14 carbons that are completely saturated by fluorine atoms and they have a functional group (primarily sulfonate and carboxylate, as in perfluoroalkyl carboxylates (PFCAs) and perfluoroalkyl sulfonates (PFSAs)) (Lau et al., 2007). These chemicals have no known route for abiotic or biotic degradation in the environment either (Martin et al., 2003). This is a great concern since perfluorinated chains exceeding more then 6-7 carbons display a great bioaccumulation potential (Martin et al., 2004). The structure and behavior of many PFCs within organism resemble the free fatty acids (FAs). They also bind to FA-binding proteins and the protein albumin, which is mainly present in blood, liver and eggs (Martin et al., 2003, Jones et al., 2003, Luebker et al., 2002). It has been suggested as an explanation for the protein-binding data of PFCs that the polar hydrophobic nature can lead to increased affinity to proteins (Biffinger et al., 2004). The highest levels of PFCs in humans, rodents and marine mammals have accordingly been found in the protein-rich blood and liver (Kudo and Kawashima, 2003, Luebker et al., 2002)

Other emerging contaminants include chlorinated flame-retardants as Dechlorane Plus and short-, medium- and long-chained chlorinated paraffins (SCCP, MCCP and LCCP). These compounds are known to bioaccumulate. Dechlorane Plus was originally introduced in the 1960 as an insecticide but is now used as a replacement of DecaBDE. SCCP, MCCP and LCCP are complex mixtures of varying chain length and degree of chlorination and are among other used as flame-retardants. There are evidences of current-used pesticides in the arctic environment including Dacthal, trifluralin, pentachlorophenol (PCP), pentachloronitrobenzene (PCNB), pentachloroanisole (PCA), chlorothalonil, chlorpyrios, diazinon, endosulfan, methoxychlor and dicofol. All pesticides were found in abiotic arctic samples, which provide evidence for long-range transport. On the other hand only endosulfan has been considered sufficiently bioaccumulative to be included in the Stockholm Convention, and in general more knowledge is required on current-used pesticides as a source of POPs (Vorkamp and Riget, 2014). Several other compounds with diverse applications and uses are found in the arctic environment. Among these are the synthetic musk compounds used in personal care and household products, phthalic acid esters (or phthalates), siloxanes and halogenated compounds. Among the halogenated compounds is hexachlorobutadiene (HCBD), octachlorostyrene (OCS), pentachlorobenzene (PeCBz) and polychlorinated naphthalene (PCN). Data on bioaccumulation is still sparse for many of these compounds and can therefore not be established (Vorkamp and Riget, 2014).

1.2 Glaucous gull (*Larus hyperboreus*) as a model organism

The glaucous gull has a circumpolar distribution and is one of the largest avian predators in the Arctic. Estimations of the breeding population in Svalbard are between 4000-10000 pairs, and they breed in small colonies or single pairs usually close to colonies of other seabirds. They winter mainly in the North Atlantic Ocean and stay there from around November to March. The glaucous gull has an apex position in the arctic food web and is an opportunistic scavenger, with a diet that varies from pelagic and marine invertebrates, fish, eggs, chicks and adults of other seabirds to carrion or humane refuse. The food preference depends on their breeding ground (Strøm, 2006).

Contaminant levels and patterns have been reported in glaucous gulls since the first survey on anthropogenic contaminants in arctic wildlife in 1972 (Bourne and Bogan, 1972). Because of bioaccumulation and biomagnification top predators as the glaucous gull can have very high concentrations of POPs, and the high levels have been linked to the low metabolizing capacity of glaucous gulls (Bustnes et al., 2000, Henriksen et al., 2000). They are also often exposed to contaminant metabolites that might be even more bioactive then their precursors (Verreault et al., 2010). The differences in feeding ecology of glaucous gulls is important for the distribution of POPs within populations (Bustnes et al., 2000). Higher contamination load of POPs like the PCBs are found in males, and this sex difference reflects that female birds have an additional important excretory pathway for lipophilic compounds resistant to biodegradation by being able to deposit contaminants into their eggs. Most POPs, with the exception of PFCs, concentrate in lipid rich tissue and can be released and distributed through the body by emaciation (Verreault et al., 2006).

Several studies indicate that high blood levels of different POPs through a variety of different effects can contribute to developmental, behavioral and reproductive stress in glaucous gulls. It has been suggested that the underlying mechanism for this is that contaminants induce modulation on the bird's hormone and/or nervous system (Bustnes et al., 2003, Bustnes et al., 2004, Verreault et al., 2004). The number of breeding glaucous gulls on Bjørnøya went from 2000 pairs in 1986 to 650 pairs in 2006, a decline by nearly 65 % (Strøm, 2007). The reason for this decline is still not established, but it was suggested that physiological stress induced by contaminants along with anthropogenic and natural stressors can be the cause (Letcher et al., 2010). The glaucous gull can be viewed as a bioindicator species and is recommended for specific effect studies (Verreault et al., 2010).

1.3 The thyroid hormone system and the transport protein transthyretin

Thyroid hormones (THs) are involved in metamorphosis, thermogenesis, hibernation, reproduction, growth and differentiation. They are found circulating in the plasma of all groups of vertebrates, and are produced in the thyroid gland follicle upon signal from thyroid stimulating hormone (TSH) as the product of the hypothalamus-pituitary gland-axis (Bentley, 1998). THs consist of a hydrophobic nucleus, a hydrophilic hydroxyl group attached to the phenolic ring and four iodine in position 3, 5, 3´, and 5´ in thyroxin (T_4) and three at position 3, 5, 3´ in triiodo-L-thyronine (T_3) (Figure 1). THs are degraded by the enzyme idothyronine-deiodinase. The main secreted product of the thyroid gland is the T_4, but by deiodination in the tissue T_4 is transformed to T_3. T_3 has a higher affinity for thyroid hormone receptors (TR) than T_4, and is the main active form (Darras et al., 1998).

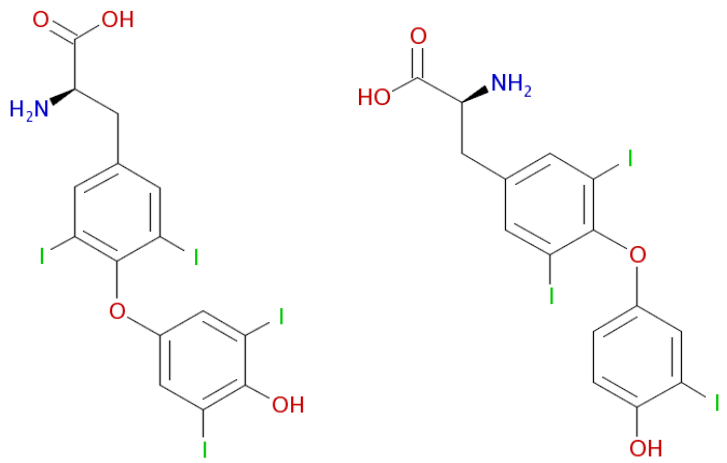

Figure 1. Chemical structure of T_4 (left) and T_3 (right) (https://www.ebi.ac.uk/chembl/, id: ChEMBL599 and ChEMBL1544).

THs are highly soluble in lipids, and this leads to a strong tendency of accumulation in cell membranes. This allows for easy transfer of information via hydrophilic signal compounds like THs. Therefore it is impossible to have an even distribution of THs without extracellular transport by serum proteins that make up an extracellular pool of THs (Schreiber, 2002). Binding of THs to serum proteins also gives a longer half-life and buffers the free hormone concentration against depletion by active tissue uptake and metabolism. It is equilibrium

between the free unbound TH and the TH bound to serum transport proteins. The main part of TH is bound, and there is only the small fraction of free TH in the serum that is available to cells. In human only 0,02 % of the total amount of T_4 is free (Schussler, 2000).

The serum protein thyroxin-binding globulin (TBG), transthyretin (TTR) and albumin (ALB) are the major transport proteins of TH in all vertebrates (Ucan-Marin et al., 2009). All the transport proteins are synthesized in the liver, but only TTR is synthesized in the brain by the choroid plexus (Dickson et al., 1987). The physiological function of TTR is thus to transport TH in the blood and cerebrospinal fluid, in addition to transport retinol by forming a complex with retinol-binding protein (RBP) (Monaco et al., 1994, Wojtczak et al., 1996).

Unlike in humans and other mammals TTR is the major TH transport protein in the bloodstream of birds, herbivorous marsupials and small eutherians (Richardson et al., 1994). In mammals TTR have higher affinity for T_4 then T_3, but non-mammalian vertebrates such as birds, teleost fish and amphibians bind T_3 stronger than T_4. During evolution selection has increased the affinity for T_4 through mutations of the TTR subunits in the N-terminus making it shorter and increasing the hydrophilicity (Chang et al., 1999). The N-terminus is the start of the polypeptide chain and is marked of in Figure 2. Alignments from previous studies showed that TTR is highly conserved among vertebrate species, but the N-terminal region present a low sequence homology (Ucan-Marin et al., 2009). Prapunpoj et al. (2006) demonstrated this relationship between N-terminal region and the affinity for THs by removing the N-terminus of the saltwater crocodile (*Crocodylus porosus*) TTR subunit replacing it with the N-terminus of human TTR resulting in a TTR with increased affinity of T_4.

The three dimensional (3D) crystal structure of TTR shows that it is a homotetramer. Each subunit is a 127 amino acids long polypeptide consisting of one short α-helix and an extensive β-structure of eight strands labelled a-h that together make up the two β-sheets dagh and cbef (Figure 2). Antiparallel hydrogen bonding interactions extend between the two dagh β-sheet from different monomers so that they form an eight-stranded sheet in the dimer. The dimers associate through hydrophilic and hydrophobic interactions forming a dimer-dimer-interface with a two-folded symmetry axis of all four subunits so that they together form a central channel of four β-sheets as shown in Figure 2. Within the central channel two buried funnel-shaped binding sites for TH are present (Blake et al., 1978).

Ucan-Marin et al. (2009) found the nucleotide sequence of glaucous gull TTR that translated into a 126 amino acid residues protein with a calculated molecular mass of 13.8 kDa (without his-tag labeling). The his-tag labelled gull TTR protein was observed as a protein monomer of 18 kDa and homodimer of 36 kDa. However there was a truncation of approximately 26 amino acids in the N-terminal end of the gull TTR and the recombinant TTR contains six histidine-tag residues (Ucan-Marin et al., 2009).

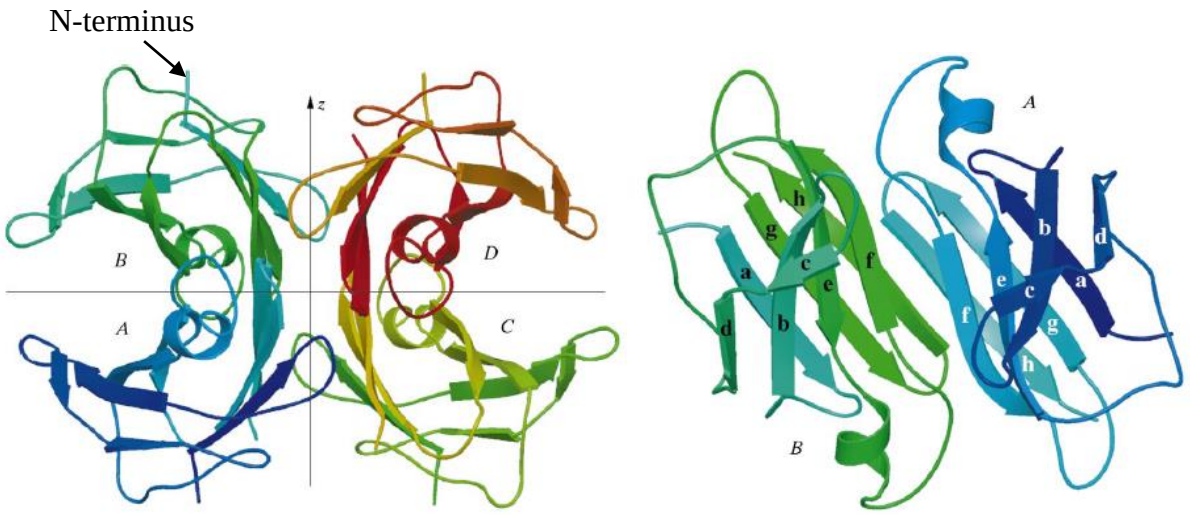

Figure 2. Ribbon diagram of TTR showing the the homotetramer ABCD with color ramping from blue to red. The central TH binding channel is along the z-axsis. Monomer A and B is connected along the side to form the dimer AB, each monomer consist of eight β-strands labelled a-h. The N-terminal region of subunit B indicating the start of the polypetid chain. (Ghosh et al., 2000).

The binding mechanism of T_4 to human TTR have been investigated by Blake et al. (1978) by solving the crystal structure of the human TTR-T_4 complex (PDB id 2PAB). The TH binding sites are very similar to each other, and are located between two dimer units so that one half of the binding site is identical to the other half along the twofold symmetry axis going through the central hormone binding channel. Based on *in vitro* studies T_4 binds to TTR with negative cooperativity so that only one molecule binds to the tetramer (Ferguson et al., 1975). However, in the crystal structures both hormone-binding pockets are occupied in a roughly similar fashion. Each pocket has a two-folded-symmetry, and T_4 binds in two mode (forward and reverse) with ~50 % occupancy. T_4 lock into the pocket by making favorable non-bonding interactions with the TTR subunits (Blake et al., 1978, Palaninathan, 2012).

The binding site of human TTR consist of a narrow inner pocket near Ser117/Ser117', a wider outer pocket near Glu54/Glu54', while a highly hydrophobic region is located between these two pockets. There are three pairs of symmetric halogen binding pockets (HBPs) with affinity for the iodine atoms of T_4 in the binding pocket. The side chains of Ala108, Leu110, Ser117 and Thr119 of both subunits form the inner binding pockets HBP3 and HBP3'. The hydroxyl groups of Ser117/Ser117' also mediate hydrogen-bonding interactions and further stability to the complex. The wider outer binding pocket that contains HBP1 and HBP1' are formed by the residues Met13, Lys15, Leu17, Thr106, Ala108 and Val121 of both subunits. Lys15 residue contains a positively charged amino group that may form direct or water-mediated electrostatic interactions with T_4. Moreover, the sidechains of Leu17, Thr106, Ala108, Thr119 and Val121 forms an accommodation region which holds the C-O-C linkage that connects the aromatic rings. In the middle of the outer and inner binding cavity HBP2 and HBP2' are positioned, comprising residues Leu17, Ala108, Ala109 and Leu110 of both subunits (Palaninathan, 2012, Banerjee et al., 2013, Cao et al., 2010).

In both the two binding conformations the iodine atoms are located in the HBPs. In the forward binding mode the inner pocket contain 3' and 5' iodine atoms of T_4 anchored to the HBP2/2' and HBP3/3' in two possible conformations and the 4' hydroxyl group forms water mediated hydrogen bonding interactions with the hydroxyl group of Ser117/Ser117' and Thr119/119' residues (through a conserved water molecule at the binding site near Ser117 and Thr119 residues). The α-amino and α-carboxylate group occupy the outer binding pocket and interact with the charged side chains of Lys15, Glu54 and His56 of both subunits. There are also hydrophobic interactions between the ligand and the hydrophobic inner of the central channel. Accordingly in the forward binding mode the carboxylate bearing aryl moiety is oriented towards the outer binding pocket. While in the reverse binding mode the carboxylate bearing aryl ring oriented towards the inner binding pocket. In both binding modes TH will have two possible symmetry-related binding confirmations because of the two-folded symmetry axis along the central binding channel, as shown in Figure 3 (Blake et al., 1978, Oatley et al., 1984, Palaninathan, 2012, Banerjee et al., 2013).

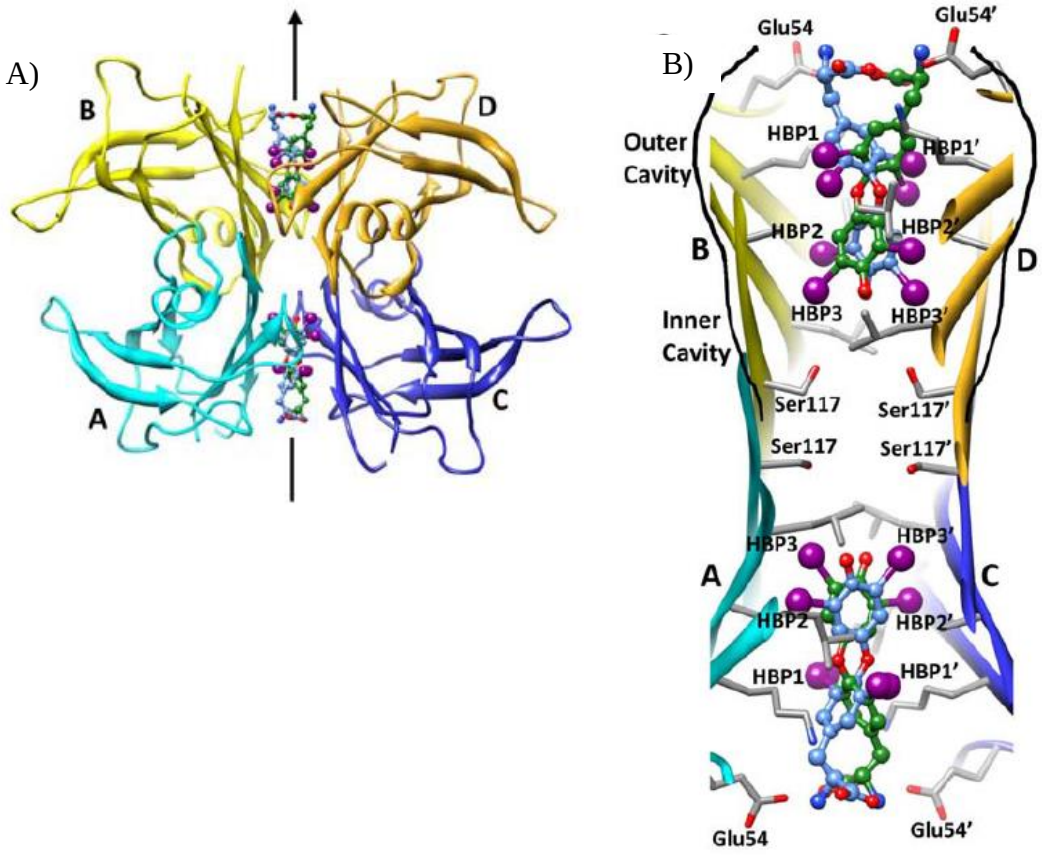

Figure 3. A) The tetrameric structure of TTR bound with T_4. B) Representation of the HBPs of T_4 binding site of TTR. Both the symmetry-related binding confirmations (blue and green) of T_4 are shown, and the carboxyl moiety of T_4 is positioned in the outer cavity at the entry of the binding site. Iodines occupy the HBP1/1´, HBP2/2´ and HBP3/3´ pockets (Palaninathan, 2012).

There are several structures in the Protein data bank (http://www.rcsb.org) of TTR in complex with T_4 and T_4-analougs from both human and other organisms. Comparative studies of these structures suggest that conformational changes and hydrogen bonding to Lys15/Lys15' in the

outer pocket and Ser117/Ser117' in the inner pocket are the controlling factors for both binding orientation and ligand affinity (Cody, 2002). Palaninathan (2012) reviewed the structural studies of TTR and based on the finding in the studies two observations were made, first the hormone molecules adopt two conformations even in absence of the two-folded-symmetry axis in the crystal structure (such as when the crystal structure only include one of the dimers). Second, the hormone show significant flexibility in their binding conformations and mode within the binding site. The capability of TTR to accommodate various different ligands in different binding modes means that many small molecules will bind. This promiscuity of the binding site however makes it more complex to predict which compounds that will bind. Small molecules that bind to the HBPs are mostly bi-aryl molecules with one or both aromatic rings equipped with halogenated, polar substituents or alkyl groups. Depending on the polarity and bulkiness of the substituents and their compatibility with the HBPs the ligand will bind in either forward or reverse binding mode (Palaninathan, 2012)

1.4 Endocrine disrupting chemicals

Endocrine disrupting chemicals (EDCs) interfere with the functions of the endocrine system, and have been associated with developmental, behavioral and reproductive abnormalities and alterations of endogenous hormone levels in laboratory and field studies (Burger et al., 2002, Dawson, 2000, Verreault et al., 2004). EDCs can alter the endocrine function through interference with the synthesis, secretion, transport, action and elimination of hormone or binding to for example membrane and nuclear receptors (Damstra et al., 2002). Beside these direct effects are indirect effects through the hypothalamus and anterior pituitary gland (Hadley, 1996). The interactions between EDCs and the endocrine system can be explained by the structural similarity of EDCs with endogenous hormones.

In recent years a variety of studies have reported interactions between OHCs and the TH system. Abnormal TH concentrations and thyroid gland structure have been linked to exposure to OHCs in reptiles, birds and mammals (Dawson, 2000, Leatherland, 2000, Rolland, 2000). Many studies have reported reduced levels of T_4 with increasing organochlorine (OC) levels with either minimal or no effect on levels of T_3. The ratio between T_4 and T_3 (T_4:T_3) seems to be a sensitive indicator of contaminants exposure (Peakall, 1992). A lower T_4:T_3 ratio is associated with increasing levels of OHCs in an organism and likely indicates alterations to the TH homeostasis through contaminant toxicity. Verreault et al. (2004) report an association between high blood levels of OHCs and alteration of TH levels in glaucous gulls breeding at Bjørnøya, and that it seems to affect males more than females.

Some laboratory and molecular modeling studies (Cao et al., 2010, Weiss et al., 2009) have reported that certain POPs can bind to the serum TH transport protein TTR and compete with TH for the binding pockets (Brouwer et al., 1998). This might affect the levels of T_4 and T_3 in the serum. OH-PBDE, $MeSO_2$-PCB, and PFCs are among the compounds reported to have high affinity for humane TTR (Weiss et al., 2009, Cao et al., 2010, Yang et al., 2011). In glaucous gull Ucan-Marin et al. (2009) found that OH-PBDE and to a smaller extent MeO-PBDE and OH-PCB are ligands and TH competitors in binding to TTR.

1.5 Molecular modeling

Molecular modeling is used to construct models that imitate the behavior of molecular systems by describing the inter- and intra-molecular forces in the 3D structure of the system. The description can be quantum mechanically (QM), molecular mechanically (MM) or a combination of both (QM/MM) (Höltje and Folkers, 2008, Gabrielsen, 2011). For big molecular system like proteins and protein complexes MM is a better representation than QM. The MM representation treats atoms as individual particles, and the molecular structure is a collection of masses interacting by harmonic forces. The atoms in the molecules are represented as balls connected with bonds (Gabrielsen, 2011). Interactions and energies resulting from bond-stretching, angel-bending, torsional energy and non-bonding interactions are calculated without considering the electrons (Höltje and Folkers, 2008).

The total energy of a molecule is calculated as deviation from the unstrained bond lengths, angels and torsions plus the non-bonded interactions. The collection of these unstrained values together with the force field constants, which are empirically derived fit parameters, make up the molecules force field. The force field is the total potential energy (E_{tot}) and can be written as:

$$E_{tot} = E_{bonded} + E_{non\text{-}bonded}$$
$$E_{tot} = (E_{bond} + E_{angle} + E_{dihedral}) + (E_{vdw} + E_{elec})$$

E_{bonded} is the bonding energy and can be divided into E_{bond}, E_{angle} and $E_{dihedral}$ which is the bond stretching, angle bending and torsional energy terms respectively. $E_{non\text{-}bonded}$ is the non-bonding energy and can be divided into E_{elec} and E_{vdw}, the electrostatic and van der Waals energy terms respectively (Höltje and Folkers, 2008).

1.6 Homology modeling

If the 3D structure of a protein is unknown, the homology modeling approach can be used to construct a theoretical model of the protein. The approach takes advantage of the fact that the 3D structure of proteins is a more conserved property during evolution than the amino acid sequence of proteins in the same family (Chothia and Lesk, 1986). Homology modelling consists of the steps: 1) template identification, 2) amino acids sequence alignment, 3) model construction and 4) refinement and evaluation of the model. The known 3D structure of a protein is the template and it is used to construct the model. When choosing a template it is important to consider the resolution of the crystal structure since low resolution introduces more uncertainty to the final model. The proteins must be homologous, meaning that they descent from a common ancestor. Templates can be identified by comparing the sequence of the target protein with sequence of structurally known protein in the protein data bank (PDB). After the template is identified, the amino acid sequences of the target and template are aligned. Alignment however can be difficult if the sequences vary a lot, and then an alignment of multiple homologous can help decrease the risk of incorrect alignment. (Gabrielsen, 2011, Ravna and Sylte, 2012).

The construction of homology models is carried out in three steps: 1) Generating the amino acids backbone of structurally conserved regions, 2) constructing the non-conserved regions called loops and 3) placing of the side chains. Following construction the model is refined to remove close contacts between amino acid residues that have been added during construction, and to relax high-energy structures. This can be done through energy minimization, Monte Carlo simulations and/or molecular dynamics methods. Energy minimization is based on iterations and calculating the energy so that the model refine to an energy minimum. Monte Carlo simulations are stochastic conformational moves followed by energy minimization. The calculated energy from each move is saved and compared, and the conformation with the lowest energy is chosen. Molecular dynamic methods intent to reproduce time-dependent structural movements in molecular systems. The atoms new positions and velocities are calculated as they move, and the new conformations are recorded in a trajectory. This is repeated in a certain amount of time steps and during refinements the conformation with the lowest energy is saved. (Höltje and Folkers, 2008).

The last step is to evaluate the model. There are different structural analysis and verification servers, which examine the quality of the 3D structure and report deviations. In addition, models can be evaluated using experimental data such as sit-directed mutagenesis data and accessibility data. Docking of known binders from experimental data and expected non-binders with structural similarity to the binders can also be used to evaluate the models (Ravna and Sylte, 2012).

1.7 Docking and Scoring

Docking is a method used to predict the binding orientation of ligands to macromolecular targets such as enzymes, receptors or transport protein. Scoring is an assessment of the docked ligand, evaluating the interaction between the ligand and target in terms of free energy to predict the binding affinity. The free energy of binding (ΔG) is given by the Gibbs-Helmholtz equation:

$$\Delta G = \Delta H - T\Delta S = - RT \ln K_i$$

Where ΔH is the enthalpy, T is the temperature (Kelvin), ΔS is the entropy, K_i is the binding constant and R is the gas constant (Höltje and Folkers, 2008). The method of docking and scoring allow us to predict the binding mode of known active ligands, predict the binding affinity of ligands that are similar to active ligands and find new ligands that can potentially bind to the target (Leach et al., 2006). Docking and scoring is commonly used in drug discovery, but also work well to predict affinity of chemicals that could potentially be toxic to a target.

The ideal situation would be for the target and the ligand to be fully flexible since this reflects best the real situation. However, such a docking is often computationally unfeasible due to the number of degrees of freedom. The most used docking programs are semi-flexible where the smaller ligand is flexible and the protein is rigid (Leach et al., 2006). Another approach is ensemble docking where flexibility is introduced to the target by binding the ligand to different conformations of the binding pocket. The various conformations can be obtained from experimental crystal structures and/or computationally generated (Nabuurs et al., 2007).

Induced-fit docking can also be used where flexibility is introduced to the receptor by refinement of the side chain in the pocket after docking the ligand to the binding pocket (Sherman et al., 2006).Structural flexibility is crucial to take into account since the crystal structure that is used as a template for the model is merely a snapshot of a highly flexible protein. The snapshot may not even be a realistic representation of the protein's native form (Ravna and Sylte, 2012). Structural rearrangement a protein undergoes upon ligand binding may undergo movements ranging from local side chain movements to large domain movements, therefore docking of a ligand to a structure that is not the native structure (cross-docking) can be difficult and have lower success then by docking a ligand into its native crystal structure (self-docking) (Höltje and Folkers, 2008, Gabrielsen, 2011).

The scoring function can rank the different conformations and orientations of the ligands according to the tightness in the binding pocket. Ideally the scoring function will give the experimentally determined binding mode highest rank. There are four forms of scoring functions, force field-based, empirical, consensus and knowledge-based scoring functions. The force filed-based scoring functions are based on the non-bonding interaction energy terms of molecular mechanics. Empirical scoring functions is based on weighted energy terms described in known drug binding properties such as hydrogen bonding, ionic, lipophilic and aromatic interactions and loss of entropy. Knowledge-based scoring functions in comparison use energy potentials derived from experimental detected structural information, while the consensus scoring functions combine the empirical, force field-based and knowledge-based functions. The different functions have different accuracy and speed and in general are the more accurate more time-consuming (Huang et al., 2010).

2. AIM

Several studies have shown that POPs found in the Arctic can bind to proteins in the serum such has the thyroid hormone transport protein transthyretin, which may initiate adverse outcomes (Brouwer et al., 1998). Therefore knowledge about the relationship between molecular structure, exposure, concentration and how the contaminants interact with biological systems is important for the risk assessment of POPs. By binding to hormone transport protein such as transthyretin contaminants can possibly disrupt the hormone homeostasis in wild life. To verify experimentally if a compound binds to a particular transport protein can be time-consuming and costly. The need for cost-efficiency and rapid high-throughput screening of a high number of chemicals have therefore led to development of computational approach that uses various prediction models. Binding affinities for different compounds can be predicted by using high quality 3D models of proteins and indicate if the compounds potentially can affect hormone homeostasis. This approach can lower the costs and time of experimental testing since fewer compounds need to be tested.

The aim of this study was to use molecular modeling to construct a homology model of the TTR in glaucous gull and to dock several well-known and new emerging POPs in the models to predict the binding affinity of POPs to the TH binding site in glaucous gull TTR. The predictability of the models were tested by docking a contaminant dataset consisting of known binders and decoys. Afterwards the models were used to predict putative binding, binding modes and affinities towards transthyretin by docking a set of contaminants. In addition, the models were used to reveal information concerning molecular interactions and residues critical for interactions between the contaminants and glaucous gull TTR.

3. METHODS

3.1 Homology modeling

Homology modeling as well as docking was performed using the internal coordinate mechanics (ICM) software version 3.7 (http://www.molsoft.com).

The amino acid sequence of TTR in glaucous gull is available through the work of Ucan-Marin et al. (2009) and is uploaded to UniProt Knowledgebase (UniProtKB, http://www.uniprot.org/) under the id B0FWC5. However only parts of the sequence represented in the article is in UniProtKB, therefore a hybrid sequence was constructed from the amino acid sequence of glaucous gull and chicken (*Gallus gallus*) UniProtKB id P27731, where all the amino acid that differed from the sequence in the article was changed manually.

Templates were chosen based on the following criteria: 1) The crystal structure should have as high as possible resolution since that will make the model more accurate. 2) It is advantageous that the template have a ligand already bound in the crystal structure so that the binding pocket could be defined around the ligand. 3) The template should have high homology to the TTR sequence of glaucous gull. 4) The template structure should be a tetramer and not a dimer since that is the natural form.

The templates used in homology modeling were downloaded from the PBD. Two of the templates are crystal structures of tetramers from rat (*Rattus norvegicus*) with PBD id 1KGJ (Muziol et al., 2001b) and 1KGI (Muziol et al., 2001a). The third template has PDB id 1SN0 and is a tetramer structure from sea bream (*Sparus aurata*) (Eneqvist et al., 2004) and the last template, PDB id 4HJU, is a humane dimer (Suh et al., 2013). The templates were used to construct model 1, 2, 3 and 4 respectively. Additional information about the templates, as resolution and bound ligand are listed in Table 1 and Figure 4.

Table 1. Information about the crystal structures used as templates for homology modeling of TTR in glaucous gull.

PDB id	Species	Structure	Resolution (Å)	Ligand	Model
1KGI	Rat (*Rattus norvegicus*)	Tetramer	2,30	3,3’,5,5’-Tetraiodothyroacetic acid	1
1KGJ	Rat (*Rattus norvegicus*)	Tetramer	1,80	6,4’-Dihydroxy-3-methyl-3’,5’-dibromoflavone	2
1SN0	Sea bream (*Sparus aurata*)	Tetramer	1,90	T_4	3
4HJU	Human	Dimer	1,35	N-(3-((E)-2-(4-hydroxy-3,5-dimethylphenyl)ethenyl)phenyl)prop-2-enamide	4

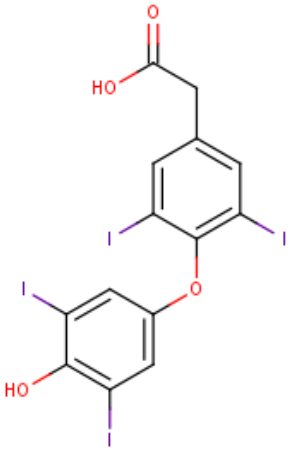

3,3’,5,5’-Tetraiodothyroacetic acid

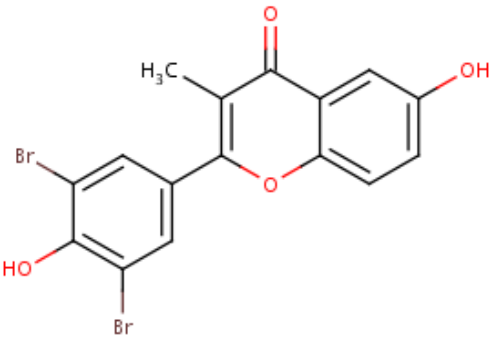

6,4’-Dihydroxy-3-methyl-3’,5’-dibromoflavone

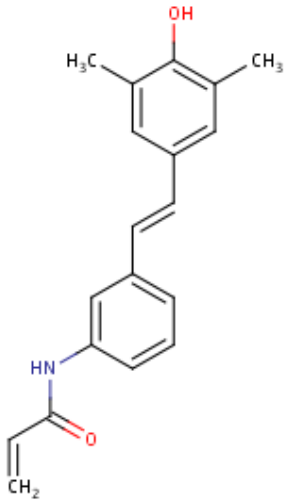

N-(3-((E)-2-(4-hydroxy-3,5-dimethylphenyl) ethenyl)phenyl)prop-2-enamide

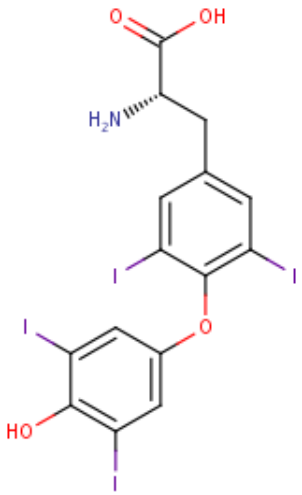

T_4

Figure 4. Ligands within the binding site of the template crystal structures 1KGI, 1KGJ, 4HJU and 1SN0 respectively.

TTR is highly conserved between taxa, and around 60-80 % of the sequences are identical between the different templates and the glaucous gull sequence. The alignments of the different sub units in the template with the sequence for glaucous gull were performed using the alignment function in ICM and ClustalW2 multiple Sequence Alignment (http://www.ebi.ac.uk/Tools/msa/clustalw2/)

To generate the homology models, ICM used a rigid body homology modeling method. The backbone conformation of the core regions from the template was transferred to the target when constructing the model. The non-conserved loop-regions were constructed by searching a loop PDB database for matching loop regions in regard to sequence similarity and steric interactions with the surroundings of the model, predicting the loop through local energy optimization. The side-chains of identical amino acid are transferred directly from the template while amino acids that are not conserved are either modeled (conservative change) or added to the target without

reference to the template (non-conservative change) using the most probable rotamer of the side chains (Gabrielsen, 2011).

The ICM refine Model macro was used to energy optimize the constructed homology models. The macro samples the conformational space of the side chain using the ICM Monte Carlo module. Then the macro performs iterative annealing of the backbone, before a second Monte Carlo simulation of the side chains. The iterations consist of random movements followed by local energy minimization. The random movements and energy minimization created an energy gradient, and side chains with energy over the gradient were selected for energy minimization. The total energy is calculated and based on the energy and temperature the iterations were accepted or rejected. The different possible conformations were combined to find the most likely conformation of the target (Abagyan et al., 1994, Gabrielsen, 2011).

3.2 Evaluation of the homology models

To evaluate the model a test set of known active binders (ligands) and predicted non-binders (decoys) was constructed. The ligands was selected by going through the PDB database collecting different ligands from the crystal structures of TTR and then clustering them using the Unweighted Pair Group Method with Arithmetic Mean (UPGMA) in ICM. The UPGMA method is a hierarchical clustering method that constructs a tree based on pairwais similarities so that the diversity of the structures is shown. Twenty compounds that were clustered with a distance range set to 0.2 were selected. Clustering was performed to avoid bias in the model evaluation to certain structures. The ligands and TTR crystal structure were from other species then glaucous gull and therefore it is possible that they will not bind in TTR of glaucous gull. The TTR structure however is highly conserved through evolution, so the ligands from human TTR crystal structures would most likely be binders to glaucous gull TTR and could therefore be used in the test set.

To construct decoys a list of the SMILES (simplified molecular-input line-entry system) codes of the ligands was sent to the database DUD.E (A Database of Useful Decoys: Enhanced, http://dude.docking.org/). For each ligand, the DUD.E returned 50 decoys, if available, that were property-matched and drawn from the database ZINC (http://zinc.docking.org/). The decoy search included only the most dissimilar decoys, by topology, from the ligands. Decoys were property-matched to the known ligands using the physicochemical properties molecular weight, estimated water-octanol partion coefficient (miLogP), rotatable bonds, hydrogen bond acceptors, hydrogen bond donors and net charge. Molecular properties were computed using Molinspiration's mib. Ligands protonation states was generated in the pH range 6-8, using Schrödinger's Epik, so that ligands that had different charges within this range get 50 decoys for each charge. Finally, in the decoy construction ECFP4 fingerprints was generated by Scitegic's Pipeline pilot for ligands and potential decoys. Decoys were sorted by their maximum Tanimoto coefficient (Tc) to any ligand and the most dissimilar 25 % were retained through the dissimilarity filter. Duplicate decoys were removed from the ligands data set (Mysinger et al., 2012).

The returned decoys and the ligands were clustered using the UMPGA in ICM. Decoys that were clustered with a distance range of 0.6 from each other and the ligands were selected so that there was a list of 102 compounds, 20 known ligands and 82 decoys that was the test set in the docking. The chemical database of European Molecular Biology Laboratory (ChEMBL, https://www.ebi.ac.uk/chembl/) was searched to find experimental half maximal inhibitory concentration (IC50) values for the ligands if available.

The homology models were evaluated on the ability to separate the ligand from the decoys in the test set, the selectivity of the TTR, by making Receiver Characteristics Operator (ROC) curves. Ligands were labeled 1 and decoys 0 and the scoring values from the docking of the test set were used to plot the number of ligands predicted as binders (true positive) against decoys predicted to bind (false positives). The true positive rate was the sensitivity of the models, while the false negative was the fall-out calculated as 1-specificty. The result was displayed as ROC-curves and the area under curve (AUC) was calculated. A diagonal signify that the model gives no preference to ligands over decoys or vice versa. Curves that are closer to the left and top border indicate a greater accuracy (Lindin et al., 2013).

3.3 Contaminant dataset

A dataset of 668 contaminants containing putative endocrine disrupters (EDs) were examined. The original dataset was obtained from Dr Lisa Bjørnsdatter Helgason and was based on the work of Howard and Muir (2010) on identifying novel organic chemicals that could be persistent and bioaccumulative in commerce that might not be included in contaminant measurement programs. Novel POPs described through the work of Vorkamp and Riget (2013), Vorkamp and Riget (2014), and Sagerup et al. (2010) that are potential contaminats in the artic wildlife were also investigated. Contaminants that have similar chemical structure to known TTR binders from other studies both experimental and molecular modeling, or found in abiotic and biotic samples in the Arctic, in particular in seabirds were especially considered. The list focus on novel POPs not under regulation, but also include known human TTR binders to see if they will bind similar in glaucous gull as in human. Among the POPs are some previously measured in blood samples from glaucous gull such as PCBs, PBDEs, PFOA and PFOS, and their toxic effects are well studied while other are unknown. The chemicals listed include well known groups as PCBs, PBDEs and their metabolites, other novel brominated and chlorinated flame retardants, PFCs, phosphorous flame retardants (PFRs), phthalates, siloxanes, polychlorinated naphthalenes, pesticides, musk xylene, nitro-PAH and other chemicals. To limit the data to analyze the focus was directed towards potential POPs that according to the literature can be found in the Arctic and be a potential threat to the glaucous gull.

3.4 Semi-flexible docking and scoring

The ICM receptor set up function was used to define the binding sites that were used for docking and scoring. The ICM PocketFinder was used to evaluated the binding sites position in protein, size of the pockets, volume and hydrophobicity. Before the docking the formal charge of the compounds was set to a pK_a corresponding to pH 7.4 which is the pH of the blood. For certain interesting groups of compounds such as the THs PBDE metabolites and PCB metabolites, with a pK_a between 6-8, the compounds were docked with both protonated and non-protonated

functional groups. The THs, contaminants dataset and test set of ligands and decoy were docked into all the four homology models using the semi-flexible method where the ligand structure was flexible while the protein structure was rigid. During docking the model was represented as a set of rigid pre-calculated grid potential maps of interacting terms as hydrogen bonds, Van de Waals, hydrophobic and electrostatic forces.

A Monte Carlo global optimization procedure predicts the binding pose of the compounds in the ICM software generating a diverse set of conformations of the compounds *in vacuo* by sampling the torsional and rotational degrees of freedom (Abagyan et al., 1994). The ligand was placed into the binding pocket and the global optimization performs iterations that randomly move the ligand torsional and positional followed by an energy minimization. The torsional moves are at an arbitrary angel and the positional mover are pseudo-Brownian random or rotations of the hold structure. Based on the energy of the different conformation they were either rejected or accepted, keeping the low energy conformation in a stack ranked after the docking energy (Bursulaya et al., 2003).

The ICM virtual ligand screening (VLS) scoring function gave a score to evaluate and compare the binding energy of the compounds in the contaminants data set and test set of ligands and decoys. The scoring function was empirical using entropy, steric, hydrophobic and electrostatic terms to calculate the score (Huang et al., 2010). The score corrected for the number of atoms to avoid biases towards larger compounds (Schapira et al., 2003).

The docking projects of both the test set and the contaminants dataset were performed in three parallels of ICM batch docking. Batch docking means that all the alternative conformations from the three runs were scored and saved. From these results a hit list can be constructed with the top ranked conformations of each of the compounds. By comparing the score of the ligands and decoys in the test set, for the different homology models threshold scoring values were set to distinguish binders and non-binders, which then were used for the docking of the contaminants. The compounds getting a higher score then the threshold were predicted to bind to TTR while the compounds with a score under the threshold were predicted to not bind to TTR.

4. RESULTS

4.1 Homology modeling

More than 200 x-ray crystal structures of TTR are available in the PDB database. The structures are mainly of the human TTR but there are also structures from rat, mice, sea bream and chicken. However almost all of the crystal structures have been crystalized as dimers separated at the dimer-dimer interface so that the structures do not have a central channel. Therefor only half of the functional protein and half of the binding pocket are present.

When choosing crystal structures as templates for homology modeling it was stressed that the resolution should be high, that a ligand was present to define the binding pocket and that crystal structure was a tetramer as the functional protein in serum. However, since the main part of available structures were dimers, also dimers were considered as possible templates. The crystal structures that were finally chosen as templates were two tetramer structures from rat (PDB id 1KGI and 1KGJ), a tetramer from sea bream (PDB id 1SN0) and one dimer structure from human (PDB id 4HJU). These x-ray structures were used to construct model 1, 2, 3 and 4 respectively.

The amino acid sequence of glaucous gull TTR was described by Ucán-Marín et al., however only parts of the sequence is uploaded to UniProtKB (code B0FWC5) therefore a hybrid amino acid sequence of glaucous gull and chicken (code P27731) was constructed. From the alignment of the amino acid sequences from template 1KGI, 1KGJ, 1SN0 and 4HJU with the amino acid sequence of glaucous gull TTR the identity was 81 %, 80 %, 65 % and 78 % respectively (Figure 5). The amino acid sequences for rat, sea bream and human TTR have UniProtKB code P02767, Q9PTT3 and P02766 respectively. All of the uploaded sequences to UniProtKB includes a signal peptide at the beginning that was in included in the alignment in Figure 5. However since the signal peptide was not a part of the protein TTR and therefore not a part of the constructed models the numbering in Figure 5 start at the beginning of the human TTR sequence. This numbering was used to easier compare the binding site in the different models with the description of the human TTR binding site in the literature. In the alignment the symbol asterisk (*) indicates positions which have a single fully conserved residue. Colon (:) indicates conservation between groups of strongly similar properties. Period (.) indicates conservation between groups of weakly similar properties. The alignment in Figure 5 was constructed using ClustaIW2. All the TTR crystal structures reported have a disordered N-terminal (residues 1-9) and C-terminal (residues 125-127) which are not visible in electron density maps (Palaninathan, 2012). Therefore, the constructed models from the crystal structure miss amino acids from the N-terminal and C-terminal.

Figure 5. Alignment of the hybrid chicken-glaucous gull TTR sequence with the TTR sequences of the crystal structure templates used in construction of the homology models. The sequences include a signal peptide in the beginning and therefore the numbering start at the beginning of the actual TTR polypeptide. The numbering for the human TTR sequence was used to easier compare the binding site in the different models with the description of the human TTR binding site in the literature.

The alignment between the different template subunits and amino acid sequence of glaucous gull was used to construct the homology models After construction, the homology models were refined. Figure 6 shows two of the constructed models after refinement. Homology model 1 had subunits of 121, 121, 121 and 122 amino acids. The homology model 2 had subunits of 121, 122, 122 and 124 amino acids. The homology model 3 had subunits of 115, 117, 117 and 119 amino acids. In the homology model 4 both subunits had 116 amino acids. The variation in number of amino acid is in the N-terminal, and the variation between subunits in one model and between models is because of differences in number of amino acid in the template structure used to construct the model. In many of the crystal structures there are truncations in the N-terminal. The N-terminal is however not a part of the central channel and the binding pocket.

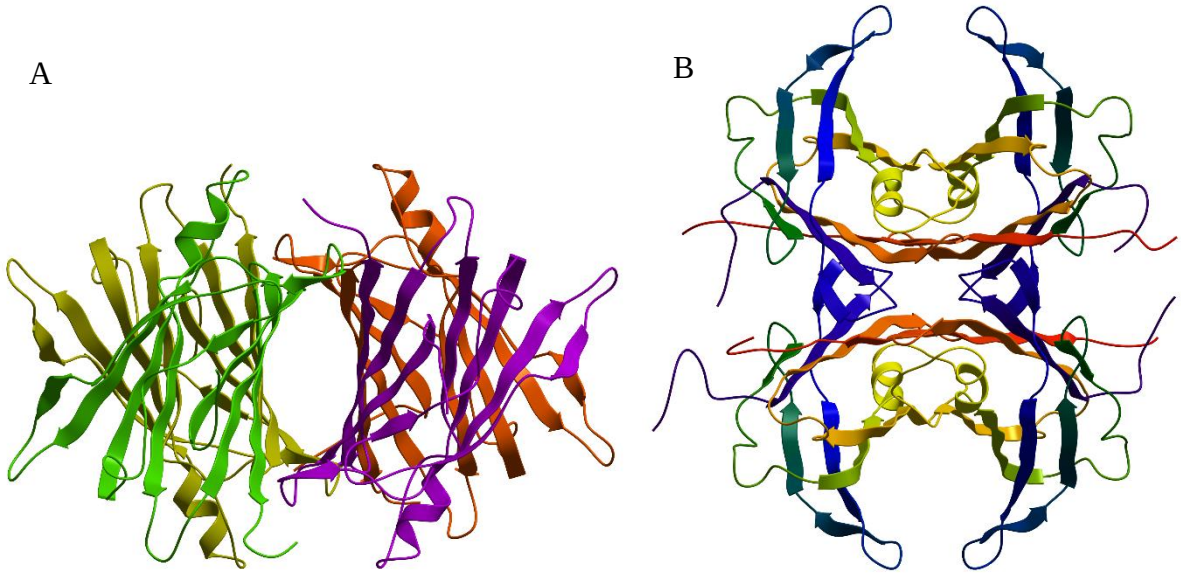

Figure 6. Two of the constructed homology models of glaucous gull TTR. A) Homology model 1, were each color represent the different subunits in TTR. B) Homology model 2, each subunit change color from the N-terminal to the C-terminal, from blue to red.

All the four templates had a ligand in the binding site of the crystal structure (Figure 4). After the construction of the homology models these ligands were used in ICM receptor set up function to define the binding sites that were used in docking and scoring of the test set and contaminants dataset. The receptor set up function include all amino acids that were in a 3.0 Å sphere radius around the ligand from the template crystal structure. The amino acids in the defined binding pockets of the models are listed in Table 2. The ligands in the template crystal structure will affect the constructed homology models since the TTR binding site will have a slightly different conformation with the different ligands at the binding site, and therefore contribute to the differences in the binding site of the models. Amino acids in the defined binding sites were compared to the amino acids reported to form the binding site in studies of human TTR. The major differences in Table 2 are highlighted in red.

In the models amino acids Glu54 and His56 were not a part of the binding site (except of Glu54 in model 1) even though they were described in studies to make up the outer part of the binding site of the human TTR. The amino acids Met13 and Ser117 that were a part of the binding site of human TTR were not a part of the binding site of all the models. Amino acids Val16 and Thr118 which were not included in the binding pocket described for the human TTR were included in the pocket of some of the models (Table 2). The numbering of the amino acids was from the human TTR subunits amino acid sequence. The original numbering of the models were different since the subunit chains have different length. However based on the alignment (Figure 5) the amino acids were given the same numbers so that it is easier to compare. These amino acids in the binding site were conserved between the different templates and the glaucous gull sequence.

Table 2. Three letter abbreviation and number of the amino acids in the defined binding pockets (3.0 Å sphere radius around the template ligand) of the four constructed homology models, and the amino acids reported in studies of human TTR binding site. The numbering of each amino acid is from the numbering of chain of 127 amino acids of the human TTR subunits and based on the alignment performed during the construction of the models.

Amino acid in the define binding sites of the homology models of TTR and described in studies of human TTR				
Model 1	**Model 2**	**Model 3**	**Model 4**	**Human**
Met13	-	-	Met13	Met13
Lys15	Lys15	Lys15	Lys15	Lys15
Val16	-	Val16	-	-
Leu17	Leu17	Leu17	Leu17	Leu17
Glu54	-	-	-	Glu54
-	-	-	-	His56
Thr106	Thr106	Thr106	Thr106	Thr106
Ala108	Ala108	Ala108	Ala108	Ala108
Ala109	Ala109	Ala109	Ala109	Ala109
Leu110	Leu110	Leu110	Leu110	Leu110
Ser117	Ser117	-	Ser117	Ser117
Thr118	Thr118	-	Thr118	-
Thr119	Thr119	Thr119	Thr119	Thr119
Val121	Val121	Val121	Val121	Val121

The ICM Pocket Finder method was used to predict the position and size of possible binding pocket, and calculated volume, area, hydrophobicity, buridness and how compact the binding sites were. After removing the template ligand, the icmPocketFinder detected two binding pockets in the models positioned at the same place as the ligands in the templates in each end of the central channel. The volume and hydrophobicity of the binding pockets in the different models are listed in Table 3. The volume are in Å and the hydrophobicity represents the percentage of the pocket surface in contact with hydrophobic protein residues (values can range from 0-1).

Table 3. Volume and hydrophobicity of the binding site in the homology models, calculated using the icmPocketFinder.

Model		**Volume (Å)**	**Hydrophobicity (0-1)**
1	Pocket 1	216,5	0,6596
	Pocket 2	180,5	0,6556
2	Pocket 1	129,9	0,6303
	Pocket 2	134,8	0,6867
3	Pocket 1	187,5	0,5068
	Pocket 2	147,6	0,5393

4.2 Evaluation of the homology models

To evaluate the constructed homology models a test set of known TTR binders and expected non-binders was constructed. The known ligands were from crystal structures of TTR in the PDB database. Few of the ligands had their binding affinity reported in the ChEMBEL database. There were large varieties of ligands in the different crystal structures and to select 20 representatives and avoid bias by selecting similar structures to the test set the UMPGA cluster method was used. The selected ligands had a distance range of 0.2. The ligands were used for obtaining decoys from the DUD.E database that returned 50 decoy compounds for each ligand that have physiochemical properties that were dissimilar to the ligands and therefor expected not to bind to the TTR. The decoys were also clustered, and the decoys with a distance range of 0.6 to the ligands and to each other were selected to avoid bias of having only similar structures included in the test set.

The test set were docked into the homology models and scored. In Table 4, the scoring values of the different ligands in the four homology models are listed. The negative values equal high scores and indicated strong binding to the model. The score however was not a quantitative measure of the binding of the ligand to proteins, and the score will vary depending on the structure of the protein model. It was therefore necessary to estimate a threshold by docking already experimentally confirmed binders into the model and set the threshold based on their score. In models 1, 2, 3 and 4 the mean scoring values of the ligands were: -23.93, -22.30 -19.56 and -15.66, respectively. This showed that the compounds bound weaker to the model that was a dimer. The scoring values of the models were not particularly high compared to results from models of nuclear and membrane bound receptors like thyroid hormone receptor isoform α (TRα) and β (TRβ) (Mæhre, 2012). However, this probably just reflected that THs have lower affinity for TTR compared to the TH receptors. T_4 have a IC50 of 7170 nM to TTR and T_3 have a EC50 of 1.3 nM to TRα in human (Collazo et al., 2006, Gupta et al., 2007).

The scoring values of the twenty selected known binders in the homology models (Table 4) were used to estimate a threshold scoring value for the compounds that could be used to predict if the compounds in the contaminant dataset could be regarded as TTR binders. Compounds with a much lower score than the other ligands in one model was excluded when setting the threshold since the low score indicates that they will not bind. From Table 4 it is clear that there is a large variation in the reported scoring values of the ligands and decoys, and therefore it was estimated that the threshold should be equal to the lowest scores in the different models. In model 1 compounds with a scoring value better than -18 was regarded as possible binders. The corresponding values for models 2, 3, and 4 were -17, -16 and -14 respectively.

From the scoring value of ligands and decoys in the test set a ROC-curve was made for each of the models, Figure 7 to 10. The closer AUC of the graph is to 1 or 100 % the better the model is anticipated to separate between the binders and non-binders. A AUC-value of 50 means that the model cannot separate between the two. For the homology models 1, 2, 3, and 4 is the AUC 96, 95, 88 and 87 respectively. The results from the docking ofthe test set tell that model 1 and 2 are better at separating between binder and non-binders then model 3 and 4.

Table 4. Scoring values and IC50 values, if available, for the ligands selected as active TTR binders in the test set. The scoring values were used to evaluate if the models can separate between compounds that bind or not. The ligands were selected from different crystal structures of human TTR. Hgh scores (negative values) indicate that the compounds were predicted to have a high binding affinity to TTR.

PDB id TTR	**Ligand from the crystal structure**	**Scoring value in the models**				**IC50 (nM)**
		1	**2**	**3**	**4**	
3CN1	2,6-dibromo-4-[(E)-2-phenylethenyl]phenol	-28.23	-25.01	-23.66	-17.05	
4ABQ	3-(5-sulfanyl-1,3,4-oxadiazol-2-yl)phenol	-27.83	-28.48	-9.99	-11.17	
4L1T	(E)-3-(dimethylamino)-5-(4-hydroxy-3,5-dimethylstyryl)benzoic acid	-27.82	-29.14	-21.70	-15.64	
4HJU	N-(3-[(E)-2-(4-hydroxy-3,5-dimethylphenyl)ethenyl]phenyl)prop-2-enamide	-27.23	-29.04	-25.51	-17.77	
4HIS	2-(3,5-dichlorophenyl)-1,3-benzoxazole-6-carboxylic acid	-26.02	-20.53	-20.28	-14.62	
4HJS	N-(4-[(E)-2-(4-hydroxy-3,5-dimethylphenyl)ethenyl]phenyl)ethanesulfonamide	-25.98	-23.38	-20.31	-17.73	
4IK7	Indomethacin	-25.35	-13.55	-17.88	-15.81	
3CN3	2,6-dibromo-4-phenoxyphenol	-24.63	-20.28	-19.54	-14.99	
3CN0	3,5-Dimethyl-4-hydroxystilbene	-24.57	-24.19	-22.57	-16.28	3800
4I89	Diflunisal	-24.03	-17.62	-20.45	-16.90	
1DVT	Flurbiprofen	-23.45	-21.75	-18.30	-16.42	
4AC4	3-methoxy-4-phenoxy-benzoic acid	-23.38	-18.79	-16.78	-14.15	41000
1SN5	T_3	-22.89	-19.98	-19.89	-14.82	
3CN2	3,5-Dibromo-4-hydroxybiphenyl	-22.61	-21.56	-18.97	-12.78	
4DEW	Luteolin	-22.33	-32.49	-17.04	-16.94	
4N86	Glabridin	-22.11	-16.88	-20.68	-14.80	
4IK6	Lumiracoxib	-21.41	-17.58	-18.93	-16.46	
4ACT	3-hydroxy-4-phenoxybenzaldehyde	-20.30	-23.40	-19.83	-17.31	
4ABV	5-(chloromethyl)-2-(2,4-dichlorophenoxy)phenol	-19.61	-18.00	-20.88	-16.15	850
3OZL	Flufenamic acid	-18.90	-24.44	-18.08	-15.45	2900
Mean scoring values		-23.93	-22.30	-19.56	-15.66	

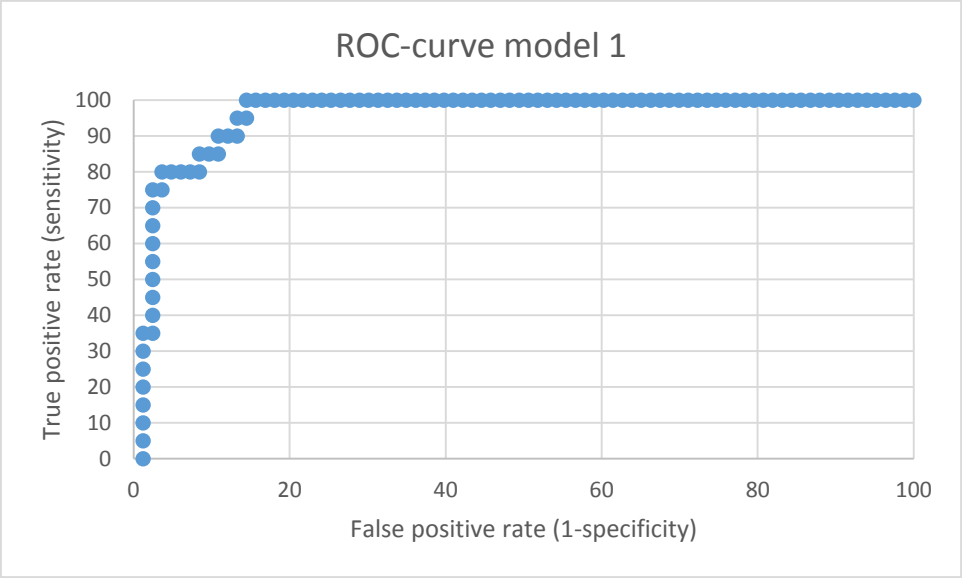

Figure 7. ROC-curve of the scoring values of ligands and decoys in the test set for model 1. The AUC of the curve is 96. The curve shows how well the model separate the 20 docked TTR binding compounds from the 82 docked non-binding compounds. The closer the area underneath the curve is to 100 the more accurate is the model.

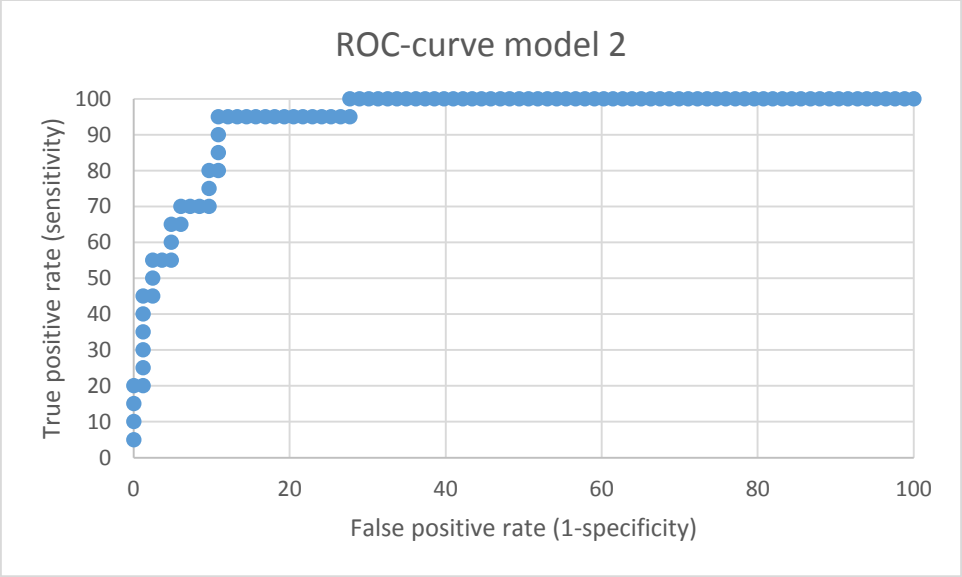

Figure 8. ROC-curve of the scoring values of ligands and decoys in the test set for model 2. The AUC of the curve is 95. The curve shows how well the model separate the 20 docked TTR binding compounds from the 82 docked non-binding compounds. The closer the area underneath the curve is to 100 the more accurate is the model.

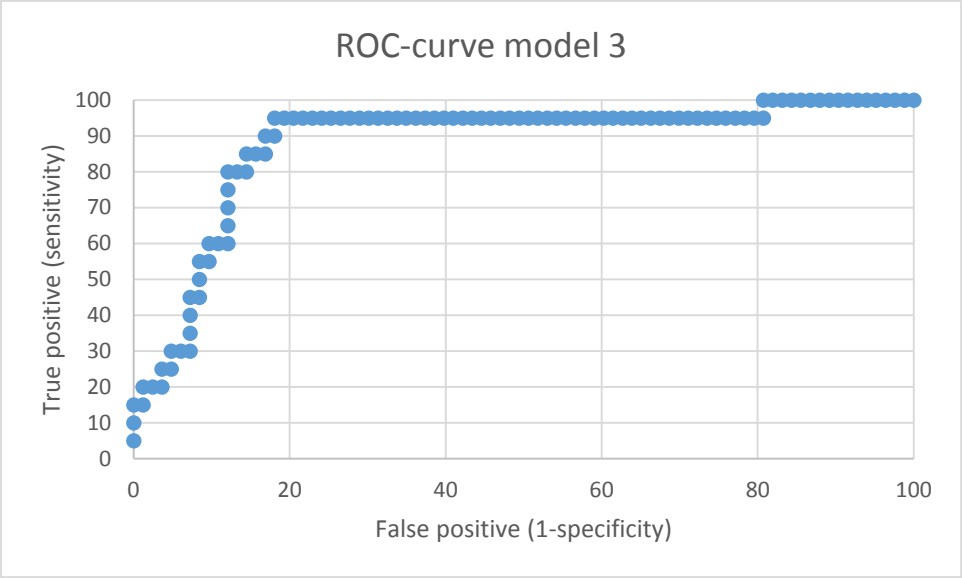

Figure 9. ROC-curve of the scoring values of ligands and decoys in the test set for model 3. The AUC of the curve is 88. The curve shows how well the model separate the 20 docked TTR binding compounds from the 82 docked non-binding compounds. The closer the area underneath the curve is to 100 the more accurate is the model.

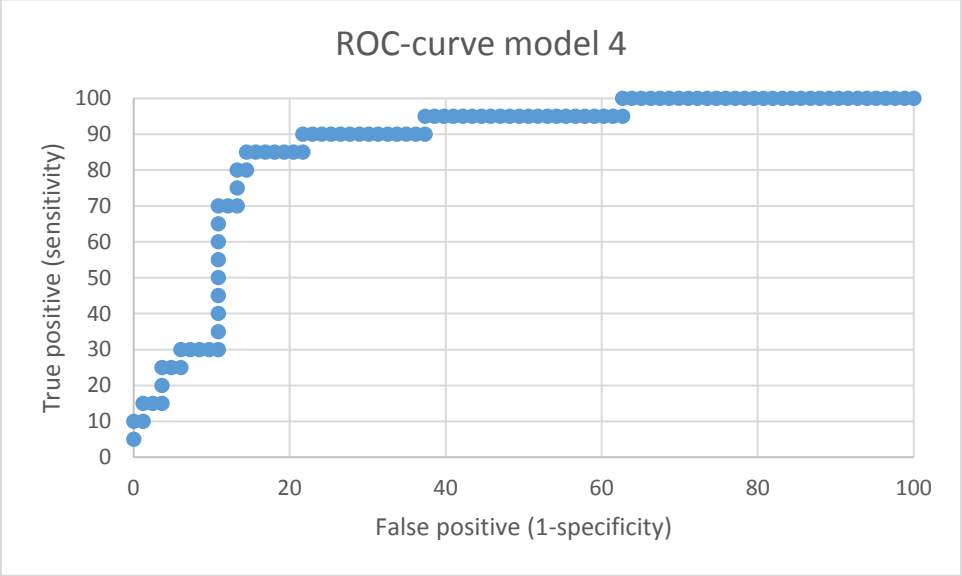

Figure 10. ROC-curve of the scoring values of ligands and decoys in the test set for model 4. The AUC of the curve is 87. The curve shows how well the model separate the 20 docked TTR binding compounds from the 82 docked non-binding compounds. The closer the area underneath the curve is to 100 the more accurate is the model.

4.3 Docking and scoring of thyroid hormones

Both T_3 and T_4 have three functional groups, a hydroxyl group, an amine group and a carboxyl group that depending on the pH will be either protonated or deprotonated. The blood of glaucous gull is expected to have a pH around 7.4 which is highly regulated to maintain homeostasis. Compounds that have a functional group with a pK_a-value around 6-8 will at pH 7.4 be present in the blood as an equilibrium between protonated and deprotonated. This is the case for THs, and therefore both T_3 and T_4 were docked with different charge of the hydroxyl group and carboxyl group, giving three different configurations.

The scoring values of the docked THs predicted THs to bind stronger to TTR when both the functional groups were charged and weakest when they were not charged. The score was higher for T_3 then T_4, predicting that T_3 bind stronger to TTR (Table 5). Model 4 predicted that the THs were poor TTR binders, indicating that the model is not very accurate. The ICM docking program return for each configuration of THs a stack of the ten bindings positions in TTR model with the highest scoring values. The binding positions predicted that THs were able to bind to TTR in both forward and reversed mode, meaning that the carboxyl bearing aryl ring can either be in the outer or inner part of the central channel respectively (Figure 11). This was in agreement with the T_4 forward and reversed binding mode in human TTR (Palaninathan, 2012). Both modes in the models had a scoring value above the threshold.

Table 5. Scoring values of T_3 and T_4 with different charge of the functional groups in the different homology models of TTR. The more negative the scoring values were the stronger the compounds were predicted to bind TTR.

Hormone	Charge	Model 1	Model 2	Model 3	Model 4
T_3	$-O^-$ and $-COO^-$	-30.75	-19.28	-19.89	-13.99
	-OH and $-COO^-$	-29.24	-17.19	-21.52	-13.5
	-OH and -COOH	-28.41	-20.44	-21.29	-14.37
T_4	$-O^-$ and $-COO^-$	-32.44	-18.86	-17.19	-14.95
	-OH and $-COO^-$	-28.84	-13.08	-20.74	-16.76
	-OH and -COOH	-27.35	-21.80	-20.77	-12.15

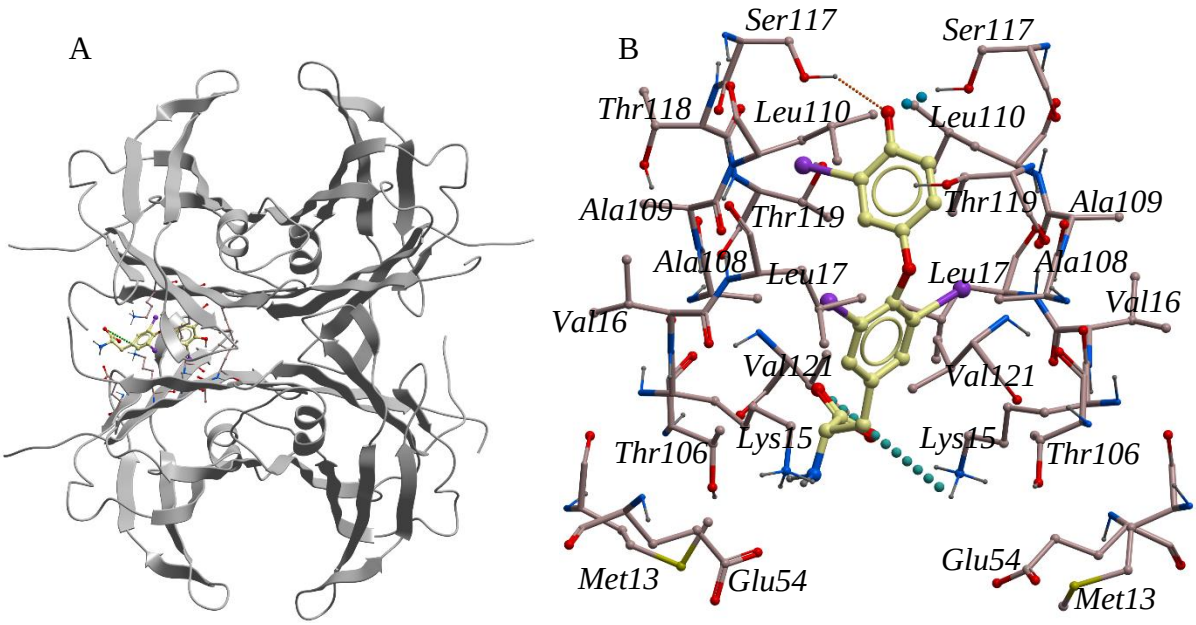

Figure 11. TH in the binding site of TTR model 1. A) Overview of the positioning of T_4 inside the funnel shaped binding site in the central channel of TTR. B) Amino acid residues in a 3.0 Å sphere radius around T_3. There is a hydrogen bond between the hydroxyl group of Ser117 and the deprotonated hydroxyl group of T_3. There is also a hydrogen bond between the amine group of Lys15 and the carboxyl group of T_3.

4.4 Docking and scoring of the contaminants

The contaminant data set of over 600 compounds were docked and scored in the different homology models of glaucous gull TTR to predict if they would bind, and the strength of the binding compared to the THs. The data set include contaminants predicted to bind to human TTR, either through experimental or molecular modeling. The dataset also include PBDEs, PCB and their metabolites where some of the compounds in these groups already through the study of Ucan-Marin et al. (2009) were found to bind to TTR in glaucous gull. The data set also include compounds that are emergent POPs used in industry and commerce for example as flame-retardants, possible metabolites, industrial biproducts, pesticides and more. The chemical properties of the emergent POPs are less known, and presences in glaucous gull serum are not measured for all compounds. The percentage of predicted TTR binders in the contaminants set was 24.0 %, 24.5 %, 36.9 % and 26.7 % in model 1, 2, 3 and 4 respectively.

4.4.1 PCB and metabolites

All the PCBs and the PCB metabolites that were docked in the models have been detected in plasma samples of glaucous gull in other studies from Svalbard and Bjørnøya (Verreault et al., 2005c, Verreault et al., 2007c, Verreault et al., 2006). Not all the highly chlorinated PCB congeners had a scoring value higher than the selected threshold separating binders and non-binders, and therefore is the mean scoring value for PCBs just below the threshold for model 1 and 2, but model 3 and 4 predict clearly that PCB are TTR binders (Table 6).

Table 6. Scoring values of PCBs docked in the different homology models. The more negative scoring values the stronger was the compound predicted to bind to TTR. To separate TTR binding compounds from non-binding a threshold scoring value was set based on the results of the test set. The thresholds are -18, -17, -16 and -14 for model 1, 2, 3 and 4 respectively.

Compound	Model 1	Model 2	Model 3	Model 4
CB-99	-18.84	-18.38	-20.79	-14.08
CB-118	-17.80	-16.58	-21.92	-14.28
CB-138	-19.09	-15.19	-20.63	-14.54
CB-153	-18.28	-16.94	-20.13	-14.92
CB-180	-17.35	-15.05	-20.45	-14.62
CB-187	-16.60	-13.80	-20.07	-13.08
Mean score	-17.99	-15.99	-20.67	-14.25

Table 6, 7 and 8 show the scoring values of PCB and the PCB metabolites in the different homology models of TTR. The mean scoring value for the OH-PCB was highest of the PCB and metabolites in model 1, 2 and 3, and the mean scores can be ranked in the order OH-PCB>PCB> $MeSO_2$-PCB. For model 4, however, the mean scoring values were highest for the $MeSO_2$-PCB. The $MeSO_2$-PCBs had low scores in model 1 and 2. They were not predicted to bind in model 2, and in model 1 only the lower chlorinated were predicted to bind. They had good scoring values in model 3 and predicted to bind with high affinity. Looking at the different docking conformations, the top scoring values predicted that the OH-PCB and $MeSO_2$-PCB will bind in both forward and reverse mode so that the functional group point to the inner binding cavity or outer binding cavity respectively (Figure 13). Hydrogen bonds were also predicted between the functional groups of the PCB metabolites (-OH and -MeO) and the polar amino acid residues of the Ser117 in forward binding mode (Figure 12) or Lys15 in revers binding mode. Most of the $MeSO_2$-PCBs were in reversed mode in the highest scoring position.

Table 7. Scoring values of OH-PCBs docked in the homology models. The negative scores predict good TTR. To separate TTR binding compounds from non-binding a threshold scoring value was set based on the results of the test set. The thresholds are -18, -17, -16 and -14 for model 1, 2, 3 and 4 respectively.

Compound	Model 1	Model 2	Model 3	Model 4
4-OH-CB-107	-24.66	-25.82	-23.97	-13.03
4-OH-CB-120	-23.92	-22.60	-21.59	-12.74
4´-OH-CB-130	-24.70	-21.31	-22.44	-13.39
3´-OH-CB-138	-19.29	-20.25	-20.84	-13.82
4-OH-CB-146	-24.47	-21.23	-22.11	-13.43
4-OH-CB-163	-23.11	-23.10	-23.42	-13.95
4´-OH-CB-172	-20.97	-21.61	-22.40	-13.85
4-OH-CB-187	-22.20	-20.74	-21.13	-13.93
4-OH-CB-193	-24.67	-23.18	-24.88	-14.08
Mean score	-23.11	-22.20	-22.53	-13.58

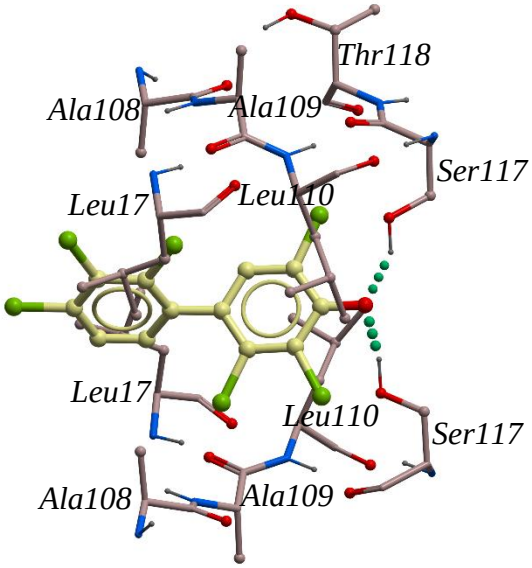

Figure 12. Amino acid residues in a 3.0 Å sphere radius around 4´-OH-CB-130 inside the TTR binding site of model 1. There is a hydrogen bond between the polar hydroxyl group of the Ser117 amino acid residue and the hydroxyl group of 4´-OH-CB-130.

Table 8. Scoring values of $MeSO_2$-PCBs docked in the different homology models. The more negative scoring values the stronger was the compound predicted to bind to TTR. To separate TTR binding compounds from non-binding a threshold scoring value was set based on the results of the test set. The thresholds are -18, -17, -16 and -14 for model 1, 2, 3 and 4 respectively.

Compound	Model 1	Model 2	Model 3	Model 4
3-$MeSO_2$-CB-49	-19.88	-16.16	-20.34	-13.93
4-$MeSO_2$-CB-49	-18.80	-17.88	-19.99	-15.01
3-$MeSO_2$-CB-52	-18.85	-14.64	-21.19	-13.24
4-$MeSO_2$-CB-52	-15.59	-15.77	-19.23	-14.40
3-$MeSO_2$-CB-87	-18.52	-13.05	-20.73	-14.13
4-$MeSO_2$-CB-91	-17.60	-13.46	-17.51	-13.79
3-$MeSO_2$-CB-101	-18.89	-13.34	-20.85	-13.18
4-$MeSO_2$-CB-101	-17.25	-14.50	-21.47	-14.75
3-$MeSO_2$-CB-110	-14.96	-13.14	-20.06	-13.96
4-$MeSO_2$-CB-110	-16.10	-10.68	-21.10	-15.70
3-$MeSO_2$-CB-132	-15.88	-13.29	-17.66	-13.10
4-$MeSO_2$-CB-132	-16.56	-10.15	-18.91	-13.96
3-$MeSO_2$-CB-141	-17.95	-15.77	-21.05	-14.54
4-$MeSO_2$-CB-141	-14.86	-13.92	-20.51	-14.52
3-$MeSO_2$-CB-149	-16.31	-10.75	-17.81	-13.70
4-$MeSO_2$-CB-149	-16.88	-13.15	-18.86	-15.46
4-$MeSO_2$-CB-174	-15.52	-10.77	-19.41	-15.84
Mean score	-17.08	-13.55	-19.81	-14.31

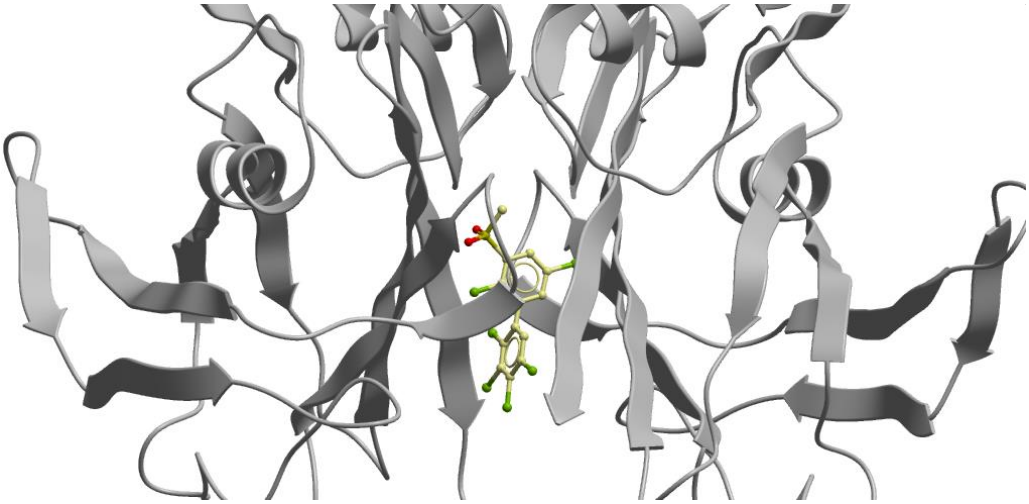

Figure 13. 3-$MeSO_2$-CB-141 bound in forward mode in the binding site of TTR model 3.

4.4.2 PBDE and metabolites

All the docked PBDEs and their metabolites have previously been measured in samples from glaucous gull from Svalbard and Kongsfjorden (Verreault et al., 2007c, Verreault et al., 2005a, Verreault et al., 2007a). The PBDEs and PBDE metabolites had a more negative mean scoring value then the PCB and PCB metabolites (Table 9, 10 and 11). The two phenyls rings, connected by an ether binding between is present in the structure of both the PBDEs, PBDE metabolites, and the THs. From Figure 11, 14, and 15 it is possible to see that the THs and the PBDEs bound in a similar binding mode in the TTR binding pocket. The PBDEs had high scoring values and were therefore predicted to be good binders, however the highly brominated congeners, BDE-203, BDE-206 and BDE-209 were not predicted to bind in all the models (Table 9).

Table 9. Scoring values of PBDEs docked in the different homology models. The more negative scoring values the stronger was the compound predicted to bind to TTR. To separate TTR binding compounds from non-binding a threshold scoring value was set based on the results of the test set. The thresholds are -18, -17, -16 and -14 for model 1, 2, 3 and 4 respectively.

Compound	Model 1	Model 2	Model 3	Model 4
BDE-49	-25.70	-24.32	-24.85	-16.63
BDE-47	-25.08	-23.31	-25.14	-15.25
BDE-99	-24.87	-23.60	-26.25	-15.61
BDE-154	-22.89	-22.03	-22.51	-14.17
BDE-100	-21.90	-22.14	-22.58	-16.13
BDE-153	-21.56	-21.06	-22.16	-14.55
BDE-206	-21.01	-14.05	-22.51	-14.10
BDE-203	-20.60	-17.55	-20.39	-15.61
BDE-209	-17.60	-13.73	-20.14	-15.19
Mean score	-22.36	-20.20	-22.95	-15.25

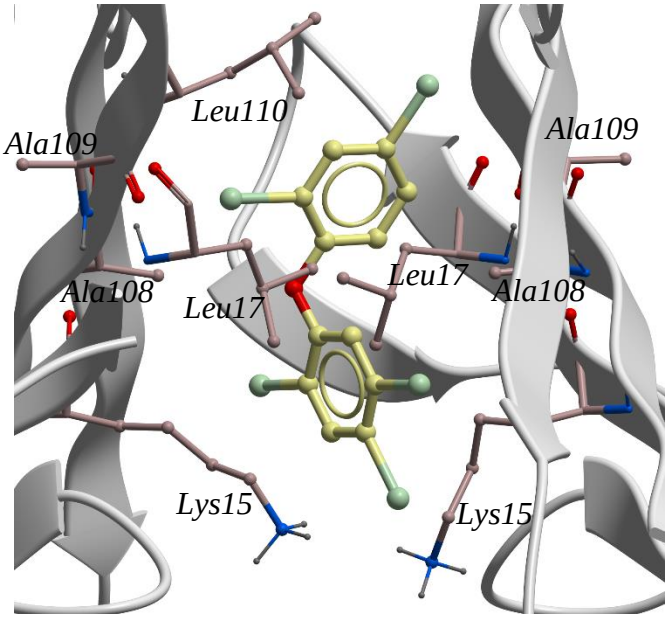

Figure 14. Amino acid residues in a 3.0 Å sphere radius around BDE-99 inside the TTR binding site of model 2.

The docking results predicted that the PBDE metabolites bound to the TTR binding site in both forward and reverse binding mode, so that the functional groups (-OH and -MeO) could form hydrogen bonds with the amino acid residues of Ser117 or Lys15 respectively. The mean scoring values were very similar for the MeO-PBDEs and OH-PBDEs in all models. For models 1 and 2 the MeO-PBDEs had a mean score slightly better than the OH-PBDEs, while in model 3 and 4 the mean scoring of the OH-PBDEs were slightly better than that of the MeO-PBDEs.

Table 10. Scoring values of MeO-PBDEs docked in the different homology models. The more negative scoring values the stronger was the compound predicted to bind to TTR. To separate TTR binding compounds from non-binding a threshold scoring value was set based on the results of the test set. The thresholds are -18, -17, -16 and -14 for model 1, 2, 3 and 4 respectively.

Compound	Model 1	Model 2	Model 3	Model 4
4-MeO-BDE-90	-25.71	-24.55	-25.16	-16.35
4´-MeO-BDE-49	-24.18	-25.23	-25.14	-16.80
4-MeO-BDE-42	-23.75	-23.50	-21.83	-16.56
6-MeO-BDE-47	-23.43	-22.01	-24.01	-15.46
6´-MeO-BDE-99	-21.91	-23.30	-21.80	-15.85
Mean score	-23.80	-23.72	-23.59	-16.20

Table 11. Scoring values of OH-PBDEs docked in the different homology models. Negative scores indicate good TTR binders and a threshold was set to separate binders from non-binders. The thresholds are -18, -17, -16 and -14 for model 1, 2, 3 and 4 respectively.

Compound	Model 1	Model 2	Model 3	Model 4
4´-OH-BDE-49	-25.32	-25.28	-24.98	-15.44
5-OH-BDE-47	-24.42	-20.24	-24.13	-16.22
3-OH-BDE-47	-24.41	-23.74	-24.45	-15.82
6-OH-BDE-47	-23.86	-20.24	-25.58	-15.69
4-OH-BDE-42	-23.69	-25.00	-23.68	-21.07
2´-OH-BDE-68	-21.56	-21.94	-21.66	-14.89
6´-OH-BDE-49	-20.50	-19.59	-21.56	-16.67
Mean score	-23.39	-22.29	-23.72	-16.54

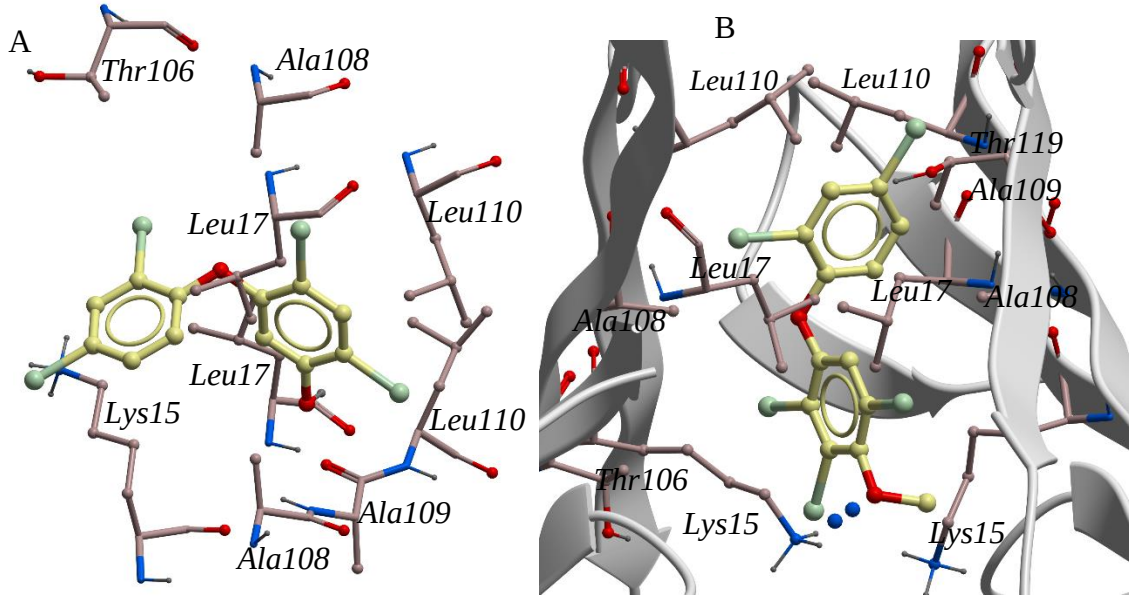

Figure 15. A) Amino acid residues in a 3.0 Å sphere radius around 5-OH-BDE-47 inside the TTR binding site of model 1. B) Amino acid residues in a 3.0 Å sphere radius around 4-MeO-BDE-99 inside the TTR binding site of model 2. There is a hydrogen bond between the amino group of the Lys15 amino acid residue and the methoxyl group of 4-MeO-BDE-99.

4.4.3 PFCs

The scoring values of some of the docked PFCs are shown in Table 12. Those that are listed are the best scoring PFCs. In addition those that were highlighted in the studies of among other Howard and Muir (2010) and Vorkamp and Riget (2014) are listed. The scoring values were best in model 2 which predict that several of the PFCs will be good binders. Model 4 on the other hand predicted that many of the PFCs will bind poorly. The PFCAs had best scoring values of the PFCs (Table 12). The PFSA as well were predicted to bind to TTR. Together with PFCA, PFSA are deprotonated at pH 7.4. The list includes other PFCs with different functional polar groups such as esters, ketones, sulfonamidoethanol, phosphorus acid and perfluoro-telomere alcohols. Most of these compounds except the phosphorus acid were neutral at pH 7.4, but could still have hydrogen bonds to polar amino acid as the results of the docking showed

(Figure 17). Some of the perfluorotelomere alcohols are predicted to bind to TTR, but the C8-PFPA was only predicted to be a weak binder in model 2. The fluorotelomers with sulfonamide (N-Et-FOSA and N-Me-FOSA) group were predicted to not bind to TTR while those with a slufonamidoethanol group (N-Et-FOSE and N-Et-FOSE) were predicted to bind in model 2 and 3. The fluorotelomer flourides were predicted to bind to TTR in model 1 and 2. The fluorotelomer acrylates were predicted to bind to TTR in model 1, 2 and 3. While the fluorotelomer methacrylates were predicted to bind to TTR in model 1 and 2 (Table 12).

Table 12. Scoring values of PFCs docked in the different homology models. Negative scores indicate good TTR binders and a threshold was set to separate binders from non-binders. The thresholds are -18, -17, -16 and -14 for model 1, 2, 3 and 4 respectively (Abbreviation list include full names of all compounds).

Compound	Model 1	Model 2	Model 3	Model 4
PFTeA	-23.41	-24.76	-21.83	-15.14
PFTriA	-16.75	-19.85	-15.09	-13.00
PFDoA	-16.51	-22.37	-18.15	-11.99
PFUnA	-19.49	-22.78	-18.23	-11.18
PFDcA	-21.77	-20.57	-19.39	-12.23
PFNA	-19.40	-19.56	-19.99	-10.32
PFOA	-23.71	-20.22	-15.99	-10.28
PFHpA	-23.50	-22.75	-15.57	-8.463
PFHxA	-20.89	-27.39	-15.51	-9.053
PFPA	-19.50	-23.44	-13.99	-8.032
PFDS	-15.49	-16.48	-15.50	-14.90
PFOS	-18.53	-16.90	-17.32	-13,84
PFHpS	-15.78	-13.33	-12.50	-9.05
PFHxS	-20.18	-16.10	-14.29	-9.031
N-Et-FOSE	-18.09	-19.60	-17.80	-13.36
N-Me-FOSE	-17.24	-24.10	-18.79	-13.61
N-Et-FOSA	-13.40	-14.81	-13.77	-12.82
N-Me-FOSA	-13.00	-14.78	-12.96	-10.89
12:2 FTOH	-17.04	-19.98	-15.96	-12.36
10:2 FTOH	-10.88	-19.41	-11.49	-9.063
8:2 FTOH	-18.46	-20.04	-19.03	-9.454
6:2 FTOH	-17.18	-18.54	-15.38	-8.904
POF	-23.32	-24.92	-15.77	-11.52
PHpF	-23.09	-24.31	-15.77	-11.80
PBF	-19.14	-16.93	-12.15	-9.865
12:2 FTAC	-15.54	-25.97	-14.63	-15.19
14:2 FTAC	-14.69	-23.84	-13.13	-16.35
12:2 FTMAC	-24.50	-27.44	-12.33	-13.30
6:2 FTMAC	-26.50	-27.62	-16.58	-13.76
C8-PFPA	-13.10	-18.25	-15.26	-13.94

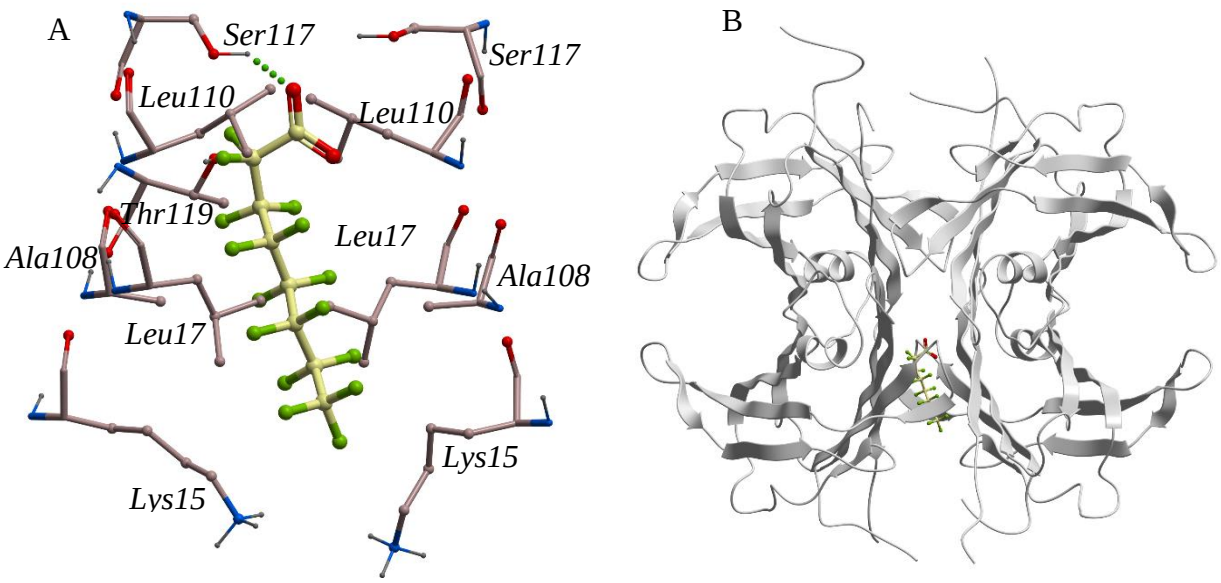

Figure 16. PFOA in the TTR binding site of homology model 2. A) Amino acid residues in 3.0 Å sphere radius around PFOA are inincluded. A hydrogen bond is present between the polar hydroxyl group of Ser117 and the deprotonaited carboxyl group of PFOA. B) Overwiev of the PFOA within the binding site of TTR model 2.

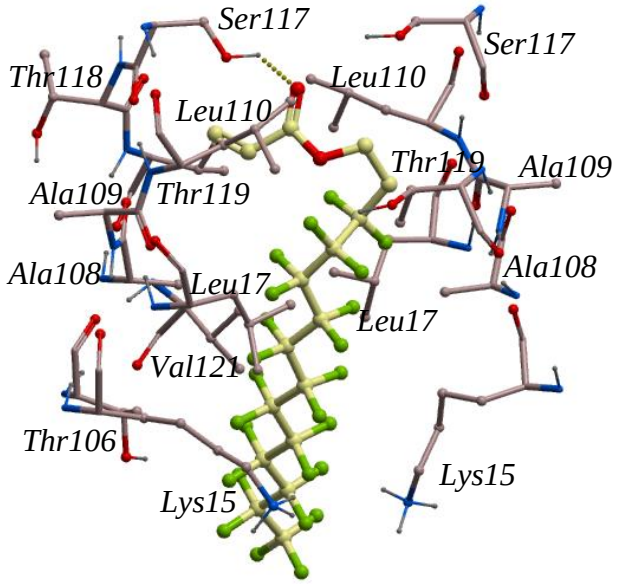

Figure 17. 12:2 FTAC, a PFCs with a ester group, inside the TTR binding site of model 2, displaying the amino acid residue within a 3.0 Å sphere radius of the ligand A hydrogen bond is present between the hydroxyl group of Ser117 and the carbonyl group of the ester.

4.4.4 Emergent flame-retardants, current used pesticides and other emergent POPs

The current used pesticides, dacthal, chlorthalonil, chlorpyrifos, diazinon, endosulfan, methoxychlor, difocol and Deca Plus, had scoring values below the threshold and were therefore not predicted to be glaucous gull TTR binders. The siloxanes and musk xylenes were also not predicted to bind. Several of the new emergent BFRs had scoring values that predicted binding to TTR such as 2,4,6-tribromophenol (2,4,6-TBP), 2,4-dibromophenol (2,4-DBP), 2-

bromoallyl-2,4,6-tribromophenyl ether **(**BATE), allyl-2,4,6-tribromphenylether (ATE), BTBPE and DPTE (Table 13 and Figure 18 and 19). Of the new emerging BFRs were TBB, TBHP, PBEB, HBBz and TBBPA not predicted to bind to TTR. DBDPE was predicted to be a TTR binder in model 3 only. Some of the tested chlorinated compounds also had good scores such as Bis-(4-chlorophenyl)sulfone (BCPS) (Table 13). The chlorinated chemical that were predicted not do bind include the emerging chemicals PCP, PCNB, PCA, HCBD and PeCBz. Among the compounds not predicted to bind or predicted to be very weak binders to glaucous gull TTR were different chlorophenols and TBBPA that were predicted to have high affinity in studies that investigated human TTR (Meerts et al., 2000). The phosphorus flame-retardant Triphenylphosphate (TPhP) was the only one in that class of chemicals that was predicted to bind in three of the models. One phthalates, butylbenzyl phthalates (BBP) was predicted to bind to TTR in model 3. The compounds triclocarban, N-(4-bromo-2,6-dichloro-3-methylphenyl)acetamide (68399-95-1), 2,4-dichlorobenzoyl peroxide (133-14-2), 3-(2-chloro-4-trifluoromethylphenoxy)benzoic acid (63734-62-3) and 3-(2-chloro-4-(trifluoromethyl)-phenoxy)phenyl acetate (50594-77-9) described in Howard and Muir (2010) study on emerging POPs were predicted to be bind strongly to glaucous gull TTR (Table 13 and Figure 18B).

Table 13. Scoring values of selected emergent POPs docked in the different homology models. The more negative scoring values the stronger was the compound predicted to bind to TTR. To separate TTR binding compounds from non-binding a threshold scoring value was set based on the results of the test set. The thresholds are -18, -17, -16 and -14 for model 1, 2, 3 and 4 respectively.

Compound	Model 1	Model 2	Model 3	Model 4
2,4,6-TBP	-23.22	-20.18	-14.94	-11.61
2,4-DBP	-21.77	-20.83	-12.65	-12.36
BTBPE	-22.05	-16.45	-21.60	-15.40
BATE	-19.27	-16.41	-18.32	-11.49
DPTE	-18.07	-16.40	-16.69	-10.91
ATE	-18.69	-15.15	-17.55	-11.03
TBBPA	-14.63	-11.26	-18.04	-12.86
DBDPE	-12.72	-11.12	-17.90	-13.90
PCP	-16.39	-15.10	-9.636	-9.976
HCBD	-14.71	-14.64	-15.49	-10.24
BCPS	-21.53	-18.19	-19.93	-15.25
Triclocarban	-22.54	-14.37	-16.47	-14.10
68399-95-1	-29.79	-28.52	-17.35	-15.76
133-14-2	-28.95	-20.06	-18.01	-16.34
63734-62-3	-26.32	-25.03	-20.70	-18.95
50594-77-9	-20.07	-26.13	-22.60	-18.36
BBP	-15.88	-16.44	-18.39	-13.79
TPhP	-13.94	-17.81	-18.31	-15.73

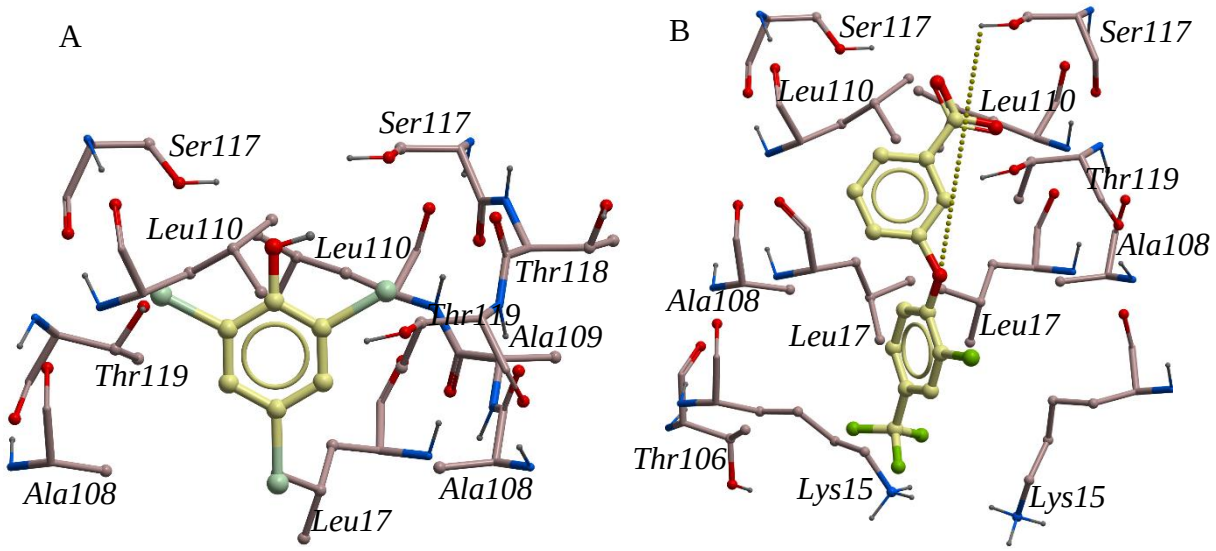

Figure 18. Amino acid in a 3.0 Å sphere radius of A) 2,4,6-TBP and B) 63734-62-3 docked in the TTR binding site of model 2

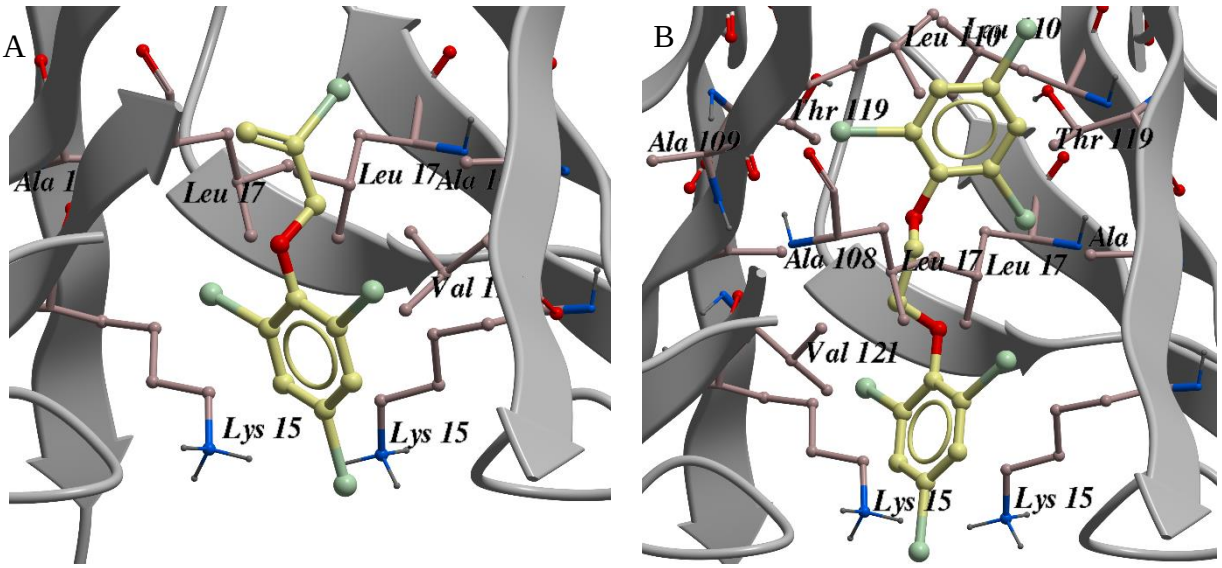

Figure 19. Amino acid in a 3.0 Å sphere radius of A) BATE and B) BTBPE docked in the TTR binding site of model 3

5. DISCUSSION

The results show that there is a large group of chemically diverse compounds that were predicted to bind to glaucous gull TTR. They vary in physicochemical properties and size, ranging from small phenols to long telomers. Some compounds are neutral while others are charged. They are all halogenated either chlorinated, brominated or fluorinated except from BBP and TPhP. The chemical structure of the compounds expected to bind to glaucous gull are in appendix A. Many of the compounds like OH-PCB, PBDEs, PBDE metabolites, emergent BFRs, 133-14-2, 63734-62-3, 68399-95-1 and some of the PFCs had high scoring values closed to the score of the THs or above, predicting that they could be strong competitors with THs for binding to TTR. The prediction of some compounds binding affinity in to TTR in glaucous gull differed from the binding affinity to TTR in other species indicating species-specific differences in binding to TTR. Displacement of THs could potentially lead to perturbation of circulating THs level and affect TH homeostasis.

5.1 Construction and evaluation of homology models

The ROC-curves and AUC-values from the test set indicates that the constructed homology models gives a good prediction of compounds that will bind to glaucous gull TTR in reality (Figure 7, 8, 9 and 10). This especially clear from model 1 and 2 AUC-values, 96 and 95 respectively. When selecting compounds for the test set, ligands from human TTR crystal structures were selected since these compounds were consequently known to bind to human TTR but not necessarily in glaucous gull TTR. A bad scoring value could therefore indicate that the models were not able to differentiate between binding and non-binding compounds or that the ligand actually was not a binder to glaucous gull TTR. The evolutionary highly conserved sequence on the other hand made it reasonable to predict that they will bind to TTR also in glaucous gull. Since the ligand T_3 in the test set is the innate hormone, should T_3 also bind in the model. The resulting scores of the test set ligands were much more negative than for the decoys indicating that the ligands will bind, and the test set therefore confirmed that the models were good in predicting the real glaucous gull TTR structure.

The binding sites of the models have a high hydrophobicity consistent with binding of hydrophobic compounds such as TH and most of the chemicals with POP properties. Studies of human TTR have found that the central channel is highly hydrophobic and that this is important for binding of TH and other lipophilic compounds (Ren and Guo, 2012, Ishihara et al., 2003). The volume of the binding pocket found by icmPocketFinder was quite small, and seems not to include the entry of the central channel, which was the widest part of the funnel-shaped binding site (Figure 11).

The region of the central channel that makes up the binding pocket is highly conserved between the gull sequence and the templates, making the modelling more accurate. However, the N-terminal of the TTR in the template crystal structure is short and lacks some amino acids so that modeling the complete N-terminal of the glaucous gull sequence was not possible. The N-terminal is not part of what is described in literature as the binding site, but it is has however been hypothesized that the N-terminal affect the binding affinity. It is suggested that this might

even be part of the reason that TTR in birds and fishes bind T_3 over T_4, contrary to TTR in mammals (Chang et al., 1999). If this is correct it could affect the accuracy of the binding predictions in the models depending on the species-specific differences in the TTR structure.

There is a possibility that the constructed models representing slightly different conformation of the binding site may not represent the best conformation for ligand binding. By constructing additional models from different crystal structures with slight structural differences in the binding site one could perhaps obtain a better conformation that could accept more ligands. Another possible improvement to the modelling could be to use molecule dynamic simulations or Monte Carlo simulations to generate more conformations of the binding site. The program Modeller can also be used to make more homology models that have some nuances in the structure/conformation. With additional models it is possible that the test set containing ligands and decoys could separate between good and bad models for ligand recognition and binding. The sterochemical properties of a model may be evaluated using the Structural Analysis and Verification Server (SAVES, http://services.mbi.ucla.edu/SAVES/) as well. However, ROC curves show that our models are quite good in separating binders from decoys, indicating that the models are predictive.

For the models to make accurate predictions the docked compounds need to have the right protonation/charge. In some cases such as with the PCB metabolites, PBDE metabolites and the THs the compounds were docked several times with different charge of functional groups (charged or neutral). The results of these dockings showed that having charged functional groups appeared to increase the predicted affinity for the binding site. This point out how important correct charge of the compound is. To make sure the compounds had the correct charge the formal charge was set to correspond to a pH of 7.4. The ICM program calculates a theoretical pK_a-value for the compound to set the charge. That means the charge could be incorrect if the real pK_a-values differ from the theoretically calculated. An experimentally decided value would be more accurate. However, this was not available for all the compounds and would be very time-consuming since over 600 compounds were docked in the models. Also compounds with pK_a (6-8) close to the pH would not be present only in charged or neutral conformation, both conformations would be present in the solution in equilibrium.

5.2 Binding of thyroid hormones and contaminants to TTR

The docking and scoring predicted binding of 24 %, 24.5 %, 36.9 % and 26.7 % of the compound in the contaminant data set in model 1, 2, 3 and 4 respectively. This number was however affected by the fact that some compound groups like the $MeSO_2$-PCBs were represented in the list with many congeners compared to other groups, and for some compounds different confirmations with different charge was represented. Still a variety of compounds were identified to bind to the models. Previous studies has shown that some of the compounds predicted to bind to glaucous gull TTR are identified as binders to human TTR (Meerts et al., 2000, Weiss et al., 2009). There were also variations from what have previously been reported in binding studies of TTR in other species indicating species variation in TTR affinity of different compounds.

What is common for the compounds predicted to bind to TTR is that they were halogenated (with some exceptions), and often had a functional group such as hydroxyl that could make hydrogen bonds with polar or charged amino acids. Many of the compounds that were predicted to bind strongly to TTR resemble TH in structure such as PCBs, PBDEs, 63734-62-3 and 50594-77-9. However, some were very structurally dissimilar to THs such as the PFCs predicted to bind to TTR.

5.2.1 Thyroid hormones

The docking of THs predicted that THs will bind stronger to TTR when the functional groups were charged. This was likely because then compounds more easily make hydrogen bonds to the amino acids. However most of the THs have uncharged carboxyl groups at pH 7.4 and T_3 which has a higher pK_a will mostly have a protonated hydroxyl group while it is the opposite in T_4. The constructed models predicted that T_3 bind stronger to TTR than T_4 in glaucous gull just as expected since previous studies has shown that this is the case in avian TTR (Chang et al., 1999).

The docked THs bound to the binding site in the models in both forward and reversed mode. The position and interaction with amino acid residues was similar to the description of the binding site described by Blake et al. (1978) that studied the crystal structure of human TTR with T_4 inside the binding site. In Figure 13B T_3 is bound to the binding pocket in forward mode and just as described from crystal structure studies of human TTR, it is a hydrogen bond between the hydroxyl group of T_3 and the amino acid side chain of Ser117. There is also hydrogen-bonding interactions between the carboxyl group and the amino acid residue of Lys15. The amino acids Leu17, Thr106, Ala108 and Val121 holds the C-O-C linkage that connect the aromatic rings. The iodine atoms of T_3 also lie close to amino acids that constitute the binding pockets HBP2/2´ and HBP3/3´ just like the iodine atoms in the crystal structure of human TTR bound to T_4.

5.2.2 PCBs, PBDEs and their metabolites

The PBDEs and their metabolites had some of the best scoring values and were predicted to be good binders to TTR. The MeO-PBDE mean score was about the same as the mean score of OH-PBDE, being just slightly better in model 1 and 2 comparde to model 3 and 4. However, the number of tested metabolites and which congener that was docked differed between these two groups of metabolites. Looking at the same congener in the two groups revealed that for the MeO- and OH-substitution in the same position, the score was better for the hydroxyl metabolites (Table 10 and 11, compound 4´-MeO-BDE-49, 4-MeO-BDE-42, 6-MeO-BDE-47 4´-OH-BDE-49, 4-OH-BDE-42 and 6-OH-BDE-47).

That OH-PBDEs was predicted to bind stronger than MeO-PBDEs to TTR is consistent with Ucan-Marin et al. (2009) result for competitive TH binding assay with recombinant TTR from glaucous gull. That both metabolites were predicted to bind stronger to TTR then PBDEs is also consistent with these results. Ucan-Marin et al. (2009) study also confirmed the prediction that T_3 binds stronger than T_4 to glaucous gull. A considerable difference however was that the PBDEs metabolites in their experiment was found to be a much stronger competitor to T_3 and

T_4 then PBDEs (Ucan-Marin et al., 2010, Ucan-Marin et al., 2009). In the present study the scoring values for PBDEs were not much lower than the scoring values of the PBDE metabolites. Studies on PBDEs competitive binding in human TTR also showed that the binding affinity to TTR is markedly lower for the PBDEs than for the THs, and the structural analogous MeO-PBDEs and especially OH-PBDEs. No substantial TTR binding was observed in studies of 17 (Meerts et al., 2000) and 19 (Hamers et al., 2006) PBDE congeners. The docking, however in our models, predicted that the PBDEs will bind almost as strongly as the PBDE metabolites especially the congeners with four bromine substitutions (BDE47 and BDE49), but the binding affinity would decrease with higher bromination, (Table 9). The highly brominated were not predicted to bind in all the models (BDE203, 206 and 209). That the predictions in the glaucous gull TTR models was not consistent with the results from the competitive binding assay with recombinant glaucous gull TTR (Ucan-Marin et al., 2009) when it comes to PBDEs raise questions about the predictability of the models. However, both studies agree that PBDEs will bind to TTR. In addition, the scoring value of OH-PBDEs was not higher than the scores of THs in model 1 predicting that they do not bind stronger than THs. In the other three models they had similar scoring values predicting that the OH-PBDEs were strong competitors with THs and had higher binding affinity to TTR.

That the tetra-brominated PBDEs was predicted to be the strongest binders also applies to the PBDE metabolites that were docked into the models (Table 10 and 11). This was consistent with previous result showing that OH-PBDE congeners with four bromine resembling the substitution pattern in T_4 will bind stronger to human TTR (Cao et al., 2010). Ren and Guo (2012) found that TTR binding affinity was associated with the degree of brominations for OH-PBDEs. The binding increased with the number of bromine atoms up to four. Binding affinity to human TTR also depend on the position of the OH group with the affinity being highest if the OH-group is in para or meta position (Ghosh et al., 2000, Hamers et al., 2008, Meerts et al., 2000). For OH-BDE47 the binding affinities were highest for 3-OH followed by 5-OH and 6-OH position (Ren and Guo, 2012).

It has been proposed for both OH-PBDEs and OH-PCBs that for optimal competitive binding to human TTR and sea bream (*Sparidae*) TTR hydroxylation should exist at the para position relative to the aromatic ring linkage, and that there are one, but preferably two, halogen substituents on carbons adjacent to the OH-group. The affinity increases with the number of halogens substitutions (Hamers et al., 2006, Lans et al., 1993, Morgado et al., 2007). Ucan-Marin et al. (2010) found in consistence with this proposal that 4´-OH-BDE-49 with para-hydroxylated and an adjacent bromine have higher affinity in competition with T_4 to glaucous gull TTR than 6-OH-BDE-47. This was also the result from the present study of these compounds. In our models the TH-like brominated biphenyl ether backbone, and the presence of OH-group (capable of electrostatic or hydrogen bonding interactions) in meta or para position in particular was predicted to make the compounds a competitive ligand for TTR relative to both T_3 and T_4 having scoring values in the same range as the THs.

The results from the docking of PCBs and their metabolites predicted that the PCBs and $MeSO_2$-PCBs are weak binders to glaucous gull TTR or will not bind at all (Table 6 and 8).

However, the OH-PCBs were predicted to be good binders to TTR (Table 7). The results were consistent with Ucan-Marin et al. (2009) that showed by competitive binding assay with recombinant TTR that OH-PCBs were good binders to TTR and had higher affinity than PCB and $MeSO_2$-PCB. In contrast to Ucan-Marin et al. (2009) the $MeSO_2$-PCBs were not predicted to bind stronger to TTR than the PCBs in the present study. Among the docked OH-PCBs the OH-group was primarily in the 4-para position and only one of the docked OH-PCBs had a 3-OH substitution. The compound 3´-OH-CB-138 had the worst scoring value of all the OH-PCBs in three out of four models of gull TTR. This was consistent with the previous study on human TTR (Rickenbacher et al., 1986) and the competitive binding assay in Ucan-Marin et al. (2009) study on glaucous gull TTR showing that para hydroxylated OH-PCBs had the highest binding affinity of the OH-PCBs. Nevertheless, since the result of the docking is for only one non-para hydroxylated and does not include congeners with OH-group at different positions, we cannot draw any certain conclusion from the docking results.

In the present study highly chlorinated PCBs was predicted to be poor TTR binders with lower binding affinity to TTR than the lower chlorinated PCBs. Chauhan et al. (2000) study found that having both para positions (4,4´) filled in general contribute to decreased competitive binding, while having all meta positions (3,3´,5,5´) filled with halogens contributes to increased binding activity. It is hypothesized that these lateral halogens can occupy the binding pockets of TTR normally occupied by the TH phenolic ring due to structural resemblance (Rickenbacher et al., 1986). Fully ortho-only substituted PCBs lack binding activity while fewer ortho-bromines increase in binding. This is consistent with the larger size of bromine leading to more rapid widening of torsional angels and maximizing the steric constrains which limit the access to the binding site. Certain ortho-only substituted PCBs however fit into the binding site so that they overlay the phenolic rings of T_4 similar to the binding mode of lateral-substituted. Their results support the view that good binders tend to show structural resemblance to T_4 in terms of substitution pattern and the phenolic ring. According to the results of Chauhan et al. (2000) the reason why the highly chlorinated PCBs were not predicted to bind to glaucous gull TTR in the models could be that they do not fit in to the binding site because of sterical constrains (Table 6). The many substitution filled up the ortho-positions making the PCB congener less similar to THs. Our results is also consistent with Chauhan et al. (2000) in the prediction that parent PCBs bind but generally have lower affinity than OH-PCBs.

The molecular structure of EDCs contains groups that can ionize under physiological conditions, and the neutral and ionic forms could have different binding mechanisms with the macromolecular targets like TTR. This was predicted in the present study of glaucous gull TTR. The docked THs and some of the OH-PBDEs and OH-PCBs had higher score when docked with charged functional groups. Yang et al. (2013) studied this through molecular modeling and investigation of crystal structures considering phenolic compounds like OH-PBDEs binding to human TTR. They found that the anionic form of the phenolic compounds bind stronger to human TTR than their corresponding neutral forms. No dominant orientation was observed for the neutral form, while the ionized group ($-O^-$, $-COO^-$, $-SO_3^-$) tended to be orientated toward the entry of the central channel because the side chain of Lys15 residue can be protonated to form a $-NH_3^+$ group under physiological conditions. This group can form

dominant and orientational electrostatic interactions with the anionic group of the ligands and cation-π interactions with the aromatic rings. These interactions are enhanced in anionic form because the surface distribution of the electrostatic potential is more negative for anionic form then the corresponding neutral form (Yang et al., 2013). Hydrogen bonding interactions between the hydroxyl group of phenolic compounds and the side chain of Lys15 were observed for the docked compounds in the glaucous gull TTR model as well. However, there were also observed hydrogen-bonding interactions between the docked compounds and the amino side chain of Ser117 as shown in Figure 14. Together these results shows that the effect of ionization should not be neglected. Comparative studies of crystal structures of human TTR has shown that hydrogen bonding to Lys 15 in the outer binding pocket and to Ser117 in the inner binding pocket are controlling factors in both orientation and affinity of the ligand (Cody, 2002).

The Ucan-Marin et al. (2009) study on gull TTR found that the competitive potency was ~10nM for 6-OH-BDE47 and 4´-OH-BDE49, and 5-10 nM for 4-OH-CB187. Mean concentrations of the OH-PBDEs in the plasma of glaucous gulls from the Norwegian Arctic was up to 0.32 ng/g (wet weight) or ~0.6 nM. The mean concentration of 4-OH-CB187 has been reported to be up to 17.5 ng/g (wet weight) or ~40nM (Verreault et al., 2005a, Verreault et al., 2005c). This indicates that there could be a profound effect on circulating T_3 and/or T_4 levels of the OH-PBDEs and that 4-OH-CB187 is even more likely to affect circulating THs levels in free-ranging Svalbard glaucous gulls. These results demonstrate that there may be potential physiological consequences of the competitive binding of OH-containing organohalogens and perturbations of THs levels in blood via interactions with TTR. But in recent studies of Svalbard glaucous gull neither T_3 or T_4 levels were associated with concentrations of selected organohalogens including PCBs and OH-PBDEs (Verreault et al., 2007a).

5.2.3 PFCs

The scoring values of the PFCs were best in model 2 which predicted that several of the PFCs would be good TTR binders both those with charged and those with neutral functional groups. Model 4 on the other hand predicted that many of the PFCs will bind poorly, even those with charged functional groups. The PFCAs had best scoring values of the PFCs (Table 12). The PFSAs were predicted to bind to TTR but not strongly, and the neutral PFCs with ketone and ester groups were predicted to have high affinity to TTR. Some of the perfluorotelomere alcohols in particularly 8:2 FTOH were also predicted to bind, but in model 4 were none of the FTOHs predicted to bind.

The prediction that PFCs with neutral functional group will bind is not consistent with the experimental and molecular modeling study by Weiss et al. (2009) on PFCs binding to human TTR. They found that PFCs with charged functional groups were the strongest binders similarly to our results on glaucous gull TTR, but none of the neutral PFCs bound to the human TTR. Weiss et al. (2009) also found that the PFCs that were more fluorinated showed higher affinity for human TTR compared to lower fluorinated, similar to results for halogenated phenols such as BFRs and chlorophenols (Ghosh et al., 2000, Meerts et al., 2000, Van den Berg, 1990). The binding affinity increased with increasing chain length, but there was no further increase in binding affinity with chain length over eight carbons. In the present study there were no clear

association between chain length and scoring values, but for the PFASs three of the models predict binding affinity to increase with chain length up to PFOS. In addition the docked compounds were mostly longer chain PFCs over eight carbons where Weiss et al. (2009) found no further increase in affinity. Carbon chain lengths of the PFC have also been reported to affect several properties such as bioaccumulation factor (BAF). BAF for PFCA increase with chain length of more than eight carbons, while PFASs and PFCAs with a chain length shorter than seven and six carbons respectively could not be detected in most tissues and were considered to have insignificant BAFs (Martin et al., 2003).

In a TTR assay, the functional group was found to change the affinity for human TTR. This assay included 78 compounds from different chemical classes, and the nitro substituents were less effective compared to carboxylates, while compounds with a hydroxyl group on the aromatic moiety had the highest affinity (Baures et al., 1998). The same was predicted in the glaucous gull models were OH-PCBs and OH-PBDEs had higher affinity than the MeO-PBDEs and $MeSO_2$-PCBs. However, Weiss et al found that the fluorotelomer alcohols with functional hydroxyl groups did not bind to human TTR and suggested that the explanation could be that the hydroxyl group itself, without being attached to an electrophilic aromatic system, is not enough for binding (Weiss et al., 2009). The docking of the FTOHs in the glaucous gull TTR model 2 on the other hand predicted that the FTOHs were TTR binders. In the other three models the FTOHs were either just above the threshold scoring value and therefor predicted to be weak TTR binders or just below the threshold predicted not to bind to TTR in glaucous gull. This results contravenes with the results of Weiss et al. (2009) and the assumption that OH-group needs to be attached to an electrophilic aromatic system. It would be interesting to test further if the prediction of Weiss et al. (2009) is correct.

A few N-substituted perfluoroalkyl sulfonamides (N-Et-FOSA and N-Me-FOSA, Table 12) were also docked in the glaucous gull TTR models and predicted not to bind. Lack of TTR binding for the N-substituted perfluoroalkyl sulfonamides was also demonstrate in Weiss et al. (2009) for human TTR. However, the N-substituted perfluoroalkyl sulfonamidoethanol (N-Et-FOSE and N-Me-FOSE, Table 12) were predicted to be good TTR binders in model 1, 2 and 3. These results further demonstrate the importance of the functional groups. It appears both from Weiss et al. (2009) and the present study that the acidic PFCAs that were dissociated had higher TTR binding affinity than nonacidic PFCs FTOHs which has a much higher pK_a and therefore does not dissociate. Nevertheless, in the glaucous gull models it was no clear trend that the acid PFCs bind stronger to TTR then non-aicd PFCs like in Weiss et al. (2009) study when considering the predicted high affinity of the fluorotelomer acrylates, methacrylates and sulfonamidoethanols compared to the predicted lower affinity of PFASs to glaucous gull TTR (Table 12).

The levels of PFCs detected in the blood of animals and humans are caused by the strong association of the compounds to proteins. One of the main carriers is believed to be albumin because of the high concentration in serum and high affinity for PFCs. Several other serum proteins such as sex hormone-binding globulin, corticosteroid-binding globulin and liver FA-binding protein have shown to be associated to PFCs (Jones et al., 2003, Luebker et al., 2002,

Vanden Heuvel et al., 1992). The study of Weiss et al. (2009) demonstrated TTR binding of PFCs in human TTR, and the present study predict that PFCs also will bind to TTR in glaucous gull.

The scoring values of the PFCs were lower than the scores of PBDEs, PBDE metabolites and OH-PCB in three of the models. In model 2 on the other hand the scoring values of the PFCAs in particular was comparable to or even higher than the scoring values of PBDEs, PBDE metabolites and OH-PCB. Weiss et al. (2009) found that PFCs binding affinity for human TTR only was one-tenth of the natural hormone T_4 and therefore less potent than other environmental pollutants. Due to the relatively high concentrations found in the environment, particularly of PFOS do the result from our glaucous gull TTR models indicate that PFCs can contribute to TH disruption by competitive binding to TTR. Decreased TH levels after PFCs exposure have been found in monkeys and rodents (Lau et al., 2003, Thibodeaux et al., 2003, Seacat et al., 2003). Haugerud (2011)found that long chain PFCAs was correlated with effects on the TH levels in glaucous gull, and explain more of the variation of total T_3 than PCBs and PFOS. This is interesting considering that the long chained PFCAs were predicted to be good binders to TTR in our models. Further work is necessary to find a putative association between PFCs levels and THs levels in glaucous gull, and to be certain whether PFCs will compete with THs for binding to TTR experimental studies is necessary. Most of the research so far have been on phenolic compounds regarding TH disruption and binding to TTR.

5.2.4 Other compounds predicted to bind to transthyretin

In the present study none of the docked pesticides (dacthal, chlorthalonil etc.) were predicted to bind to TTR. However the docking of the different emerging BFRs and POPs predicted that compound such as 2,4,6-TBP, 2,4-DBP, BTBPE, BATE, BCPS, 68399-95-1, 113-14-2, 63734-62-3 and 50594-74-9 have strong binding affinity to glaucous gull TTR. All of the compounds have one or two aromatic ring and are halogenated some of them are also very similar to the THs structure (Appendix A for chemical structure). The scoring values of these compounds were better in model 1 and 2 than in model 3 and 4. The compounds TBBPA, bisphenol A (BPA), PCP and HCBD were predicted not to bind to gull TTR (Table 13). TBBPA was predicted to not bind to glaucous gull TTR in three of the models, but was just above the threshold in model 3. TBBPA was docked in protonated state, but the scoring value was so low that it is unlikely that it was the reason that TBBPA was expected to not bind in three of the models. However, one of the docked phthalates BBP, was predicted to bind in model 3 and just below threshold of predicted binders in the other three models. The phathalates are not halogenated like the other compounds predicted to bind to TTR, but they have a aromatic ring system like many of the predicted TTR binders and THs. The same phthalate in addition to two others were tested by Ishihara et al. (2003) and all three had a weak effect on T_3 binding in all four species chicken, human, bullfrog (*Rana catesbeiana*) and masu salmon (*Onchorhynchus masou*). The prediction that the bromophenols were good binders is consistent with the study of Morgado et al. (2007) and Meerts et al. (2000). The high binding affinity of TBBPA to human TTR (Meerts et al., 2000) as well as sea bream (Morgado et al., 2007) is inconsistent with the prediction of weak binding or no binding of TBBPA from the docking in the glaucous full TTR models.

The degree of bromine substitution appeared to play an important role for binding affinity. The models of glaucous gull TTR predicted that 2,4-DBP bind with lower affinity than 2,4,6-TBP. Bromophenols with a less degree of bromination also showed lower or no competitive binding to human and sea bream TTR (Meerts et al., 2000, Morgado et al., 2007). This is also consistent with den Besten et al. (1991) and Van Den Berg et al. (1991) studies, with chlorophenols showing an increased interaction of higher chlorinated phenols with human TTR compared with the lower chlorinated. The nature of the halogen substitution also affect the binding affinity of compounds to TTR. PBP was predicted to be a weak binder while PCP were predicted not to bind to glaucous gull TTR when docked in the models. This is consistent with Meerts et al. (2000) result that TBBPA was the most potent competitor with T_4 for binding to human TTR compared to TCBPA with the only difference being that bromine atoms were replaced with chlorine atoms. Higher affinity of brominated analogues over chlorinated analogues was also observed for PBP compared to PCP in human TTR (den Besten et al., 1991, Van den Berg, 1990)

Morgado et al. (2007) study on sea bream recombinant TTR (sbrTTR) found that the brominated flame retardants BDE-49, 47 and 99 were some of the most potent inhibitors of T_3 binding to sbrTTR, while higher brominated PBDEs did not show binding to sbrTTR just as predicted in our models of glaucous gull TTR. In contrast, PBDEs show very low binding affinities to human TTR. The binding ability to human and sea bream TTR was lost when PBDEs have over five bromine substitutions (Hamers et al., 2006, Morgado et al., 2007). The PBDEs have favorable bromine substitution but lack the para hydroxylation found in strong TTR binders. Binding of PBDEs and PCBs to recombinant glaucous gull and sea bream TTR is in consistence with previous studies using bromophenols and non-hydroxylated compounds that show strong binding to TTR even in the absence of OH group interactions (Ghosh et al., 2000). Studies of crystal structures revealed that bromophenols bind to human TTR in a reversed new binding mode where the hydroxyl group does not seem to play an important role, this may explain the TTR binding affinities of the non-hydroxylated PBDEs and PCBs. This is further substantiated by earlier findings on the existence of different binding modes of T_4 to TTR. In the forward mode were the phenolic ring pointing towards the center of the TTR central channel and reversed mode were the phenolic ring pointing towards the entry of the central channel. However, the docking of phenolic compounds in the glaucous gull TTR models predicted that they bind in both forward and revers mode.

The results form the present study differed from previous studies on other organism in the predictions of the binding affinity of some compounds. For example PCP is not predicted to bind to glaucous gull TTR and was a poor binder to sea bream TTR, but experiments has proven that it was a strong binder to human, chicken and bullfrog TTR (Morgado et al., 2007, Ishihara et al., 2003). The models predict that PBP was a weak binder to glaucous gull TTR opposite to the high binding affinity this compound has to human TTR (Meerts et al., 2000, Van den Berg, 1990). Ishihara et al. study on TTR from human, chicken, bullfrog and masu salmon also found differences in binding affinities between the species for other chemicals like diethylstilbestrol (DES) (Ishihara et al., 2003). These observations reinforce the notion of species-specific

difference in TTR binding affinities for EDCs. The reason for the different binding affinities of the compounds remain to be established but it is likely that differences in physiochemical and structural properties are important. It has been revealed that despite amino acid conservation, the shape of the TTR hormone binding channel was different when comparing human, rat, chicken and sea bream TTR (Eneqvist et al., 2004). In addition, the surface potential of TTR from sea bream and chicken appear to be more negative than human or rat TTR (Power et al., 2000). These facts could explain the discrepancies in binding affinities between species. It is also known that the amino acid sequence of the N-terminal is shorter and more hydrophilic in eutherians and longer and more hydrophobic in birds, reptiles, amphibians and fish. The significance of this have been discussed and has been proposed to influence the TH binding properties of TTR (Power et al., 2000, Yamauchi et al., 2000)

5.3 Further studies and possible consequences of binding of contaminants to TTR

OH-PCB and OH-PBDE congeners persistence in the blood of birds and other wildlife has previously been hypothesized to be caused by competitive binding to TH transport proteins and specifically TTR. Competitive binding of OH-PCB and OH-PBDEs has also been proven through experimental studies of recombinant glaucous gull TTR. However, this study predicted that several other compounds also can competitively bind to glaucous gull TTR and therefore possibly affect the THs homeostasis. Further studies will be needed to test experimentally the binding affinity of the new predicted TTR binders, for example with an *in vitro* glaucous gull TTR assay similar to the study by Ucan-Marin et al. (2009). An experimental test would also be a good verification of how good and accurate the constructed homology models are.

Table 14 below list the compounds that were predicted to bind to glaucous gull TTR and found in environmental samples. The PBDEs, PCBs and their metabolites are not in the list but they have all several times been detected in previous studies (Verreault et al., 2007c, Verreault et al., 2007a, Verreault et al., 2005a). Many of the compounds listed have been detected in glaucous gull like most of the PFASs and PFCAs. Several of those not found in glaucous gull have however been found in other seabirds in arctic areas like common eider (*Somateria mollissima*), black-legged kittiwake (*Rissa tridactyla*) and northern fulmar (*Fulmarus glacialis*) which shows that they can bioaccumulate and are subject to long-range transport. Other of the predicted TTR binders have only been found in abiotic samples like sediments or not detected at all. Some of those not detected have hardly been searched for in arctic samples (e.g. the emerging BFRs). For some compounds like the perfluorotelomer alcohols,fluorides, acrylates and methacrylates are also the potential for long-range transport and bioaccumulation uncertain.

Table 14. Contaminants detected in glaucous gull from Svalbard or other samples from the Arctic (year 2004-2015) predicted to bind to glaucous gull TTR

Contaminant	Sample	Year	Reference
PFTeA	Glaucous gull plasma and not eggs from Svalbard and Bjørnøya. Glaucous gull liver from Kongsfjorden, Svalbard	2004 2011	(Verreault et al., 2005b, Mæhre, 2012)
PFTriA	Glaucous gull plasma and eggs from Svalbard and Bjørnøya Glaucous gull egg from Prince Leopold Island, Canadian Arctic. Glaucous gull liver from Kongsfjorden, Svalbard	2004 2008 2011	(Verreault et al., 2005b) (Braune and Letcher, 2013) (Mæhre, 2012)
PFDoA	Glaucous gull plasma and eggs from Svalbard and Bjørnøya	2004	(Verreault et al., 2005b)
PFUnA	Glaucous gull liver from Kongsfjorden, Svalbard. Glaucous gull egg from Prince Leopold Island, Canadian Arctic.Glaucous gull plasma and eggs from Svalbard and Bjørnøya	2011 2008 2004	(Mæhre, 2012) (Braune and Letcher, 2013) (Verreault et al., 2005b)
PFDcA	Glaucous gull plasma and eggs from Svalbard and Bjørnøya. Glaucous gull liver from Barents Sea east of Svalbard.	2004 2004	(Verreault et al., 2005b, Haukås et al., 2007)
PFNA	Glaucous gull plasma and not eggs from Svalbard and Bjørnøya. Glaucous gull liver from Barents Sea east of Svalbard.	2004 2004	(Verreault et al., 2005b, Haukås et al., 2007)
PFOA	Glaucous gull plasma and not eggs from Svalbard and Bjørnøya. Glaucous gull liver from Kongsfjorden, Svalbard	2004 2011	(Verreault et al., 2005b) (Mæhre, 2012)
PFHpA	Northern fulmar eggs from Faroe Island	2004	(Kallenborn et al., 2004)
PFHxA	Glaucous gull liver from Barents Sea east of Svalbard.	2004	(Haukås et al., 2007)
PFPA	Glaucous gull plasma and not eggs from Svalbard and Bjørnøya. Glaucous gull liver from Kongsfjorden, Svalbard	2004 2011	(Verreault et al., 2005b) (Mæhre, 2012)
PFDS	Glaucous gull egg from Prince Leopold Island, Canadian Arctic.	2008	(Braune and Letcher, 2013)
PFOS	Glaucous gull egg from Prince Leopold Island, Canadian Arctic. Glaucous gull liver from Barents Sea east of Svalbard. Glaucous gull plasma and eggs from Svalbard and Bjørneøya	2008 2004 2004	(Braune and Letcher, 2013) (Haukås et al., 2007, Verreault et al., 2005b)
PFHpS	Glaucous gull liver from Kongsfjorden, Svalbard	2011	(Mæhre, 2012)
PFHxS	Glaucous gull egg from Prince Leopold Island, Canadian Arctic. Glaucous gull liver from Barents Sea east of Svalbard. Glaucous gull plasma and eggs from Svalbard and Bjørnøya	2008 2004 2004	(Braune and Letcher, 2013) (Haukås et al., 2007, Verreault et al., 2005b)

N-Me-FOSE	In bile of dabs (*Limanda limanda*) from Iceland and the North Sea	2008	(Ahrens and Ebinghaus, 2010)
N-Et-FOSA	Guillemot (*Uria aalge*) eggs from Iceland, north of Norway and Sweden but not the Faroe Island	2002-2005	(Löfstrand et al., 2008)
N-Me-FOSA	Common eider eggs and european shag (*Phalacrocorax aristotelis*) eggs from Røst and Sklinna, Norway not found in herring gull from same area	2012	(Huber et al., 2014)
10:2 FTOH	Not detected in thick-billed murres (*Uria lomvia*) and northern fulmars from the Canadian Arctic	2007-2008	(Braune et al., 2014)
8:2 FTOH	Not detected in thick-billed murres and northern fulmars from the Canadian Arctic	2007-2008	(Braune et al., 2014)
6:2 FTOH	Not detected in thick-billed murres and northern fulmars from the Canadian Arctic	2007-2008	(Braune et al., 2014)
C8-PFPA	Canadian surface water and wastewater treatment plant.	2004-2007	(D'Eon et al., 2009)
2,4,6-TBP	Found in common eider liver, but not in black-legged kittiwake liver and Brünnich's guillemot *(Uria lomvia)* eggs from Bjørnøya and Kongsfjorden Svalbard	2008-2009	(Sagerup et al., 2010)
2,4-DBP	Found in Atlantic cod (*Gadus morhua*) liver but not in black guillemot (*Cepphus* grylle) eggs Faroe Island	2009	(Schlabach et al., 2011)
BTBPE	Glaucous gull plasma and egg yolk, Bjørnøya Norwegian Arctic.	2006	(Verreault et al., 2007b)
BATE	Black guillemot eggs from Faroe Island	2009	(Schlabach et al., 2011)
ATE	Black guillemot eggs from Faroe Island	2009	(Schlabach et al., 2011)
DPTE	Not found in common eider liver, black-legged kittiwake liver and Brünnich's guillemot eggs from Bjørnøya and Kongsfjorden Svalbard	2008-2009	(Sagerup et al., 2010)
DBDPE	Not found in common eider or black-legged kittiwake liver, but found in Brünnich's guillemot eggs from Bjørnøya and Kongsfjorden Svalbard	2008-2009	(Sagerup et al., 2010)
50594-77-9	Not measured suspected to be moderately volatile and have low bioaccumulation potential	2009	(USEPA, 2009) (Vorkamp and Riget, 2013)
BBP	Found in sediments from Greenland. Found in seawater and air samples from the North Sea to the high Arctic	2004	(Vorkamp and Riget, 2013) (Xie et al., 2007)
TPhP	Black-legged kittiwake and common eider liver, Kongsfjorden and Liefdefjorden, Svalbard	2008	(Evenset Anita, 2009)

The PFCs mainly detected in biota samples from the Arctic and glaucous gull is the PFASs and PFCAs. The highest concentrations of PFCs detected in glaucous gull are of PFOS, and in general do the long chain PFASs and PFCAs dominate. The PFCAs and in particular the long chained congeners are predicted to be the PFCs with highest affinity for TTR. PFCs as a group is not predicted to be as strong TTR binders as the metabolites of PCBs and PBDEs but should still be investigated more thorough given the high levels of some PFASs and PFCAs measured in glaucous gull. The available data on different groups of PFCs is much more scarce, but for the compounds that have been measured the concentrations are lower than for the PFASs and PFCAs or not detected (Table 14). However, more research is necessary. C8-PFPA is a volatile precursor compounds that biologically or in the atmosphere is degraded to fluorotelomer alcohols and perfluorinated sulfonamides (D'Eon et al., 2009). Both N-Et-FOSE, N-Me-FOSE, N-Et-FOSA and N-Me-FOSA have been measured in glaucous gull but found to be below detection levels (Axelson, 2014). The fluorotelomer alcohols are highly volatile and seems to not having been investigated in glaucous gull, but in a study of air samples from Ny-Ålesund were all the FTOHs from this study measured and below the detection level. The FTOHs will hydrolyze to PFCA such as PFOA (Green et al., 2008).

The fluorotelomer acrylates and fluorotelomer methacrylate constitute a group of compounds that are highly volatile and expected to hydrolyze within a few years in the environment. The polymeric acrylates and metacrylates are expected to be hydrolyzed more slowly. Acrylates and methacrylates hydrolyzed into n:m FTOHs with $n \geq 8$ and $m \geq 1$ including their polymers and can therefor lead to release of PFCAs like PFOA (Nielsen, 2014). The fluorotelomer fluorides (POF, PHpF and PBF, Table 13) are extremely corrosive/reactive and quickly hydrolyze to corresponding acids (Howard and Muir, 2010). That these compounds are so reactive and easily hydrolyze means that they probably want accumulate. However, if they are precursor to PFCAs then they are still a potential risk since the PFCAs are predicted to be even stronger binders to TTR. There is need for more data on the propensity of accumulation of PFCA and PFSA precursors and identification of new classes to predict the possible risk of these compounds.

TPhP is a phosphorus flame retardant and has been found in black-legged kittiwake and common eider liver samples from Kongsfjorden and Liefdefjorden, Svalbard. TPhP was predicted in three of the models (model 2, 3 and 4) to bind to TTR. BBP have been detected in sediments samples from Greenland. BCPS have no data from the Arctic, but has been found in herring (*Clupea harengus*), salmon (*Salmo salar*), perch (*Perca fluviatilis*) from the Swedish coast, the inland fish species arctic char (*Salvelinus alpinus*) and grey seal (*Halichoerus gryphus*) and guillemot from the Baltic Sea. The other compounds in Table 13 predicted to bind to glaucous gull TTR, triclocarban, 68399-95-1, 113-14-2, 63734-62-3 and 50594-77-9 have not been search for in samples from the Arctic, and the potential for long-range transport is uncertain. Triclocarban have been found in aquatic environment and can bioaccumulate. 68399-95-1 and 63734-62-3 are persistent, while 113-14-2 and 50594-77-9 are suspected to degrade (Howard and Muir, 2010).

Ucan-Marin et al. (2010) found in their study on recombinant TTR and albumin that the levels of 4-OH-CB187 in free-ranging glaucous gull appeared high enough to effectively displace T_3

or T_4 binding to TTR and thus may have an impact on circulating TH levels. Considering this and all the other predicted TTR binders in the present study it is important to be aware of the potential of the combined effect all these compounds could have together as several of them have been measured in glaucous gull and some even in high concentration. The result form the docking of different POPs in the present study revealed that a large and varied group of compounds could potentially bind to glaucous gull TTR. In combination the compounds can disrupt circulating TH homeostasis via competitive binding with THs to TTR and possibly result in perturbation of the cellular TH levels and/or the ratio of T_3 and T_4 changing the apparent affinity. This would diminish the cellular uptake of THs, and possibly affect TH homeostasis in target tissues depending on the affinity and capacity of TTR for EDCs. There can also be effects on TH-dependent function. For example one possible disruption from the displacement of T_4 from TTR could be less T_4 at target tissue and thus decrease the conservation to active T_3. (Ishihara et al., 2003). The potential in biological effects binding of POPs to glaucous gull TTR remains to be investigated.

Although the TTR amino acid sequence have been conserved through evolution giving high similarity between glaucous gull and human TTR sequences, the human TTR cannot be used as a surrogate to assess the competitive binding effects on circulating THs and how this can potentially affect reproductive, nutritional and physiological processes. The present study and previous showed that there were differences in the binding affinity of THs and several environmentally relevant POPs for both human and glaucous gull TTR (Ucan-Marin et al., 2010, Ishihara et al., 2003). In addition, other TH binding factors can affect the binding affinity among species and in different stages of development (Richardson 1994).

T_4 and particularly the primary metabolically active T_3 are the prime controllers for the regulation of metabolic functions and thermogenesis in mammals and birds. High concentrations of contaminants may alter circulating TH status, basal metabolism and capacity for adaptive thermogenesis. Verreault et al. (2007a) reported for breeding glaucous gulls negative associations between basal metabolic rate and concentrations of PCBs, DDTs and chlordanes. However, levels of THs were not associated significantly with variation of basal metabolic rate or concentrations of blood residue levels of OH-PCBs or OH-PBDEs. Haugerud (2011) on the other hand found that long chained PFCAs were strongly correlated with effects on TH levels, and explained more of the variation in total T_3 than higher concentrations of e.g. PCBs or PFOS. More studies that address competitive binding with THs and TH binding proteins like TTR interactions are needed. Studies that address the differences in species and population such as TH-related effects with TH binding proteins and the potential effect of confounding factors such as physiological status and timing, nutritional status, sensitivity as a function of other stressors (e.g. climate change) deleterious (chronic) effects and environmental factors. All this factors can influence circulating THs levels and subsequently the TH-dependent processes (Ucan-Marin et al., 2010).

To understand the actions of EDCs competitive binding with THs to TTR is there two areas that need to be investigated: 1) possible biological responses and 2) the destiny of chemicals after binding to TTR. Better understanding of the binding with TTR (and other TH transport

proteins) is important with respect to effects on target organs and the thyroid system. For example, TTR may be a transporter for OH-PCBs and OH-PBDEs to TH receptors in the target organs. POPs may displace T_4 from TTR and subsequently release free T_4 which may enhance T_4 metabolism and excretion (Brouwer et al., 1998). A sufficiently increase of T_4 excretion could decrease the circulating T_4 level potentially leading to effects such as hypothyroidism (Ucan-Marin et al., 2009). Studies have for example shown that administration of PCP to rat decrease both plasma TH levels (Van Den Berg et al., 1991) and uptake of T_4 into cerebrospinal fluid (Vanraaij et al., 1994) which could be TTR-mediated. Correlation between TTR-activity and plasma levels of OH-PCBs have also been found in polar bear cubs (Bytingsvik et al., 2013).

The results of Ucan-Marin et al. (2009) suggest that T_3 binding relative to T_4 is less susceptible to competitive displacement by exogenous ligands present in the blood, which mean that T_4 delivery targeting organs like the liver and brain could be more perturbed relative to T_3. However THs synthesizes and release into circulation is primarily of T_4 (95 % T_4, 5 % T_3) the active precursor that subsequently deiodinates to T_3 at the target tissue. Since much more T_4 relative to T_3 is associated with circulating TTR this would suggest that circulating and target organ levels of T_4 would be less sensitive to exogenous ligand competition (Ucan-Marin et al., 2009).

Grimm et al reports that PCB sulfates had weaker interactions with the second binding site which is consistent with the negative cooperativity between the sites that is observed with T_4 (Ferguson et al., 1975). Under physiological conditions concentrations of T_4 are too low to allow binding to the low affinity binding site (Liz et al., 2010). Consequently displacement of T_4 by xenobiotic primarily affect the high affinity binding site *in vivo*, whereas both sites may have relevance in the (inter-tissue) transport and retention of xenobiotics.

In the cerebrospinal fluid, TTR is the only TH transporter, while in serum there are additional transport proteins that contribute in the saturation of TH binding sites of TTR. TTR has additional relevance owing to its function as mediator for the transport of TH across the blood-brain-barrier and may facilitate transport of compounds to the cerebrospinal fluid (Grimm et al., 2013, Brouwer et al., 1998). Also albumin is involved in the transport of THs in the serum. TTR may be of lesser importance because in birds the proportion of circulating TH-binding transport protein is low for TTR. McNabb and Fox (2003) found that in chicken the circulating T_4 is bound 75 % to ALB, 17 % to TTR and 7.5 % to an α-globulin. Ucan-Marin et al. (2010) research on expression and purification of ALB in gull species assess the binding affinities of PCB, PBDE and MeO-metabolites to be stronger to recALB from gull than from recTTR, while it was opposite for the OH-metabolites. This indicate that binding to albumin may potentially have a stronger effect on TH system.

When EDCs are bound to TTR they can be mediated by receptors on cell surfaces and metabolized in the cells (Sousa and Saraiva, 2001). Another possibility is a receptor-mediate pathway found in chicken oocytes where TTR accumulates in the yolk (Vieira et al., 1995). Chemicals transported into the yolk by TTR are of high risk to developing embryos. This could

also possibly happen in glaucous gull and should be investigated. These pathways give different biological outcomes and it is therefore important to elucidate the tissue distribution of chemicals bound to TTR.

TTR also function in maintain of retinol levels in plasma through interactions with retinol binding protein (RBP) (Robbins, 1996). POPs could potentially disrupt the retinol transport or formation of RBP-TTR complexes in glaucous gull. Brouwer and Vandenberg (1986) found that a metabolite of 3,4,3´,4´-tetrachlorobiphenyl interacted directly with TTR and inhibited the formation of the TTR-RBP complex leading to reduced serum vitamin A transport. A reduction in plasma retinol level was also reported in the common seals fed PCP-contaminated fish and their levels of total T_4, free T_4 and total T_3 also decreased (Brouwer et al., 1989). However Ishihara et al. (2003) found that none of the chemicals (10 µM) investigated including 2,4,6-TBP and PCP prevented formation of the TTR-RBP complex in human bullfrog, chicken and masu salmon. This discrepancy might be due to species-specific or ligand-dependent differences in the conformation of the TTR-RBP complex. In mammals, OH-PCB binding affinity to TTR has been link to alterations of THs and vitamin A levels in exposed laboratory rats (Hallgren et al., 2001, Hallgren and Darnerud, 2002). OH-PCB congeners have also been shown to bind to the human TH receptor (You et al., 2006). Mæhre (2012) predicted through molecular modelling that long chained PFCAs, OH-PCB and OH-PBDE would bind to TR in glaucous gull. Kimura-Kuroda et al. (2005) reported that 4´-OH-CB106 and 4´-OH-CB159 inhibited T_3-dependent extension of Purkinje cell dendrites extracted from mouse cerebellum *in vitro*. It has been hypothesized that binding of PCBs to TTR is a major contributing factor for the reduction in circulating THs and for certain biological effects related to PCB exposure. For example certain neurological effects of PCB may be the result of altered TH availability to critical tissue and cellular systems (Chauhan et al., 2000).

As a continuation of this study the binding affinity of the compounds predicted to bind to glaucous gull TTR should be studied by *in vitro* competitive binding assays. Measurements of the concentration levels of these compounds in glaucous gull should also be done. In that way it can be determined if the compounds potentially could displace THs in wild populations of glaucous gull living in the Arctic. Further on, one can see whether the compounds will be correlated with the level of circulating THs and the ratio between T_4 and T_3. It would also be very interesting to investigate whether changes in TH-dependent functions could be associated with binding of compounds to TTR or to any of the other TH transport proteins in serum of glaucous gull.

.

6. CONCLUSION

The docking of the contaminant data set in the four constructed glaucous gull homology models predicted that structurally dissimilar compound such as PCB, OH-PCB, $MeSO_2$-PCB, PBDEs, OH-PBDEs, MeO-PBDEs, bromophenols, BATE, BTBPE, ATE, DPTE, triclocarban, TPhP, 68399-95-1, 63734-62-3, 5059-77-9 and several PFCs (e.g. PFCAs, PFASs, fluorotelomer acrylate, methacrylate and fluorides) can bind to glaucous gull TTR inside the THs binding site in the central channel.

All the compounds predicted to bind to TTR were halogenated except BBP and TPhP. The present of functional groups on the compounds such as hydroxyl groups were predicted to increase the binding affinity for the TH binding site, and in case the functional groups were ionized was the binding affinity predicted to further increase. However, the high scores of PBDEs indicate that hydroxylation or other functional groups are not necessary for the compounds to bind to TTR. The models also predicted that brominated analogues had higher affinity to TTR than the corresponding chlorinated analogues. T_3 were predicted to bind stronger to TTR than T_4, and the THs bound to the binding site in both forward and revers mode. The docked compounds were also predicted to bind in both forward and reverse binding modes and had hydrogen-bonding interactions with the amino acids Lys15 and Ser117. The predicted binding affinity for some compounds like PCP and TBBPA differ from the results of competitive binding to TTR in other species- This indicate that there is species-specific difference in binding of compounds to TTR. The docking of THs and the ROC-curves from the docking of the test set showed that the constructed homology models of glaucous gull TTR are accurate in the predictions of whether a compound will bind to glaucous gull TTR or not.

Competitive binding of the POPs with TTR in glaucous gull can potentially disrupt circulation THs and possibly affect the TH homeostasis and TH-dependent function. The potential effects are predicted to be many. This study predicted that a diverse group of chemicals could bind to glaucous gull TTR competing with THs. Many of these chemicals have been detected in samples from glaucous gull as well. The POPs not yet detected should be measured in sample from glaucous gull. Further studies should investigated the binding affinity of the compound to TTR and their potential of competitive displacement of TH in the binding site of TTR. Studies looking at the potential effects on individual and population level of POPs binding to TTR are also necessary.

REFERENCES

ABAGYAN, R., TOTROV, M. & KUZNETSOV, D. 1994. ICM - A New Method for Protein Modeling and Design: Applications to Docking and Structure Predictions from the Distorted Native Conformation. *Journal of Computational Chemistry,* 15**,** 488-506.

AHRENS, L. & EBINGHAUS, R. 2010. Spatial distribution of polyfluoroalkyl compounds in dab (Limanda limanda) bile fluids from Iceland and the North Sea. *Marine Pollution Bulletin,* 60**,** 145-148.

AXELSON, S. 2014. *Perfluoroalkyl substances in Arctic birds - a comparison between glaucous gull nd black guillemots from svalbard.* Master, Swedish University of Agricultural Sciences and University Center of Svalbard.

BANERJEE, A., BAIRAGYA, H. R., MUKHOPADHYAY, B. P., NANDI, T. K. & MISHRA, D. K. 2013. Conserved water mediated H-bonding dynamics of Ser117 and Thr119 residues in human transthyretin-thyroxin complexation: Inhibitor modeling study through docking and molecular dynamics simulation. *Journal of Molecular Graphics & Modelling,* 44**,** 70-80.

BAURES, P. W., PETERSON, S. A. & KELLY, J. W. 1998. Discovering transthyretin amyloid fibril inhibitors by limited screening. *Bioorganic & medicinal chemistry,* 6**,** 1389-1401.

BENTLEY, P. J. 1998. *Comparative vertebrate endocrinology,* Cambridge University Press.

BIFFINGER, J. C., KIM, H. W. & DIMAGNO, S. G. 2004. The polar hydrophobicity of fluorinated compounds. *ChemBioChem,* 5**,** 622-627.

BLAKE, C. C. F., GEISOW, M. J., OATLEY, S. J., RERAT, B. & RERAT, C. 1978. Structure of Pre-Albumin: Secondary, Tertiary and Quaternary Interactions Determined by Fourier Refinement at 1.8-A. *Journal of Molecular Biology,* 121**,** 339-356.

BORGA, K., GABRIELSEN, G. W. & SKAARE, J. U. 2001. Biomagnification of organochlorines along a Barents Sea food chain. *Environmental Pollution,* 113**,** 187-198.

BOURNE, W. R. P. & BOGAN, J. A. 1972. Polychlorinated Biphenyls in North Atlantic Seabirds. *Marine Pollution Bulletin,* 3**,** 171-175.

BRAUNE, B. M. & LETCHER, R. J. 2013. Perfluorinated Sulfonate and Carboxylate Compounds in Eggs of Seabirds Breeding in the Canadian Arctic: Temporal Trends (1975-2011) and Interspecies Comparison. *Environmental Science & Technology,* 47**,** 616-624.

BRAUNE, B. M., GASTON, A. J., LETCHER, R. J., GILCHRIST, H. G., MALLORY, M. L. & PROVENCHER, J. F. 2014. A geographical comparison of chlorinated, brominated and fluorinated compounds in seabirds breeding in the eastern Canadian Arctic. *Environmental research,* 134**,** 46-56.

BROUWER, A. & VANDENBERG, K. J. 1986. Binding of a Metabolite of 3,4,3´,4´-Tetrachlorobiphenyl to Transthyretin Reduces Serum Vitamin-A Transport by Inhibiting the Formation of the Protein Complex Carrying Both Retinol and Thyroxine. *Toxicology and Applied Pharmacology,* 85**,** 301-312.

BROUWER, A., REIJNDERS, P. J. H. & KOEMAN, J. H. 1989. Polychlorinated Biphenyls (PCB)-Contaminated Fish Induces Vitamin-A and Thyroid-Hormone Deficiency in the Common Seal (*Phoca vitulina*). *Aquatic Toxicology,* 15**,** 99-105.

BROUWER, A., MORSE, D. C., LANS, M. C., SCHUUR, A. G., MURK, A. J., KLASSON-WEHLER, E., BERGMAN, A. & VISSER, T. J. 1998. Interactions of persistent environmental organohalogens with the thyroid hormone system: Mechanisms and

possible consequences for animal and human health. *Toxicology and Industrial Health,* 14**,** 59-84.
BURGER, J., KANNAN, K., GIESY, J., GRUE, C., GOCHFELD, M. & DELL'OMO, G. 2002. Effects of environmental pollutants on avian behaviour. *Behavioural ecotoxicology***,** 337-375.
BURKOW, I. C. & KALLENBORN, R. 2000. Sources and transport of persistent pollutants to the Arctic. *Toxicology Letters,* 112**,** 87-92.
BURSULAYA, B. D., TOTROV, M., ABAGYAN, R. & BROOKS, C. L. 2003. Comparative study of several algorithms for flexible ligand docking. *Journal of Computer-Aided Molecular Design,* 17**,** 755-763.
BUSTNES, J. O., ERIKSTAD, K. E., BAKKEN, V., MEHLUM, F. & SKAARE, J. U. 2000. Feeding ecology and the concentration of organochlorines in glaucous gulls. *Ecotoxicology,* 9**,** 179-186.
BUSTNES, J. O., ERIKSTAD, K. E., SKAARE, J. U., BAKKEN, V. & MEHLUM, F. 2003. Ecological effects of organochlorine pollutants in the Arctic: A study of the Glaucous Gull. *Ecological Applications,* 13**,** 504-515.
BUSTNES, J. O., HANSSEN, S. A., FOLSTAD, I., ERIKSTAD, K. E., HASSELQUIST, D. & SKAARE, J. U. 2004. Immune function and organochlorine pollutants in arctic breeding glaucous gulls. *Archives of Environmental Contamination and Toxicology,* 47**,** 530-541.
BUSTNES, J. O., FAUCHALD, P., TVERAA, T., HELBERG, A. & SKAARE, J. U. 2008. The potential impact of environmental variation on the concentrations and ecological effects of pollutants in a marine avian top predator. *Environment International,* 34**,** 193-201.
BYTINGSVIK, J., SIMON, E., LEONARDS, P. E. G., LAMOREE, M., LIE, E., AARS, J., DEROCHER, A. E., WIIG, O., JENSSEN, B. M. & HAMERS, T. 2013. Transthyretin-Binding Activity of Contaminants in Blood from Polar Bear (*Ursus maritimus*) Cubs. *Environmental Science & Technology,* 47**,** 4778-4786.
CAO, J., LIN, Y., GUO, L.-H., ZHANG, A.-Q., WEI, Y. & YANG, Y. 2010. Structure-based investigation on the binding interaction of hydroxylated polybrominated diphenyl ethers with thyroxine transport proteins. *Toxicology,* 277**,** 20-28.
CHANG, L., MUNRO, S. L. A., RICHARDSON, S. J. & SCHREIBER, G. 1999. Evolution of thyroid hormone binding by transthyretins in birds and mammals. *European Journal of Biochemistry,* 259**,** 534-542.
CHAUHAN, K. R., KODAVANTI, P. R. S. & MCKINNEY, J. D. 2000. Assessing the role of ortho-substitution on polychlorinated biphenyl binding to transthyretin, a thyroxine transport protein. *Toxicology and Applied Pharmacology,* 162**,** 10-21.
CHOTHIA, C. & LESK, A. M. 1986. The Realtion Beetween the Divergence of sequence and Structure in Proteins. *Embo Journal,* 5**,** 823-826.
CODY, V. 2002. Mechanisms of molecular recognition: Crystal structure analysis of human and rat transthyretin inhibitor complexes. *Clinical Chemistry and Laboratory Medicine,* 40**,** 1237-1243.
COLBORN, T., SAAL, F. S. V. & SOTO, A. M. 1993. Developmental Effects of Endocrine-Disrupting Chemicals in Wildlife and Humans. *Environmental Health Perspectives,* 101**,** 378-384.
COLLAZO, A. M. G., KOEHLER, K. F., GARG, N., FARBEGARDH, M., HUSMAN, B., YE, L., LJUNGGREN, J., MELLSTROM, K., SANDBERG, J., GRYNFARB, M., AHOLA, H. & MALM, J. 2006. Thyroid receptor ligands. Part 5: Novel bicyclic agonist ligands selective for the thyroid hormone receptor beta. *Bioorganic & Medicinal Chemistry Letters,* 16**,** 1240-1244.

D'EON, J. C., CROZIER, P. W., FURDUI, V. I., REINER, E. J., LIBELO, E. L. & MABURY, S. A. 2009. Perfluorinated Phosphonic Acids in Cadian Surface Waters and Wastewater Treatment Plant Effluent: Discovery of a New Class of Perfluorinated Acids. *Environmental Toxicology and Chemistry,* 28**,** 2101-2107.

DAMSTRA, T., BARLOW, S., BERGMAN, Å., KAVLOCK, R. & VAN DER KRAAK, G. 2002. Global Assessment of the-State of-the-Science of Endocrine Diruptors. Geneva: World Health Organization, International Programme on Chemical Safety

DARRAS, V. M., MOL, K. A., VAN DER GEYTEN, S. & KUHN, E. R. 1998. Control of peripheral thyroid hormone levels by activating and inactivating deiodinases. *In:* VAUDRY, H., TONON, M. C., ROUBOS, E. W. & DELOOF, A. (eds.) *Trends in Comparative Endocrinology and Neurobiology: From Molecular to Integrative Biology.*

DAWSON, A. 2000. Mechanisms of endocrine disruption with particular reference to occurrence in avian wildlife: A review. *Ecotoxicology,* 9**,** 59-69.

DE WIT, C., FISK, A, HOBBS, K, MUIR, D, GABRIELSEN, G, KALLENBORN, R, KRAHN, M, NORSTROM, R, SKAARE, J 2004. AMAP Assessment 2002: Persistent Organic Pollutants in the Arctic. Arctic Monitoring and Assessment Programme report. Oslo, Norway.

DE WIT, C. A., HERZKE, D. & VORKAMP, K. 2010. Brominated flame retardants in the Arctic environment - trends and new candidates. *Science of the Total Environment,* 408**,** 2885-2918.

DEN BESTEN, C., VET, J. J., BESSELINK, H. T., KIEL, G. S., VAN BERKEL, B. J. M., BEEMS, R. & VAN BLADEREN, P. J. 1991. THE LIVER, KIDNEY, AND THYROID TOXICITY OF CHLORINATED BENZENES. *Toxicology and Applied Pharmacology,* 111**,** 69-81.

DICKSON, P. W., ALDRED, A. R., MENTING, J. G. T., MARLEY, P. D., SAWYER, W. H. & SCHREIBER, G. 1987. Thyroxine Transport in Choroid-Plexus. *Journal of Biological Chemistry,* 262**,** 13907-13915.

ENEQVIST, T., LUNDBERG, E., KARLSSON, A., HUANG, S. H., SANTOS, C. R. A., POWER, D. M. & SAUER-ERIKSSON, A. E. 2004. High resolution crystal structures of piscine transthyretin reveal different binding modes for triiodothyronine and thyroxine. *Journal of Biological Chemistry,* 279**,** 26411-26416.

EVENSET ANITA, L. H., CHRISTENSEN GUTTORM N., WARNER NICHOLAS, REMBERGER MIKAHEL, GABRILSEN GEIR WING 2009. Screening of new contaminants in samples from the Norwegian Arctic. *SPFO-report 1049/2009.* Norwegian Pollution Control Authority: Akvaplan-niva.

FERGUSON, R. N., EDELHOCH, H., SAROFF, H. A. & ROBBINS, J. 1975. Negative Cooperativity in Binding of Thyroxine to Human-Serum Prealbumin. *Biochemistry,* 14**,** 282-289.

GABRIELSEN, G. W. 2007. Levels and effects of persistent organic pollutants in arctic animals. *Arctic alpine ecosystems and people in a changing environment.* Springer.

GABRIELSEN, M. 2011. *Structure, function and inhibition of the serotonin transporter studied by molecular docking, -dynamics and virtual screening.* Philosophiae Doctor, University of Tromsø.

GHOSH, M., MEERTS, I. A., COOK, A., BERGMAN, A., BROUWER, A. & JOHNSON, L. N. 2000. Structure of human transthyretin complexed with bromophenols: a new mode of binding. *Acta Crystallographica Section D: Biological Crystallography,* 56**,** 1085-1095.

GIESY, J. P., FEYK, L. A., JONES, P. D., KANNAN, K. & SANDERSON, T. 2003. Review of the effects of endocrine-disrupting chemicals in birds. *Pure and Applied Chemistry,* 75**,** 2287-2303.

GREEN, N., SCHLABACH, M., BAKKE, T., BREVIK, E. M., DYE, C., HERZKE, D., HUBER, S., PLOSZ, B., REMBERGER, M., SCHØYEN, M., UGGERUD, H. T. & VOGELSANG, C. 2008. Screening of selected metals and new organic contaminants 2007. *Rapport 1014/2008.* Norwegian Pollution Control Authority: Norwegian Institute for Water Research.

GRIMM, F. A., LEHMLER, H.-J., HE, X., ROBERTSON, L. W. & DUFFEL, M. W. 2013. Sulfated Metabolites of Polychlorinated Biphenyls Are High-Affinity Ligands for the Thyroid Hormone Transport Protein Transthyretin. *Environmental Health Perspectives,* 121**,** 657-662.

GUPTA, S., CHHIBBER, M., SINHA, S. & SUROLIA, A. 2007. Design of mechanism-based inhibitors of transthyretin amyloidosis: Studies with biphenyl ethers and new structural templates. *Journal of Medicinal Chemistry,* 50**,** 5589-5599.

HADLEY, M. E. 1996. *Endocrinology,* New Jersey, Prentice Hall.

HALLGREN, S. & DARNERUD, P. O. 2002. Polybrominated diphenyl ethers (PBDEs), polychlorinated biphenyls (PCBs) and chlorinated paraffins (CPs) in rats - testing interactions and mechanisms for thyroid hormone effects. *Toxicology,* 177**,** 227-243.

HALLGREN, S., SINJARI, T., HAKANSSON, H. & DARNERUD, P. O. 2001. Effects of polybrominated diphenyl ethers (PBDEs) and polychlorinated biphenyls (PCBs) on thyroid hormone and vitamin A levels in rats and mice. *Archives of Toxicology,* 75**,** 200-208.

HAMERS, T., KAMSTRA, J. H., SONNEVELD, E., MURK, A. J., KESTER, M. H. A., ANDERSSON, P. L., LEGLER, J. & BROUWER, A. 2006. In vitro profiling of the endocrine-disrupting potency of brominated flame retardants. *Toxicological Sciences,* 92**,** 157-173.

HAMERS, T., KAMSTRA, J. H., SONNEVELD, E., MURK, A. J., VISSER, T. J., VAN VELZEN, M. J., BROUWER, A. & BERGMAN, Å. 2008. Biotransformation of brominated flame retardants into potentially endocrine-disrupting metabolites, with special attention to 2, 2′, 4, 4′-tetrabromodiphenyl ether (BDE-47). *Molecular nutrition & food research,* 52**,** 284-298.

HAUGERUD, A. J. 2011. *Levels and Effects of Organohalogenated Contaminants onThyroid Hormone Levels in Glaucous Gulls (Larus hyperboreus) from Kongsfjorden, Svalbard.* Master thesis Master thesis in Environmental Toxicology and Chemistry, Norwegian University of Science and Technology.

HAUKÅS, M., BERGER, U., HOP, H., GULLIKSEN, B. & GABRIELSEN, G. W. 2007. Bioaccumulation of per- and polyfluorinated alkyl substances (PFAS) in selected species from the Barents Sea food web. *Environmental Pollution,* 148**,** 360-371.

HENRIKSEN, E. O., GABRIELSEN, G. W., TRUDEAU, S., WOLKERS, J., SAGERUP, K. & SKAARE, J. U. 2000. Organochlorines and possible biochemical effects in glaucous gulls (*Larus hyperboreus*) from Bjørnøya, the Barents sea. *Archives of Environmental Contamination and Toxicology,* 38**,** 234-243.

HOUDE, M., MARTIN, J. W., LETCHER, R. J., SOLOMON, K. R. & MUIR, D. C. G. 2006. Biological monitoring of polyfluoroalkyl substances: A review. *Environmental Science & Technology,* 40**,** 3463-3473.

HOWARD, P. H. & MUIR, D. C. G. 2010. Identifying New Persistent and Bioaccumulative Organics Among Chemicals in Commerce. *Environmental Science & Technology,* 44**,** 2277-2285.

HUANG, S.-Y., GRINTER, S. Z. & ZOU, X. 2010. Scoring functions and their evaluation methods for protein-ligand docking: recent advances and future directions. *Physical Chemistry Chemical Physics,* 12**,** 12899-12908.
HUBER, S., NYGÅRD, T., WARNER, N., REMBERGER, M., HARJU, M., UGGERUD, H. T., KAJ, L., SCHLABACH, M. & HANSSEN, L. 2014. Kartlegging av miljøgifter i sjøfuglegg fra Sklinna og Røst. *In:* MILJØDIREKTORATET (ed.). Norskinstitutt for luftforskning.
HÖLTJE, H.-D. & FOLKERS, G. 2008. *Molecular modeling: basic principles and applications*, John Wiley & Sons.
ISHIHARA, A., SAWATSUBASHI, S. & YAMAUCHI, K. 2003. Endocrine disrupting chemicals: interference of thyroid hormone binding to transthyretins and to thyroid hormone receptors. *Molecular and Cellular Endocrinology,* 199**,** 105-117.
JENSSEN, B. M. 2006. Endocrine-disrupting chemicals and climate change: A worst-case combination for arctic marine mammals and seabirds? *Environmental Health Perspectives,* 114**,** 76-80.
JONES, P. D., HU, W., DE COEN, W., NEWSTED, J. L. & GIESY, J. P. 2003. Binding of perfluorinated fatty acids to serum proteins. *Environmental Toxicology and Chemistry,* 22**,** 2639-2649.
KALLENBORN, R., BERGER, U. & JÄRNBERG, U. 2004. *Perfluorinated alkylated substances (PFAS) in the Nordic environment*, Nordic Council of Ministers.
KELLY, B. C., IKONOMOU, M. G., BLAIR, J. D. & GOBAS, F. A. P. C. 2008. Hydroxylated and methoxylated polybrominated diphenyl ethers in a Canadian Arctic marine food web. *Environmental Science & Technology,* 42**,** 7069-7077.
KIMURA-KURODA, J., NAGATA, I. & KURODA, Y. 2005. Hydroxylated metabolites of polychlorinated biphenyls inhibit thyroid-hormone-dependent extension of cerebellar Purkinje cell dendrites. *Developmental Brain Research,* 154**,** 259-263.
KUDO, N. & KAWASHIMA, Y. 2003. Toxicity and toxicokinetics of perfluorooctanoic acid in humans and animals. *The Journal of toxicological sciences,* 28**,** 49-57.
LANS, M. C., KLASSON-WEHLER, E., WILLEMSEN, M., MEUSSEN, E., SAFE, S. & BROUWER, A. 1993. Structure-dependent, competitive interaction of hydroxy-polychlorobiphenyls, -dibenzo-p-dioxins and -dibenzofurans with human transthyretin. *Chemico-Biological Interactions,* 88**,** 7-21.
LAU, C., ANITOLE, K., HODES, C., LAI, D., PFAHLES-HUTCHENS, A. & SEED, J. 2007. Perfluoroalkyl acids: A review of monitoring and toxicological findings. *Toxicological Sciences,* 99**,** 366-394.
LAU, C., THIBODEAUX, J. R., HANSON, R. G., ROGERS, J. M., GREY, B. E., STANTON, M. E., BUTENHOFF, J. L. & STEVENSON, L. A. 2003. Exposure to perfluorooctane sulfonate during pregnancy in rat and mouse. II: postnatal evaluation. *Toxicological Sciences,* 74**,** 382-392.
LEACH, A. R., SHOICHET, B. K. & PEISHOFF, C. E. 2006. Prediction of protein-ligand interactions. Docking and scoring: Successes and gaps. *Journal of Medicinal Chemistry,* 49**,** 5851-5855.
LEATHERLAND, J. F. 2000. *Environmental Endocrine Disrupters: A Evolutionary Perspective* New York, Taylor and Francis.
LETCHER, R. J., BUSTNES, J. O., DIETZ, R., JENSSEN, B. M., JORGENSEN, E. H., SONNE, C., VERREAULT, J., VIJAYAN, M. M. & GABRIELSEN, G. W. 2010. Exposure and effects assessment of persistent organohalogen contaminants in arctic wildlife and fish. *Science of the Total Environment,* 408**,** 2995-3043.

LETCHER, R. J., KLASSON-WEHLER, E. & BERGMAN, A. 2000. Methyl sulfone and hydroxylated metabolites of polychlorinated biphenyls. *Volume 3 Anthropogenic Compounds Part K.* Springer.

LINDIN, I., WUXIUER, Y., KUFAREVA, I., ABAGYAN, R., MOENS, U., SYLTE, I. & RAVNA, A. W. 2013. Homology modeling and ligand docking of Mitogen-activated protein kinase-activated protein kinase 5 (MK5). *Theoretical Biology and Medical Modelling,* 10.

LIZ, M. A., MAR, F. M., FRANQUINHO, F. & SOUSA, M. M. 2010. Aboard Transthyretin: From Transport to Cleavage. *Iubmb Life,* 62**,** 429-435.

LUEBKER, D. J., HANSEN, K. J., BASS, N. M., BUTENHOFF, J. L. & SEACAT, A. M. 2002. Interactions of flurochemicals with rat liver fatty acid-binding protein. *Toxicology,* 176**,** 175-185.

LÖFSTRAND, K., JORUNDSDOTTIR, H., TOMY, G., SVAVARSSON, J., WEIHE, P., NYGARD, T. & BERGMAN, A. 2008. Spatial trends of polyfluorinated compounds in guillemot (Uria aalge) eggs from North-Western Europe. *Chemosphere,* 72**,** 1475-1480.

MARTIN, J. W., MABURY, S. A., SOLOMON, K. R. & MUIR, D. C. G. 2003. Bioconcentration and tissue distribution of perfluorinated acids in rainbow trout (Oncorhynchus mykiss). *Environmental Toxicology and Chemistry,* 22**,** 196-204.

MARTIN, J. W., SMITHWICK, M. M., BRAUNE, B. M., HOEKSTRA, P. F., MUIR, D. C. G. & MABURY, S. A. 2004. Identification of long-chain perfluorinated acids in biota from the Canadian Arctic. *Environmental Science & Technology,* 38**,** 373-380.

MCNABB, F. M. A. & FOX, G. A. 2003. Avian thyroid development in chemically contaminated environments: is there evidence of alterations in thyroid function and development? *Evolution & Development,* 5**,** 76-82.

MEERTS, I., VAN ZANDEN, J. J., LUIJKS, E. A. C., VAN LEEUWEN-BOL, I., MARSH, G., JAKOBSSON, E., BERGMAN, A. & BROUWER, A. 2000. Potent competitive interactions of some brominated flame retardants and related compounds with human transthyretin in vitro. *Toxicological Sciences,* 56**,** 95-104.

MONACO, H. L., MANCIA, F., RIZZI, M. & CODA, A. 1994. Crystallization of the Macromolecular Complex Transthyretin-Retinol-Binding Protein. *Journal of Molecular Biology,* 244**,** 110-113.

MORGADO, I., HAMERS, T., VAN DER VEN, L. & POWER, D. M. 2007. Disruption of thyroid hormone binding to sea bream recombinant transthyretin by ioxinyl and polybrominated diphenyl ethers. *Chemosphere,* 69**,** 155-163.

MUZIOL, T., CODY, V., LUFT, J. R., PANGBORN, W. & WOJTCZAK, A. 2001a. Complex of rat transthyretin with tetraiodothyroacetic acid refined at 2.1 and 1.8 angstrom resolution. *Acta Biochimica Polonica,* 48**,** 877-884.

MUZIOL, T., CODY, V. & WOJTCZAK, A. 2001b. Comparison of binding interactions of dibromoflavonoids with transthyretin. *Acta Biochimica Polonica,* 48**,** 885-892.

MYSINGER, M. M., CARCHIA, M., IRWIN, J. J. & SHOICHET, B. K. 2012. Directory of Useful Decoys, Enhanced (DUD-E): Better Ligands and Decoys for Better Benchmarking. *Journal of Medicinal Chemistry,* 55**,** 6582-6594.

MÆHRE, S. 2012. *Binding of Persistent Organic Pollutants to Thyroid Hormone Receptors in Glaucous Gull (Larus hyperboreus).* master thesis Biomedicine, University of Tromsø.

NABUURS, S. B., WAGENER, M. & DE VLIEG, J. 2007. A flexible approach to induced fit docking. *Journal of medicinal chemistry,* 50**,** 6507-6518.

NIELSEN, C. J. 2014. Potential Precursors PFOA. *M-231.* Miljødirektoratet: University of Oslo.

OATLEY, S. J., BLANEY, J. M., LANGRIDGE, R. & KOLLMAN, P. A. 1984. Molecular-mechanical studies of hormone–protein interactions: The interaction of T4 and T3 with prealbumin. *Biopolymers,* 23**,** 2931-2941.

PALANINATHAN, S. K. 2012. Nearly 200 X-Ray Crystal Structures of Transthyretin: What Do They Tell Us About This Protein and the Design of Drugs for TTR Amyloidoses? *Current Medicinal Chemistry,* 19**,** 2324-2342.

PEAKALL, D. 1992. Thyroid function, retinols, haem and regulatory enzymes. *In:* PEAKALL, D. (ed.) *Animal Biomarkers as Pollution Indicators.* Netherlands: Springer.

POWER, D. M., ELIAS, N. P., RICHARDSON, S. J., MENDES, J., SOARES, C. M. & SANTOS, C. R. A. 2000. Evolution of the thyroid hormone-binding protein, transthyretin. *General and Comparative Endocrinology,* 119**,** 241-255.

PRAPUNPOJ, P., LEELAWATWATANA, L., SCHREIBER, G. & RICHARDSON, S. J. 2006. Change in structure of the N-terminal region of transthyretin produces change in affinity of transthyretin to T4 and T3. *Febs Journal,* 273**,** 4013-4023.

RAVNA, A. W. & SYLTE, I. 2012. Homology modeling of transporter proteins (carriers and ion channels). *Methods in molecular biology* 857**,** 281-99.

REN, X. M. & GUO, L.-H. 2012. Assessment of the Binding of Hydroxylated Polybrominated Diphenyl Ethers to Thyroid Hormone Transport Proteins Using a Site-Specific Fluorescence Probe. *Environmental Science & Technology,* 46**,** 4633-4640.

RICHARDSON, S. J., BRADLEY, A. J., DUAN, W., WETTENHALL, R. E. H., HARMS, P. J., BABON, J. J., SOUTHWELL, B. R., NICOL, S., DONNELLAN, S. C. & SCHREIBER, G. 1994. Evolution of Marsupial and other Vertebrate Thyroxine-Binding Plasma-Proteins *American Journal of Physiology,* 266**,** R1359-R1370.

RICKENBACHER, U., MCKINNEY, J. D., OATLEY, S. J. & BLAKE, C. C. F. 1986. STRUCTURALLY SPECIFIC BINDING OF HALOGENATED BIPHENYLS TO THYROXINE TRANSPORT PROTEIN. *Journal of Medicinal Chemistry,* 29**,** 641-648.

ROBBINS, J. 1996. Thyroid hormones transport proteins and the physiology of hormone binding. *In:* BRAVERMAN, L. E. & UTIGER, R. D. (eds.) *Werner & Ingbar´s TheThyroid: A Fundamental and Clinical Text.* 7th ed.

ROLLAND, R. M. 2000. A review of chemically-induced alterations in thyroid and vitamin A status from field studies of wildlife and fish. *Journal of Wildlife Diseases,* 36**,** 615-635.

SAGERUP, K., HERZKE, D., HARJU, M., EVENSET, A., CHRISTENSEN, G. N., ROUTTI, H., FUGLEI, E., AARS, J., STRØM, H. & GABRIELSEN, G. W. 2010. New brominated flame retardants in Arctic biota. *Rapportnr 1070/2010.* Klima- og forurensningsdirektoratet.

SCHAPIRA, M., ABAGYAN, R. & TOTROV, M. 2003. Nuclear hormone receptor targeted virtual screening. *Journal of Medicinal Chemistry,* 46**,** 3045-3059.

SCHLABACH, M., REMBERGE, M., BRORSTRÖM-LUNDÉN, KARIN, N., KAJ, L., HANNA, A., HERZKE, D., ANDERS, B. & HARJU, M. 2011. Brominated flame retardants (BFR) in the Nordic environment. *TeamNord 2011:528.* Nordic Council of Ministers.

SCHREIBER, G. 2002. The evolutionary and integrative roles of transthyretin in thyroid hormone homeostasis. *Journal of Endocrinology,* 175**,** 61-73.

SCHUSSLER, G. C. 2000. The thyroxine-binding proteins *Thyroid,* 10**,** 141-149.

SEACAT, A. M., THOMFORD, P. J., HANSEN, K. J., CLEMEN, L. A., ELDRIDGE, S. R., ELCOMBE, C. R. & BUTENHOFF, J. L. 2003. Sub-chronic dietary toxicity of potassium perfluorooctanesulfonate in rats. *Toxicology,* 183**,** 117-131.

SHERMAN, W., DAY, T., JACOBSON, M. P., FRIESNER, R. A. & FARID, R. 2006. Novel procedure for modeling ligand/receptor induced fit effects. *Journal of Medicinal Chemistry,* 49**,** 534-553.

SOUSA, M. M. & SARAIVA, M. J. 2001. Internalization of transthyretin - Evidence of a novel yet unidentified receptor-associated protein (RAP)-sensitive receptor. *Journal of Biological Chemistry,* 276**,** 14420-14425.

STRØM, H. 2006. Glaucous gull. *In:* KOVACS, K. M., LYDERSEN, C. (ed.) *Birds and mammals of Svalbard.* Norwegian Polar Institute.

STRØM, H. 2007. Distribution of seabirds on Bjørnøya. *In:* ANKER-NILSSEN T., B. R. T., BUSTNES J.O., ERIKSTAD K.E., FAUCHALD P., LORENTSEN S.-H., STEEN H., STRØM H., SYSTAD G.H., TVERAA T. (ed.) *SEAPOP studies in the Lofoten and Barents Sea area in 2006. Report no. 249.* Tromsø: Norwegian Institute for Nature Research (NINA).

SUH, E. H., LIU, Y., CONNELLY, S., GENEREUX, J. C., WILSON, I. A. & KELLY, J. W. 2013. Stilbene Vinyl Sulfonamides as Fluorogenic Sensors of and Traceless Covalent Kinetic Stabilizers of Transthyretin That Prevent Amyloidogenesis. *Journal of the American Chemical Society,* 135**,** 17869-17880.

THIBODEAUX, J. R., HANSON, R. G., ROGERS, J. M., GREY, B. E., BARBEE, B. D., RICHARDS, J. H., BUTENHOFF, J. L., STEVENSON, L. A. & LAU, C. 2003. Exposure to perfluorooctane sulfonate during pregnancy in rat and mouse. I: maternal and prenatal evaluations. *Toxicological Sciences,* 74**,** 369-381.

UCAN-MARIN, F., ARUKWE, A., MORTENSEN, A., GABRIELSEN, G. W., FOX, G. A. & LETCHER, R. J. 2009. Recombinant Transthyretin Purification and Competitive Binding with Organohalogen Compounds in Two Gull Species (*Larus argentatus* and *Larus hyperboreus*). *Toxicological Sciences,* 107**,** 440-450.

UCAN-MARIN, F., ARUKWE, A., MORTENSEN, A. S., GABRIELSEN, G. W. & LETCHER, R. J. 2010. Recombinant Albumin and Transthyretin Transport Proteins from Two Gull Species and Human: Chlorinated and Brominated Contaminant Binding and Thyroid Hormones. *Environmental Science & Technology,* 44**,** 497-504.

USEPA 2009. Initial risk-based prioritization of High Production Volume (HPV) Chemicals. RH-35,201 Crude (47-51%) (CASRN 50594-77-9) CA Index Name: Phenol, 3-[2-chloro-4- (trifluoromethyl)phenoxy]-,1-acetate). .

VAN DEN BERG, K. 1990. Interaction of chlorinated phenols with thyroxine binding sites of human transthyretin, albumin and thyroid binding globulin. *Chemico-biological interactions,* 76**,** 63-75.

VAN DEN BERG, K. J., VAN RAAIJ, J. A. G. M., BRAGT, P. C. & NOTTEN, W. R. F. 1991. Interactions of Halogenated Industrial Chemicals with Transthyretin and Effects on Thyroid Hormone Levels *in vivo*. *Archives of Toxicology,* 65**,** 15-19.

VANDEN HEUVEL, J. P., KUSLIKIS, B. I. & PETERSON, R. E. 1992. Covalent binding of perfluorinated fatty acids to proteins in the plasma, liver and testes of rats. *Chemico-biological interactions,* 82**,** 317-328.

VANRAAIJ, J., FRIJTERS, C. M. G., KONG, L. W. Y., VANDENBERG, K. J. & NOTTEN, W. R. F. 1994. Reduction of Thyroxine Uptake into Cerebrospinal Fluid an Rat Brain by Hexachlorobenzene and Pentachlorophenol. *Toxicology,* 94**,** 197-208.

VERREAULT, J., SKAARE, J. U., JENSSEN, B. M. & GABRIELSEN, G. W. 2004. Effects of organochlorine contaminants on thyroid hormone levels in arctic breeding glaucous gulls, Larus hyperboreus. *Environmental Health Perspectives,* 112**,** 532-537.

VERREAULT, J., GABRIELSEN, G. V., CHU, S. G., MUIR, D. C. G., ANDERSEN, M., HAMAED, A. & LETCHER, R. J. 2005a. Flame retardants and methoxylated and hydroxylated polybrominated diphenyl ethers in two Norwegian Arctic top predators: Glaucous gulls and polar bears. *Environmental Science & Technology,* 39**,** 6021-6028.

VERREAULT, J., HOUDE, M., GABRIELSEN, G. W., BERGER, U., HAUKAS, M., LETCHER, R. J. & MUIR, D. C. G. 2005d. Perfluorinated alkyl substances in plasma, liver, brain, and eggs of glaucous gulls (Larus hyperboreus) from the Norwegian Arctic. *Environmental Science & Technology,* 39**,** 7439-7445.

VERREAULT, J., LETCHER, R. J., MUIR, D. C. G., CHU, S. G., GEBBINK, W. A. & GABRIELSEN, G. W. 2005n. New organochlorine contaminants and metabolites in plasma and eggs of glaucous gulls (Larus hyperboreus) from the Norwegian Arctic. *Environmental Toxicology and Chemistry,* 24**,** 2486-2499.

VERREAULT, J., VILLA, R. A., GABRIELSEN, G. W., SKAARE, J. U. & LETCHER, R. J. 2006. Maternal transfer of organohalogen contaminants and metabolites to eggs of Arctic-breeding glaucous gulls. *Environmental Pollution,* 144**,** 1053-1060.

VERREAULT, J., BECH, C., LETCHER, R. J., ROPSTAD, E., DAHL, E. & GABRIELSEN, G. W. 2007a. Organohalogen contamination in breeding glaucous gulls from the Norwegian Arctic: Associations with basal metabolism and circulating thyroid hormones. *Environmental Pollution,* 145**,** 138-145.

VERREAULT, J., GEBBINK, W. A., GAUTHIER, L. T., GABRIELSEN, G. W. & LETCHER, R. J. 2007e. Brominated flame retardants in glaucous gulls from the Norwegian Arctic: More than just an issue of polybrominated diphenyl ethers. *Environmental Science & Technology,* 41**,** 4925-4931.

VERREAULT, J., SHAHMIRI, S., GABRIELSEN, G. W. & LETCHER, R. J. 2007f. Organohalogen and metabolically-derived contaminants and associations with whole body constituents in Norwegian Arctic glaucous gulls. *Environment International,* 33**,** 823-830.

VERREAULT, J., GABRIELSEN, G. W. & BUSTNES, J. O. 2010. The Svalbard Glaucous Gull as Bioindicator Species in the European Arctic: Insight from 35 Years of Contaminants Research. *In:* WHITACRE, D. M. (ed.) *Reviews of Environmental Contamination and Toxicology, Vol 205.*

VIEIRA, A. V., SANDERS, E. J. & SCHNEIDER, W. J. 1995. Transport of Serum Transthyreti into Chicken Oocytes - A Receptor-Mediated Mechanism. *Journal of Biological Chemistry,* 270**,** 2952-2956.

VORKAMP, K. & RIGET, F. F. 2013. Nye kontaminanter med relevans for det grønlandske miljø. Aarhus Universitet, DCE-Nationalt Center for Miljø og Energi.

VORKAMP, K. & RIGET, F. F. 2014. A review of new and current-use contaminants in the Arctic environment: Evidence of long-range transport and indications of bioaccumulation. *Chemosphere,* 111**,** 379-395.

WEISS, J. M., ANDERSSON, P. L., LAMOREE, M. H., LEONARDS, P. E. G., VAN LEEUWEN, S. P. J. & HAMERS, T. 2009. Competitive Binding of Poly- and Perfluorinated Compounds to the Thyroid Hormone Transport Protein Transthyretin. *Toxicological Sciences,* 109**,** 206-216.

WOJTCZAK, A., CODY, V., LUFT, J. R. & PANGBORN, W. 1996. Structures of human transthyretin complexed with thyroxine at 2.0 angstrom resolution and 3',5'-dinitro-N-acetyl-L-thyronine at 2.2 angstrom resolution. *Acta Crystallographica Section D-Biological Crystallography,* 52**,** 758-765.

XIE, Z., EBINGHAUS, R., TEMME, C., LOHMANN, R., CABA, A. & RUCK, W. 2007. Occurrence and air-sea exchange of phthalates in the arctic. *Environmental Science & Technology,* 41**,** 4555-4560.

YAMAUCHI, K., PRAPUNPOJ, P. & RICHARDSON, S. J. 2000. Effect of diethylstilbestrol on thyroid hormone binding to amphibian transthyretins. *General and Comparative Endocrinology,* 119**,** 329-339.

YANG, W., SHEN, S., MU, L. & YU, H. 2011. Structure-Activity Relationship Study on the Binding of PBDEs with Thyroxine Transport Proteins. *Environmental Toxicology and Chemistry,* 30**,** 2431-2439.

YANG, X., XIE, H., CHEN, J. & LI, X. 2013. Anionic Phenolic Compounds Bind Stronger with Transthyretin than Their Neutral Forms: Nonnegligible Mechanisms in Virtual Screening of Endocrine Disrupting Chemicals. *Chemical Research in Toxicology,* 26**,** 1340-1347.

YOU, S.-H., GAUGER, K. J., BANSAL, R. & ZOELLER, R. T. 2006. 4-hydroxy-PCB106 acts as a direct thyroid hormone receptor agonist in rat GH3 cells. *Molecular and Cellular Endocrinology,* 257-8**,** 26-34.

APPENDIX A: CHEMICAL STRUCTURE OF THE PREDICTED TTR BINDERS

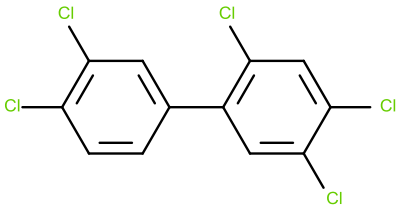

CB-99

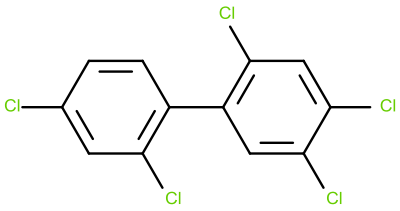

CB-118

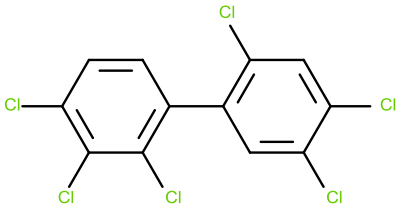

CB-138

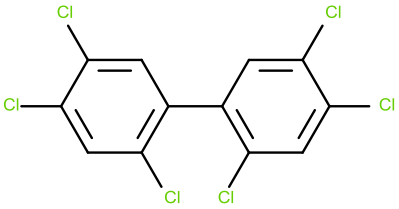

CB-153

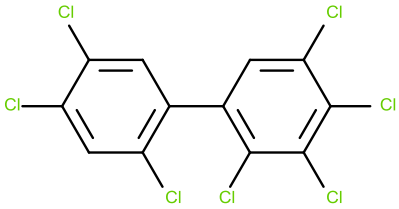

CB-180

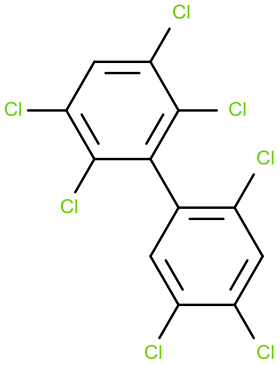

CB-187

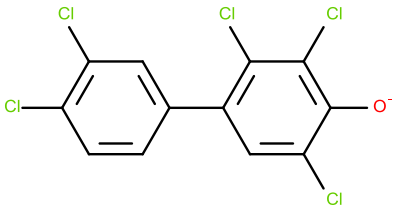

4.OH-CB-107

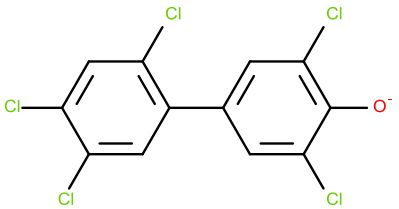

4-OH-CB-120

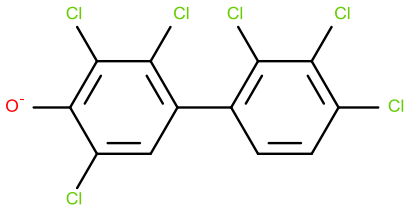

4´-OH-CB-130

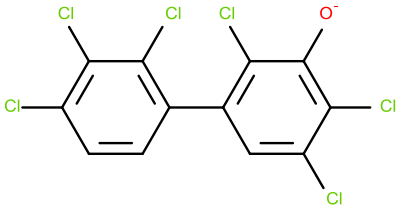

3´-OH-CB-138

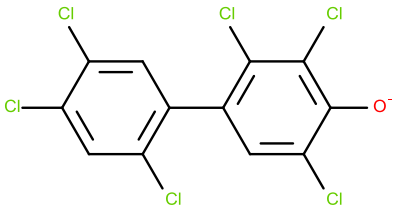

4-OH-CB-146

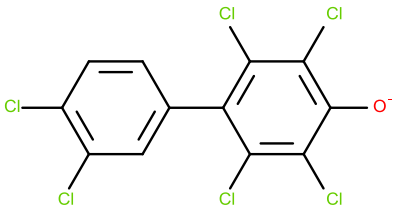

4-OH-CB-163

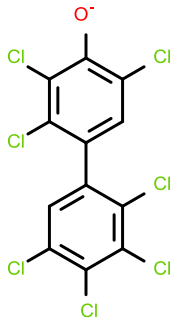

4´-OH-CB-172

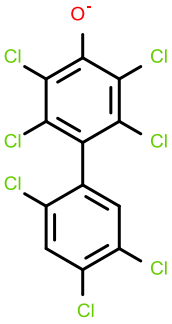

4-OH-CB-187

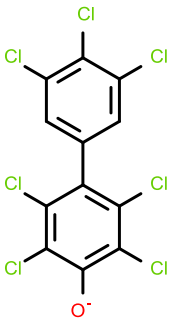

4-OH-CB-193

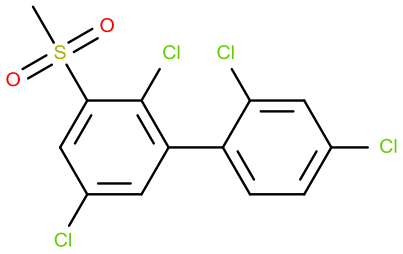

3-MeSO$_2$-CB-49

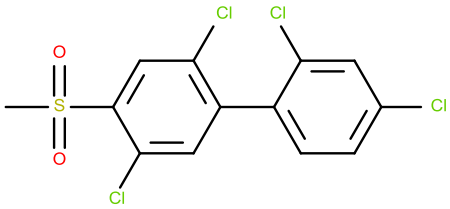

4-MeSO$_2$-CB-49

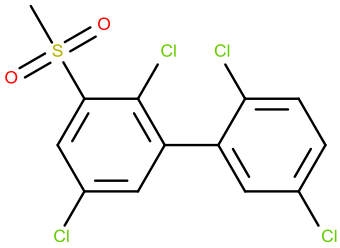

3-MeSO$_2$-CB-52

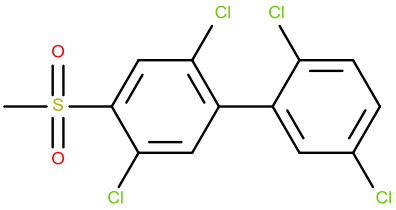

4-MeSO$_2$-CB-52

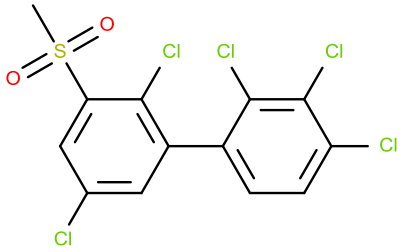

3-MeSO$_2$-CB-87

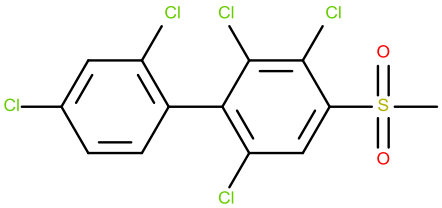

4-MeSO$_2$-CB-91

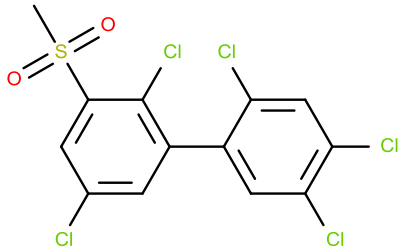

3-MeSO$_2$-CB-101

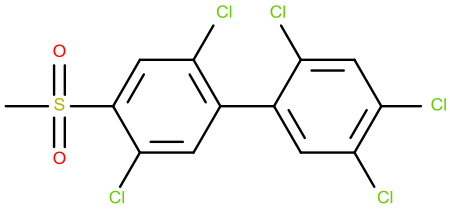

4-MeSO$_2$-CB-101

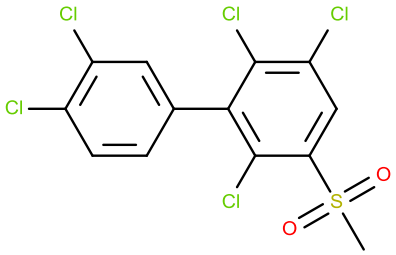

3-MeSO$_2$-CB-110

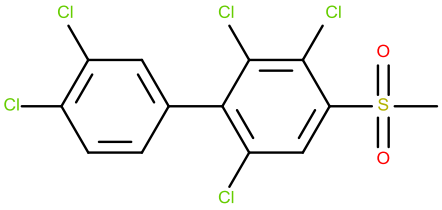

4-MeSO$_2$-CB-110

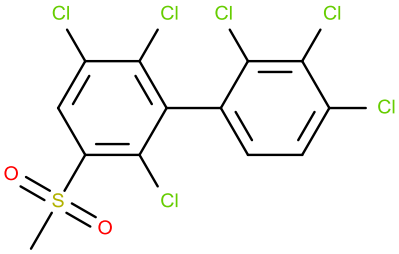

3-MeSO$_2$-CB-132

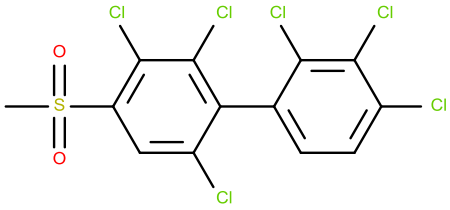

4-MeSO$_2$-CB-132

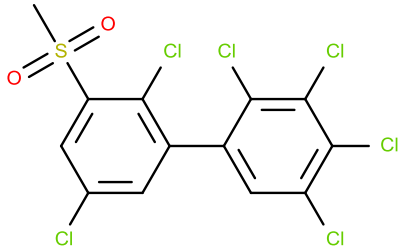

3-MeSO$_2$-CB-141

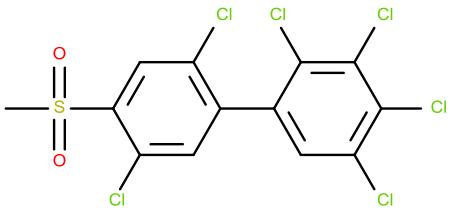

4-MeSO$_2$-CB-141

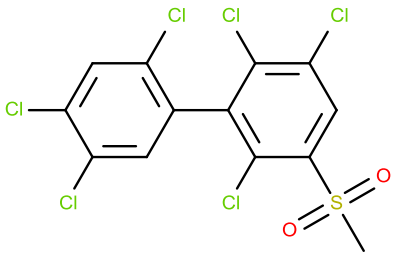

3-MeSO$_2$-CB-149

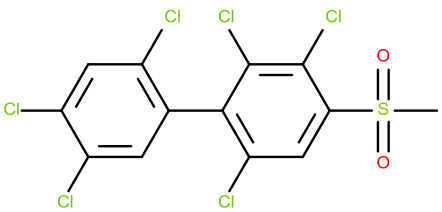

4-MeSO$_2$-CB-149

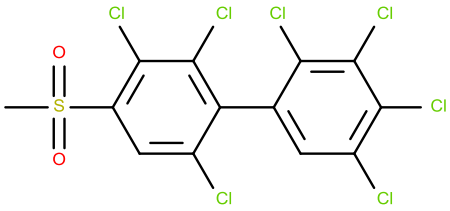

4-MeSO$_2$-CB-174

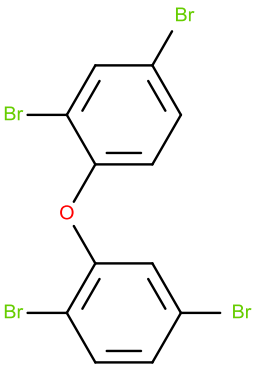

BDE-49

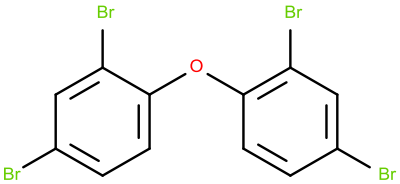

BDE-47

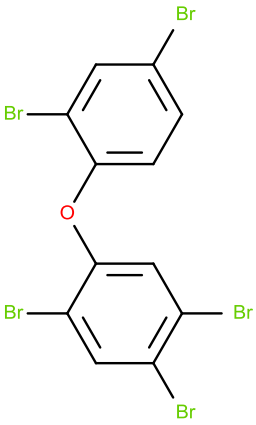

BDE-99

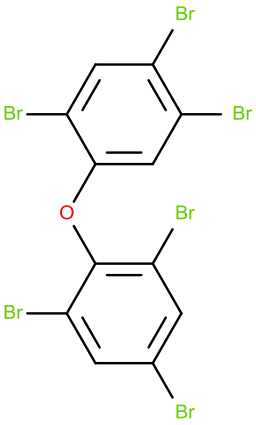

BDE-154

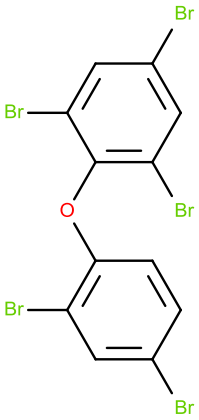

BDE-100

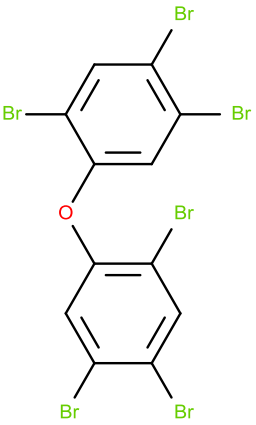

BDE-153

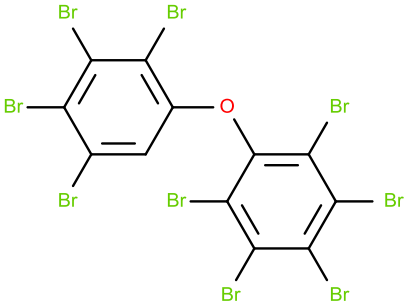

BDE-206

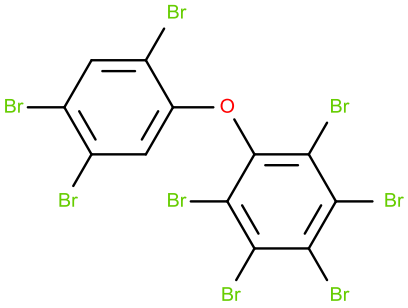

BDE-203

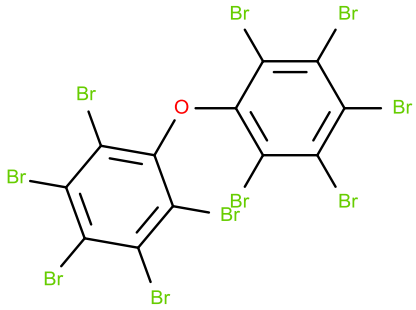

BDE-209

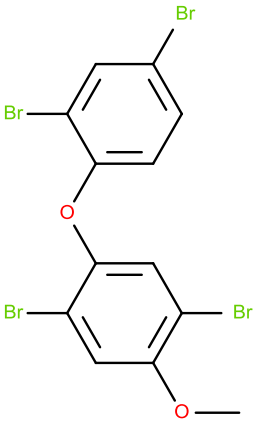

4-MeO-BDE-90

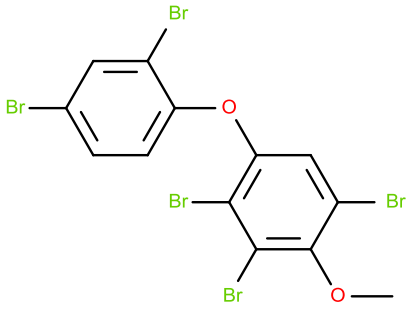

4´-MeO-BDE-49

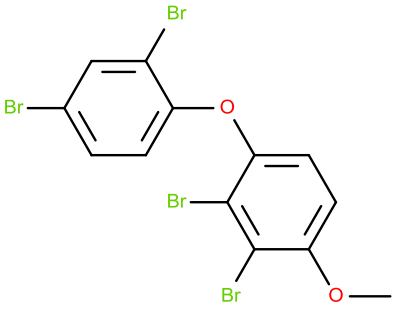

4-MeO-BDE-42

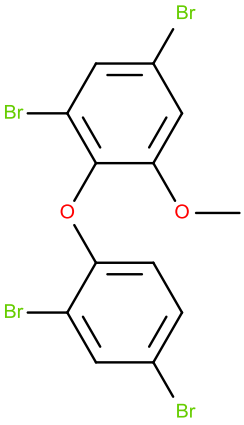

6-MeO-BDE-47

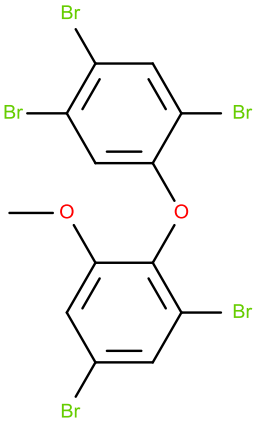

6´-MeO-BDE-99

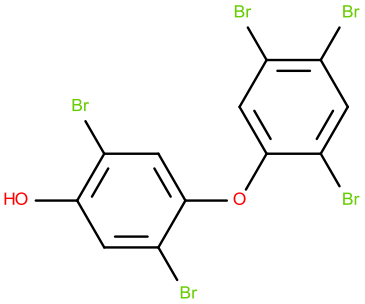

4´-OH-BDE-49

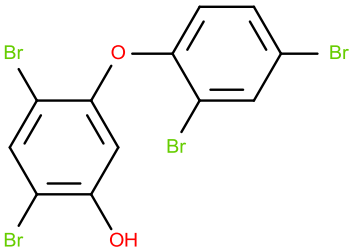

5-OH-BDE-47

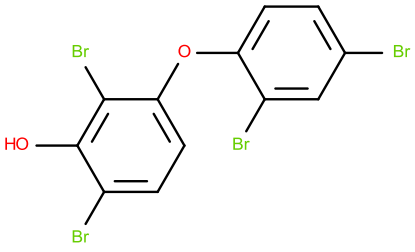

3-OH-BDE-47

F

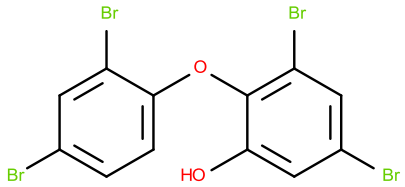

6-OH-BDE-47

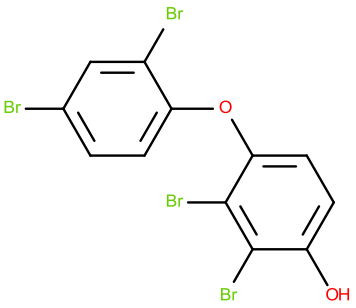

4-OH-BDE-42

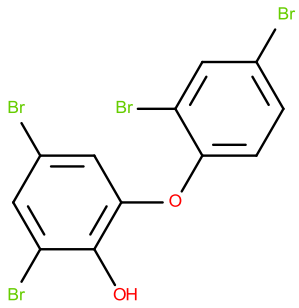

2´-OH-BDE-68

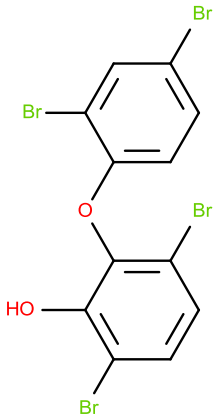

6´-OH-BDE-49

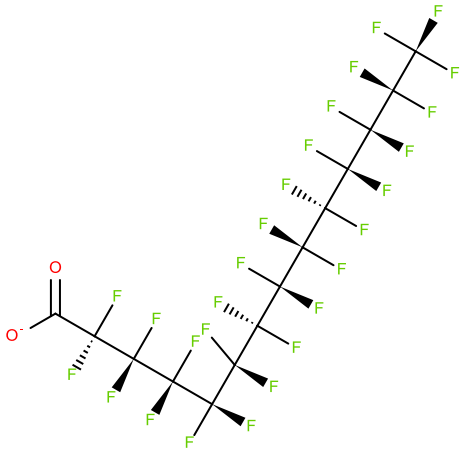

PFTeA

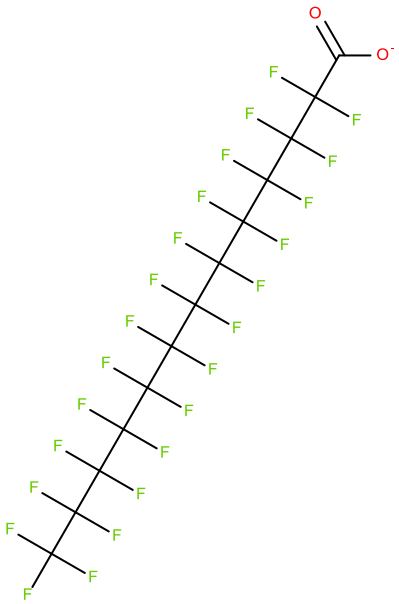

PFTriA

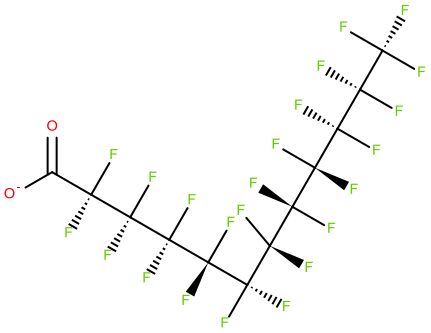

PFDoA

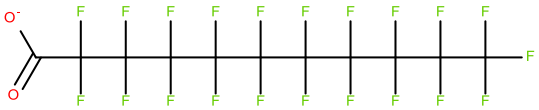

PFUnA

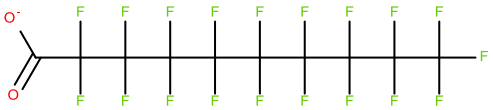

PFDcA

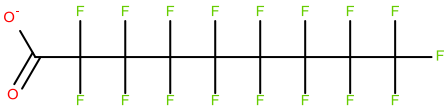

PFNA

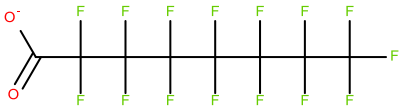

PFOA

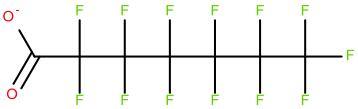

PFHpA

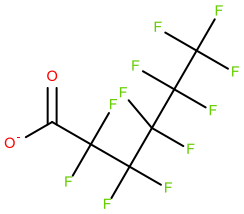

PFHxA

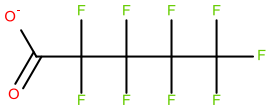

PFPA

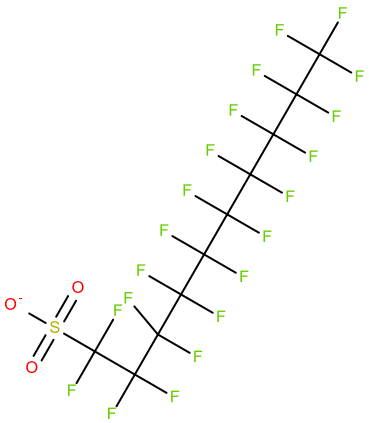

PFDS

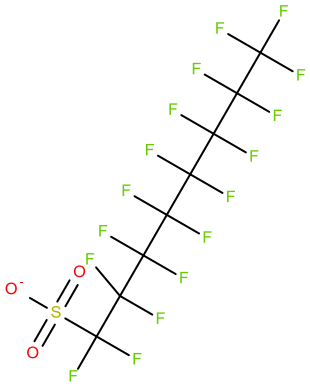

PFOS

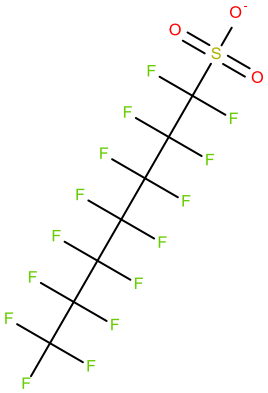

PFHpS

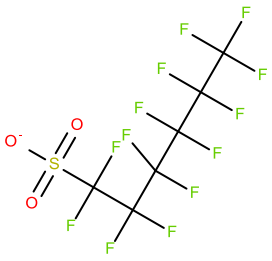

PFHxS

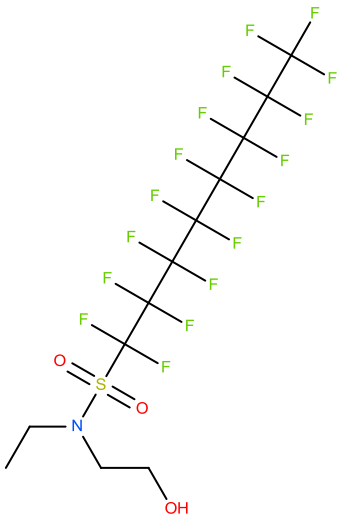

N-Et-FOSE

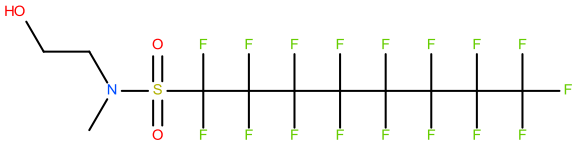

N-Me-FOSE

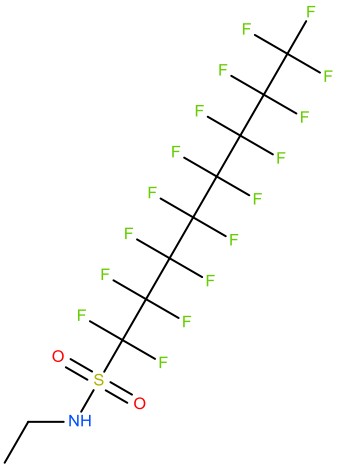

N-Et-FOSA

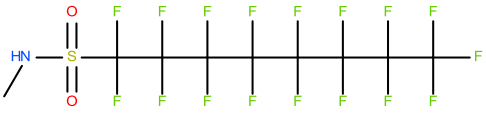

N-Me-FOSA

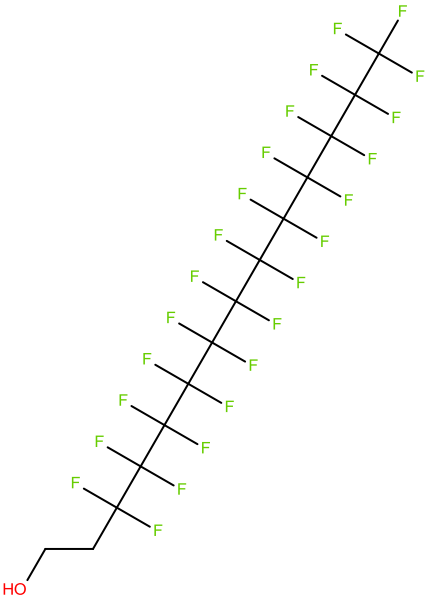

12:2 FTOH

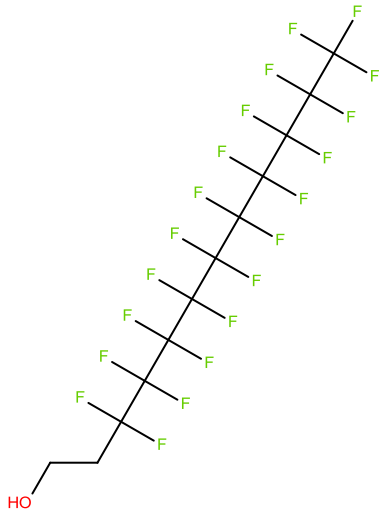

10:2 FTOH

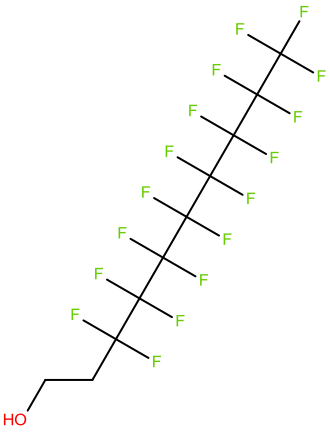

8:2 FTOH

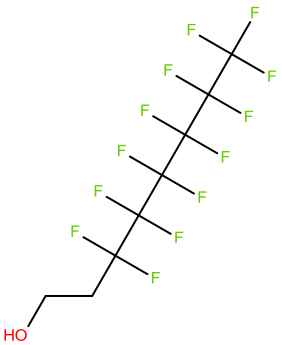

8:2 FTOH

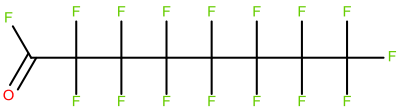

POF

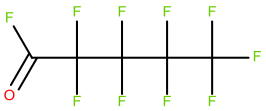

PHpF

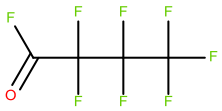

PBF

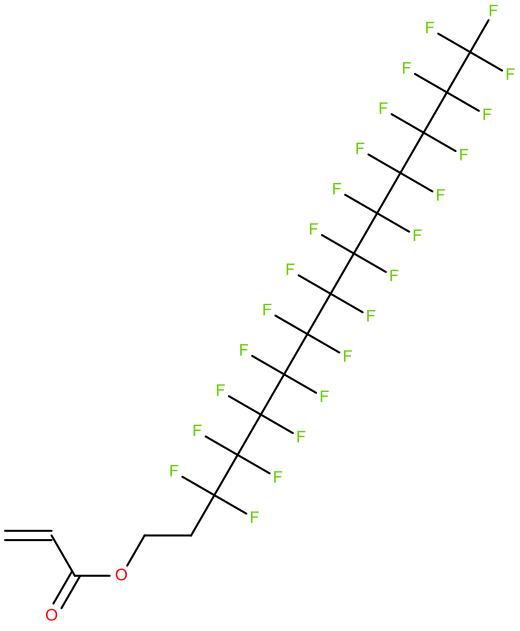

12:2 FTAC

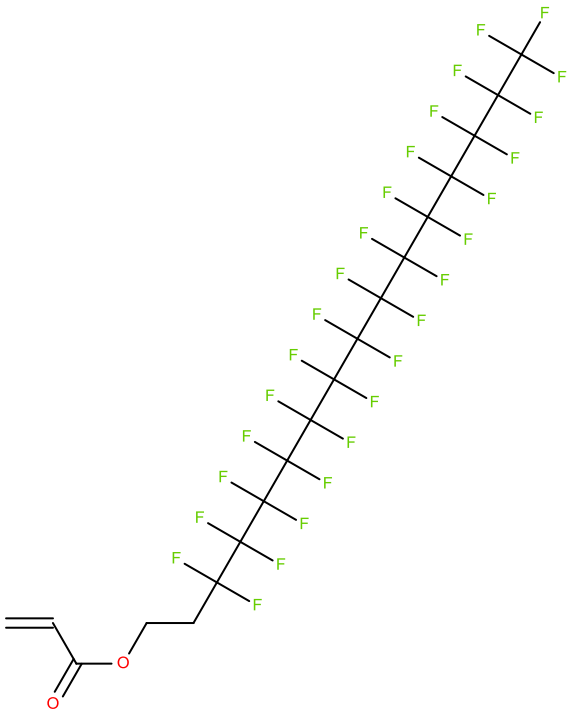

14:2 FTAC

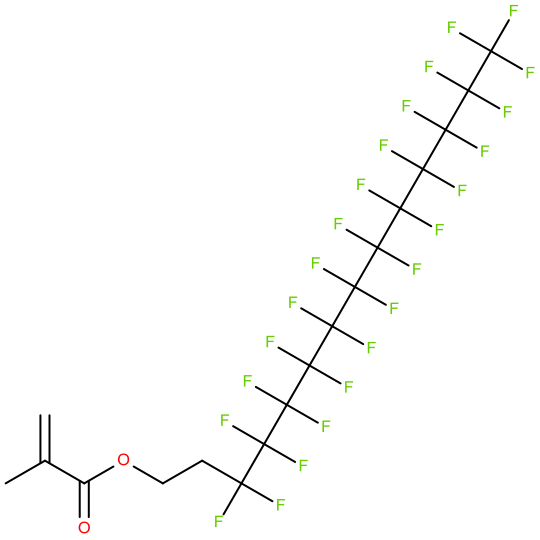

12:2 FTMAC

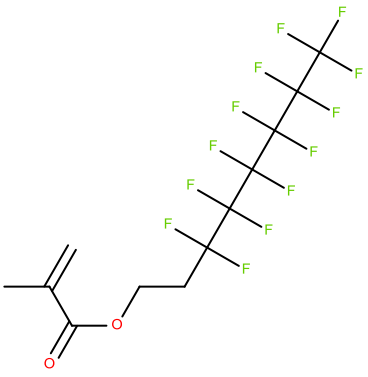

6:2 FTMAC

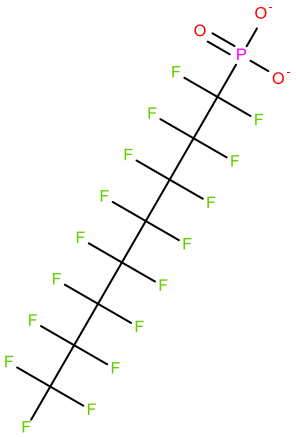

C8-PFPA

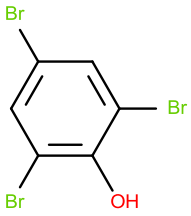

2,4,6-TBP

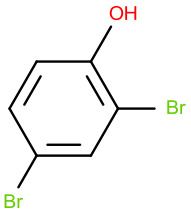

2,4-DBP

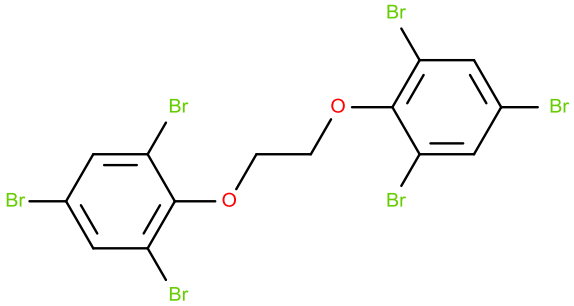

BTBPE

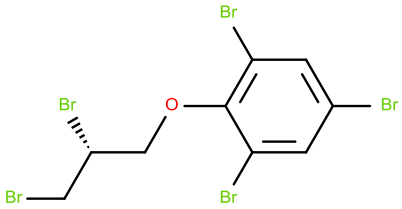

DPTE

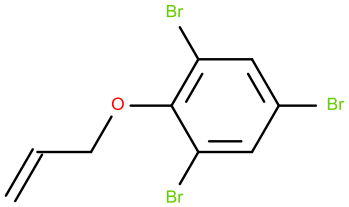

BATE

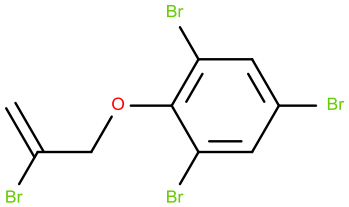

ATE

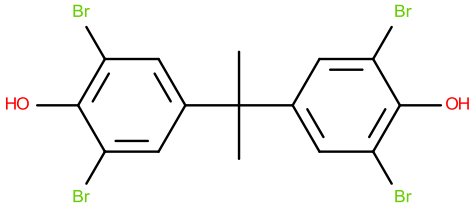

TBBPA

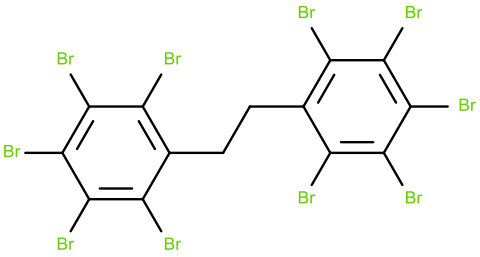

DBDPE

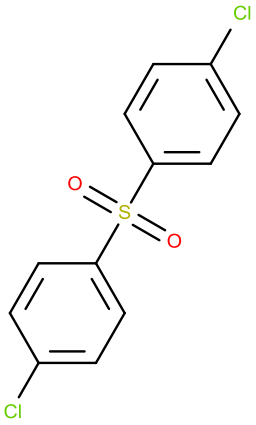

BCPS

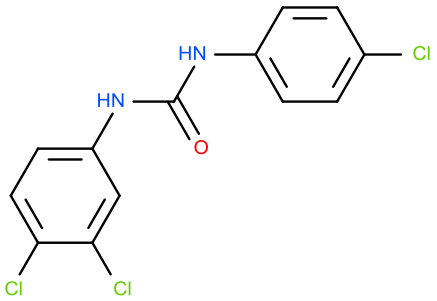

Triclocarban

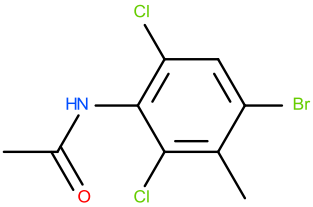

68399-95-1

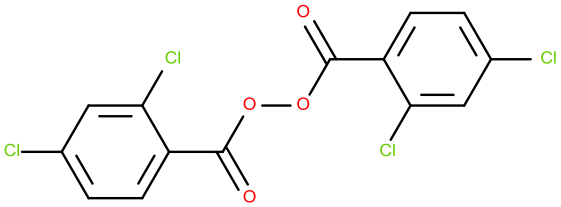

133-14-2

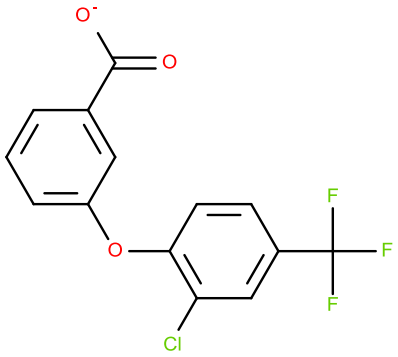

63734-62-3

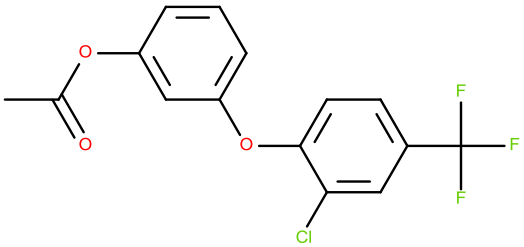

50594-77-9

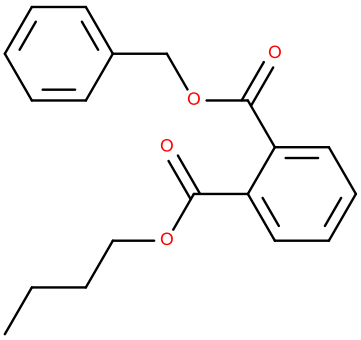

BBP

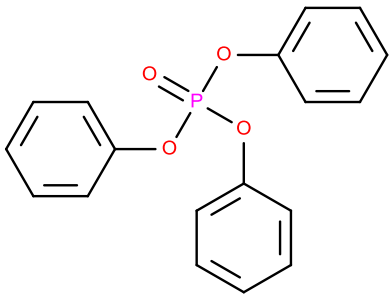

TPhP